Development of a Bio-Based Adhesive for the Encapsulation of Urea in order to Control its Dissolution Rate in Water and Improving its Degradation Rate in Soil

Yihun Wasie Anteneh

A Thesis Submitted to

The Department of Chemical Engineering

School of Mechanical, Chemical and Material Engineering

Presented in Partial Fulfillment of the Requirement for the Degree of Master's

in Chemical Engineering (Specialization in Process Engineering)

Office of Graduate Studies

Adama Science and Technology University

September, 2022

Adama, Ethiopia

Encapsulation of Urea into a Bio-Based Adhesive to Control its Dissolution Rate in Water and Improving its Degradation Rate in Soil

Yihun Wasie Anteneh

Advisor: P. Selvakumar (Ph.D.)

Co- Advisor: Melaku Tesfaye (Ph.D.)

A Thesis Submitted to

The Department of Chemical Engineering

School of Mechanical, Chemical and Material Engineering

Presented in Partial Fulfillment of the Requirement for the Degree of Master's

in Chemical Engineering (Specialization in Process Engineering)

Office of Graduate Studies

Adama Science and Technology University

September, 2022

Adama, Ethiopia

DECLARATION

I hereby declare that this Master Thesis entitled “Development of a Bio-Based Adhesive for the Encapsulation of Urea in order to Control its Dissolution Rate in Water and Improving its Degradation Rate in Soil” is my original work. That is, it has not been submitted for the award of any academic degree, diploma, or certificate in any other university. All sources of materials that are used for this thesis have been duly acknowledged through citation.

Yihun Wasie Anteneh	_____	_____
Name of the student	Signature	Date

RECOMMENDATION

We, the advisors of this thesis, hereby certify that we have read the revised version of the thesis entitled “Development of a Bio-Based Adhesive for the Encapsulation of Urea in order to Control its Dissolution Rate in Water and Improving its Degradation Rate in Soil” prepared under our guidance by Yihun Wasie Anteneh submitted in partial fulfillment of the requirements for the degree of Masters of Science in Chemical Engineering. Therefore, we recommend the submission of the revised version of the thesis to the department following the applicable procedures.

Dr. P. Selvakumar	_____	_____
Major advisor	Signature	Date
Dr. Melaku Tesfaye	_____	_____
Co-advisor	Signature	Date

APPROVAL PAGE

We, the advisors of the thesis entitled "Development of a Bio-Based Adhesive for the Encapsulation of Urea in order to Control its Dissolution Rate in Water and Improving its Degradation Rate in Soil" and developed by Yihun Wasie Anteneh; hereby certify that the recommendation and suggestions made by the board of examiners are appropriately incorporated into the final version of the thesis.

Dr. P. Selvakumar	_____	_____
Major Advisor	Signature	Date
Dr. Melaku Tesfaye	_____	_____
Co-advisor	Signature	Date

We, the undersigned, members of the Board of Examiners of the thesis by Yihun Wasie Anteneh have read and evaluated the thesis entitled "Encapsulation of Urea into a Bio-Based Adhesive to Control its Dissolution Rate in Water and Improving its Degradation Rate in Soil" and examined the candidate during the open defense. This is, therefore, to certify that the thesis is accepted for partial fulfillment of the requirement of the degree of Master of Science in Chemical Engineering (Specialization in Process Engineering).

_____	_____	_____
Chairperson	Signature	Date
_____	_____	_____
Internal Examiner	Signature	Date
Dr. Wondalem Misganaw	_____	04-11-2022
External Examiner	Signature	Date

Finally, approval and acceptance of the thesis is contingent upon submission of its final Copy to the Office of Postgraduate Studies (OPGS) through the Department Graduate Council (DGC) and School Graduate Committee (SGC).

_____	_____	_____
Department Head	Signature	Date
_____	_____	_____
School Dean	Signature	Date
_____	_____	_____
Office of Postgraduate Studies, Dean	Signature	Date

ACKNOWLEDGEMENT

First and foremost, praises and thanks to **God**, the Almighty, for His showers of blessings throughout my research work to complete the research successfully. Next, I would like to express my deepest and heartfelt gratitude to my advisors Dr. P. Selvakumar and Dr. Melaku Tesfaye for their valuable guidance, assistance and continuous encouragement throughout this research.

I would like to thank my Special Parents with the deepest gratitude for their love, prayers, caring and all unlimited helps throughout my journey. **God bless you all!**

Lastly and certainly not in the least, I would like to thank my friends for their encouragement, motivation and support throughout the research work.

TABLE OF CONTENTS

LIST OF TABLES

LIST OF FIGURES

LIST OF ACRONYMS AND ABBREVIATIONS

AMO	Ammonia Monooxygenase
ANOVA	Analysis of Variance
CRF	Controlled Release Fertilizer
CRU	Controlled Release Urea
CU	Coated Urea
FTIR	Fourier Transform Infrared Spectroscopy
GA	Gum Acacia
HAO	Hydroxylamine Oxidoreductase
LA	Lactic Acid
LAO	Lactic Acid Oligomer
LAO-g-GA	Lactic acid Oligomer Grafted With Gum Arabic
NI	Nitrification Inhibitor
NMR	Nuclear Magnetic Resonance
NF	Nano Fertilizer
NUE	Nitrogen Use Efficiency
PC	Polymer Coated
RSM	Response Surface Method
U-e-LAO-g-GA	Urea Encapsulated Lactic Acid Oligomer Grafted Gum Acacia
UI	Urease Inhibitor
USG	Urea Super Granules
S-CRF	Slow or Controlled Release Fertilizer
SRF	Slow Release Fertilizer

ABSTRACT

Nitrogen (N) is the most essential and very important nutrient for the plant growth. Urea contains 46% of N which is the highest content of those solid nitrogenous fertilizers, but urea has a limitation on its delivery system. Most plants require the essential nutrient N from urea throughout their lifetime. Since different plants have different lifetime, the release of N from urea must to be in a controlled manner. In this research work urea was encapsulated in a biodegradable adhesive, which was synthesized through poly-condensation reaction of lactic acid (LA) and gum acacia (GA), to control its dissolution rate in water, and to improve its degradation rate in soil. The poly-condensation reaction was performed in an oven with conventional heating system at different temperatures (between 165 ^{0}C to 195 ^{0}C), reaction time (between 1.5-2.5hrs), and GA to LA mixing ratio (between 8.3 to 12.5 w/w%) based on the Box-Behnken method of design expert software. The effect of those independent variables on the grafting efficiency of lactic acid oligomer grafted gum acacia (LAO-g-GA), and on its release rate after urea encapsulation was studied. The result shows that the grafting efficiency and the urea release rate were inversely proportional. Therefore, the urea release rate of urea encapsulated LAO-g-GA (U-e-LAO-g-GA) can be controlled simply by controlling the grafting efficiency of LAO-g-GA. The grafting of lactic acid oligomer (LAO) chains at the O-H and N-H functional groups of GA backbone was confirmed with the help of FTIR and NMR analyses. The results of solubility and hydrophobicity tests of LAO-g-GA exhibits that as the grafting efficiency of LAO-g-GA increases, both its solubility in chloroform and its hydrophobicity increases. The increase in temperature of a medium, and the urea concentration encapsulated in the synthesized LAO-g-GA increases the urea release rate, but the increase in pH of the medium decreases the urea release rate. The soil degradation test result shows that all U-e-LAO-g-GAs were entirely degrade in soil, and as the grafting efficiency of the LAO-g-GA increases its degradation rate decreases. The amount of urea encapsulated into the LAO-g-GA affects its soil degradation rate in a positive manner. The N release rate of U-e-LAO-g-GAs in water was studied using Kjeldhal method, and from the four studied release kinetic model equations, the Korsmeyer-Peppas equation exhibits a best fit with correlation coefficients (R^2 > 0.99), and the release exponent (n) values for all U-e-LAO-g-GAs were greater than 0.89, implies the release of N from U-e-LAO-g-GAs was a combination of diffusion and erosion mechanisms.

Keywords: dissolution rate, release kinetics, urea encapsulation, bio-adhesive

CHAPTER ONE

1. INTRODUCTION

1.1. Background of the Study

Working on increasing agricultural productivity continues as the most crucial task for attaining the great challenge of feeding 9.5 billion peoples of the world estimated by 2050 (Fertahi et al., 2021). So, in order to meet the food need for increasing population, use of fertilizers as an input of crop production is very important. Fertilizer, a very important chemical substance in agriculture, performs a vital role in preserving soil fertility, increasing crop yields, and enhancing harvest quality (Shan et al., 2021). Plants require more than 14 nutrients for their optimal growth and productivity. From those nutrients the three macro nutrients nitrogen, phosphorus and potassium are very important and required in largest quantity, found in most packaged fertilizers that are commonly used in agriculture (Hasanuzzaman et al., 2018). However, from those nutrients, nitrogen is the most significant and very important nutrient for the growth of crops, since it is a basic component of protein and almost all the necessary processes in the plants growth requirement are related with it (Dimkpa, Fugice, et al., 2020).

Consequently, N-fertilizer has long been used as a very important component for agriculture, predicted to meet 48% demand of the world's population (Galloway et al., 2008; Xia et al., 2022). It has been playing an important role in global food security, presently accounting for more than half of the world's food production (Dimkpa, Andrews, et al., 2020; X. Zhang et al., 2015) and is possible to say that it continues in fulfilling the food challenge in the future. Urea is the most well-known fertilizer used in the world by suppling the highest amount of nitrogen to the plants (Beig et al., 2020). Urea delivers 46% of nitrogen, which is very essential nutrient for plant growth and it has a favourable characteristics in terms of manufacturing cost, handling, storage, and transport (Herrera et al., 2016), it has a limitation in its nutrient delivery. Urea has a major limitation of easily dissolved in water and rapid nitrification rate. Thus, the essential nutrient nitrogen from urea is vulnerable to losses through nitrous emission, ammonia volatilization, leaching, and surface runoff (Azeem et al., 2020; Ma et al., 2019).

As a result, many researchers have tried to solve these problems by developing fertilizers, which have slow release rate of nutrients in order to improve the nitrogen use efficiency of plants (An et

al., 2021; Beig et al., 2020; El Assimi et al., 2021; Lyu et al., 2021; Madzokere et al., 2020; Pan et al., 2021; Salimi et al., 2020; Zafar et al., 2021). Slow or controlled-release fertilizers (S-CRFs) are those containing a plant nutrient in a form, which delays its availability for plant uptake. Beside to enhancing plants nutrients uptake ability, S-CRFs reduces human health and environmental problems caused by leaching and volatilization due to a high dissolution and nitrification rate of commercial urea fertilizer (Lawrencia et al., 2021). Researchers have tried to develop these fertilizers by using the following developing mechanisms: 1) Coating fertilizer with semipermeable or impermeable membranes such as sulfur, gypsum, lignin and polymers; 2) Urea super granules (USG); 3) Using urease and nitrification inhibitors; and 4) Using of Nano technology, i.e., Nano fertilizers. Although developing of a slow or controlled release fertilizers using these mechanisms play great role in reducing nutrient loss, it has its own limitations such as high processing cost, non-biodegradability and easily cracking nature of coating materials, still venerable to nutrient loss and human health and environmental impacts (Dimkpa, Fugice, et al., 2020); labor-intensive and time-consuming while using urea super granules (L. Liu et al., 2018); Decrease osmotic shock along with delayed urea hydrolysis during the application of urease and nitrification inhibitors (Abalos et al., 2014); and high production cost and toxicity of using Nano-fertilizers (Zulfiqar et al., 2019). So, working on improving the mechanisms of developing a slow or controlled released fertilizer has been continued to find out a mechanism for developing a fertilizer for efficient delivery of nitrogen, which is technically and economically viable to allow the controlled release of fertilizer to significantly reduce loss of nutrients in to the environment and to the water bodies.

Bio-based polymers like cellulose, chitosan, and gum acacia have received a lot of attention recently to develop a slow or controlled release fertilizers (Abd El-Aziz et al., 2021; Mohammadbagheri et al., 2021; Zonatto et al., 2017), since they are safe for the environment, non-toxic, biodegradable, and have a low carbon footprint (Katiyar & Tripathi, 2019). As bio-based polymers are often hydrophilic in their natural forms, there are currently just a few viable applications for them. However, the polymers' potential applications drastically expand, if they can be made into hydrophobic materials. Gum acacia (GA) is a hydrophilic biopolymer in its nature, however, if certain modifications are performed on its structure, it becomes hydrophobic and can be used for the nutrient encapsulation applications (Lamsen, 2019). And also its hydrophobicity can be controlled during its modification reaction, making it suitable for a

controlled nutrient delivery system application. Here, a poly-condensation reaction was conducted to modify gum acacia (GA) with lactic acid oligomer (LAO) in order to synthesis a biodegradable and hydrophobic adhesive. And a controlled dissolution rate fertilizer with an improved soil degradation rate was formulated successfully by encapsulating urea into the synthesized hydrophobic and biodegradable adhesive.

1.2. Statement of Problem

Urea is the most well-known and highly significant fertilizer used in agricultural production in the world by suppling the highest amount of nitrogen to the plants (Beig et al., 2020), and it has favourable characteristics in terms of manufacturing cost, handling, storage, and transport (Herrera et al., 2016). However, urea has a limitation in its nutrient delivery. It has a major limitation of easily dissolved in water and rapid nitrification rate. Thus, its essential nutrient nitrogen is vulnerable to losses through ammonia volatilization, leaching, and surface runoff (Azeem et al., 2020; Ma et al., 2019). Consequently, approximately 40% - 70% of nitrogen is lost (Fertahi et al., 2021), which is a cause for a great economic crisis, since a low nitrogen use efficiency of plants leads to; a reduction in crops yield potential and higher cost of investment in agricultural inputs by farmers. Besides, the nitrogen released in to the water bodies and to the atmosphere through leaching and volatilization, leads to cause human health problem's such as: respiratory ailments, cardiac disease and cancer, and other environmental problems such as greenhouse gas effects may happen (Lawrencia et al., 2021). Therefore, it is very important to establish a new type of controlled release fertilizer by encapsulating urea into a hydrophobic and bio-degradable adhesive to minimize the above limitations of urea fertilizer.

1.3. Research Questions and Choice of Systems

The present research work aims to answer the following major research questions;

- What would be the effect of lactic acid oligomer grafted gum acacia copolymer synthesizing factors (i.e. reaction temperature, reaction time and mixing ratio) on its grafting efficiency, and on its nitrogen release rate after urea encapsulation?
- What role that the lactic acid oligomer grafted gum acacia copolymer contributes in the development of a controlled dissolution rate fertilizer?
- Is it possible to control the hydrophobicity of lactic acid oligomer grafted gum acacia copolymer?

- Is the lactic acid oligomer grafted gum acacia copolymer degraded in natural soil?

Based on the above research questions the choice of the systems is formed as follows;

Urea, lactic acid and gum acacia, are selected as a base and focal point due to:

- Urea is one of the world's leading nitrogen fertilizer due to its high nitrogen content (about 46%), low cost, able to handle and transport, and commercially available.
- Lactic acid oligomer grafted with gum acacia copolymer, which was synthesized from gum acacia and lactic acid was used due to its favorable biodegradability and hydrophobic properties, recognized from the preliminary experiment.

1.4. Objectives of the Study

1.4.1. General Objective

The major objective of this research work is to encapsulate urea into a bio-based adhesive to control its dissolution rate in water and improve its degradation rate in soil.

1.4.2. Specific Objectives

In order to achieve the above mentioned general objective, the following specific objectives are articulated as follows:

- To synthesize and characterize a bio-based adhesive and study the effect of its synthesizing factors (i.e. reaction temperature, reaction time and mixing ratio) on the grafting efficiency and on the release rate of urea.
- To study the effect pH, temperature and urea concentration on the urea release rate of urea encapsulated bio-adhesives in water.
- To study the urea release rate of urea encapsulated bio-adhesives in soil.
- To study the soil degradation rate of the urea encapsulated bio-adhesives as compared with pure urea and the effect of urea concentration on its degradation rate.
- To study the total nitrogen release rate of urea encapsulated bio-adhesives as compared with pure urea in water using Kjeldhal method, and studding its release kinetics using different kinetic models.

1.5. Significance of the Study

This study has a great significance in terms of assuring the synthesize of a biodegradable controlled dissolution rate fertilizer for efficient delivery of nitrogen to the plants. The major significance of this study is to reduce volatilization, leaching, and runoff of nutrients from urea fertilizer. It has a great role in accordance with the government policy of increasing food production and diversification of the present farming so as to attain sustainable food security and subsequent poverty reduction. Besides, it reduces environmental and human health problems caused by utilization of commercial urea fertilizer.

1.6. Scope of the Study

This research is mainly focused on:

- Synthesis of a bio-based adhesive i.e., lactic acid oligomer grafted gum acacia copolymer (LAO-g-GA).
- Study the effect of reaction temperature, reaction time and GA to LA mixing ratio on the grafting efficiency of a synthesized LAO-g-GA, and on its urea release rate after urea was encapsulated in it.
- The solubility and hydrophobicity of a synthesized LAO-g-GA was evaluated.
- FTIR and NMR analyses of a LAO-g-GA was also conducted.
- Study the effect of factors such as pH, temperature and urea concentration on the urea release rate in water.
- Study the urea release rate in the soil of a urea encapsulated LAO-g-GAs.
- Study the soil degradation rate of urea encapsulated LAO-g-GA as compared with commercial urea fertilizer and the effect of grafting efficiency on the soil degradation rate.
- Study the effect of urea concentration on the soil degradation rate.
- Finally, the release kinetics of nitrogen from urea encapsulated LAO-g-GA was studied using four different kinetic models.

CHAPTER TWO

2. LITERATURE REVIEW

2.1. Overview of Fertilizers

A fertilizer is an organic or inorganic chemical substance which is used to increase plant growth and fertility. It can also improve water retention and filter any extra liquid, subsequently improving soil effectiveness. Organic fertilizers are prepared from natural substances specifically manure generated from sheep, poultry litter, green manures, sewage sludge, and press mud, compost, or other different animal and plant products (Hammad et al., 2020). They generally tend to work slowly and over the long-time period (R. P. Singh, 2012). Inorganic fertilizers are fertilizers that are either industrially produced via chemical methods or mined from mineral reserves with little processing (Gupta & Hussain, 2014). They are used for effective short-term growth, after ascertaining the nutrient required for the plant and use an inorganic fertilizer containing that nutrient (Ma et al., 2019). Inorganic fertilizers are fertilizers mined from mineral deposits with little processing (e.g., lime, potash, or phosphate rock), or industrially manufactured through chemical processes (e.g., urea).

Plants require a number of chemical elements to grow. The most important are: carbon, hydrogen, and oxygen which are available in air and water. Macro nutrients, such as potassium, phosphorus and nitrogen, and micronutrients, such as boron, cobalt, copper, iron, manganese, molybdenum and zinc, and secondary nutrients, such as sulfur, calcium and magnesium are required for the optimal growth and productivity of plants (Hasanuzzaman et al., 2018). Nutrients such as nitrogen, phosphorus, potassium, magnesium, manganese, chlorine and iron are directly involved in plant photosynthetic activities; calcium, boron, copper, zinc and molybdenum are involved in enzymatic activities; N and S are involved in protein synthesis (Hasanuzzaman et al., 2018). Basically, macro nutrients nitrogen, phosphorus and potassium are the most important nutrients for plant growth and needed in the largest quantity. They are necessary for basic building blocks. For example, every amino acid contains nitrogen, every molecule making up ATP (the main energy source of all cells) contains phosphorus, and so does every molecule making up every cells membrane (the membrane molecules known as phospholipids). Although all macro nutrients are important and needed in largest quantity, Nitrogen is the most essential nutrient for plant growth and required in greatest amount (Xia et al., 2022).

2.2. Sources of Nitrogen

Table 2.1. Nitrogen sources and their compositions (Herrera et al., 2016)

Source	Nitrogen Content (%)
Anhydrous ammonia	82
Urea	46
Ammonium nitrate	33.5-34
Urea-ammonium nitrate solution	28-32
Calcium ammonium nitrate	21-27
Ammonium nitrate sulfate	26
Ammonium chloride	26
Aqua ammonia	20-25
Ammonium sulfate	21
Diammonium phosphate	18
Sodium nitrate	16
Calcium nitrate	15.5
Potassium nitrate	13
Ammonium thiosulfate	12
Monoammonium phosphate	10-11

From those inorganic fertilizers, anhydrous ammonia contains the highest concentration of N (82%) as shown in the Table 2.1. above, which has cheap cost in a number of countries. But, as it is a gas it is difficult to handle and it must be pressurized in order to store it as a liquid, so, it needs special equipment for storage, handling, and application. In addition, the effect on soil pH produced by this source might require lime to maintain a desired soil pH (Herrera et al., 2016). This later effect is not exclusively from anhydrous ammonia but all ammoniacal sources.

Urea ($CO(NH_2)_2$) contains 46% of N, which is the second highest N content next to anhydrous ammonia, but the highest of those solid nitrogenous fertilizers. Favourable characteristics of manufacturing costs, handling, storage, and transport make urea very competitive N source. As a result, it is the most widely used fertilizer in the current worldwide.

2.3. Limitations of Using Commercial Fertilizers

Direct utility of chemical fertilizers to plants become proven to have low usage performance, only 30–35% of the nutrients are absorbed by the plants (Iftime et al., 2019; Lawrencia et al., 2021)**.** Urea, a well-known usually used N-fertilizer, become suggested to have the most effective nitrogen use efficiency. Unfortunately, around 40% - 70% of nitrogen from urea is lost (Beig et al., 2020; Fertahi et al., 2021), in which 2–20% is lost by volatilization, 15–25% reacts with natural compounds within the soil and 2–10% is lost through leaching into water bodies, prominent to urgent environmental concerns (Lawrencia et al., 2021). Urease enzyme in the soil turns urea into ammonium carbonate, which is highly unstable and converted into ammonia and carbon dioxide causes to volatilize nitrogen to the atmosphere in the form of ammonia. A certain amount of ammonia is then converted into ammonium by the presence of water in the soil. And also nitrifying bacteria's, Nitrobacter and Nitrosomonas converts ammonium into nitrite and then to nitrate, which are highly mobile in nature and leached with rain to the water bodies as shown in the Figure 1.1 below

Nitrogen (N) transformation process from urea;

$(NH_2)_2CO + 2H_2O + \text{Enzyme Urease} \longrightarrow (NH_4)_2CO_3$

$(NH_4)_2CO_3 + H_2O \longrightarrow 2NH_3 + CO_2 + H_2O$

$NH_3 + H_2O \longrightarrow NH_4^+ + OH^-$

$2NH_4^+ + 3O_2 + \text{Ammonification bacteria nitrosomonas} \longrightarrow 2NO_2^- + 2H_2O + 4H^+$

$2NO_2^- + O_2 + \text{Ammonification bacteria nitrobacter} \longrightarrow 2NO_3^-$

$2NO_3^- + \text{Microorganisms} \longrightarrow N_2 + N_2O$

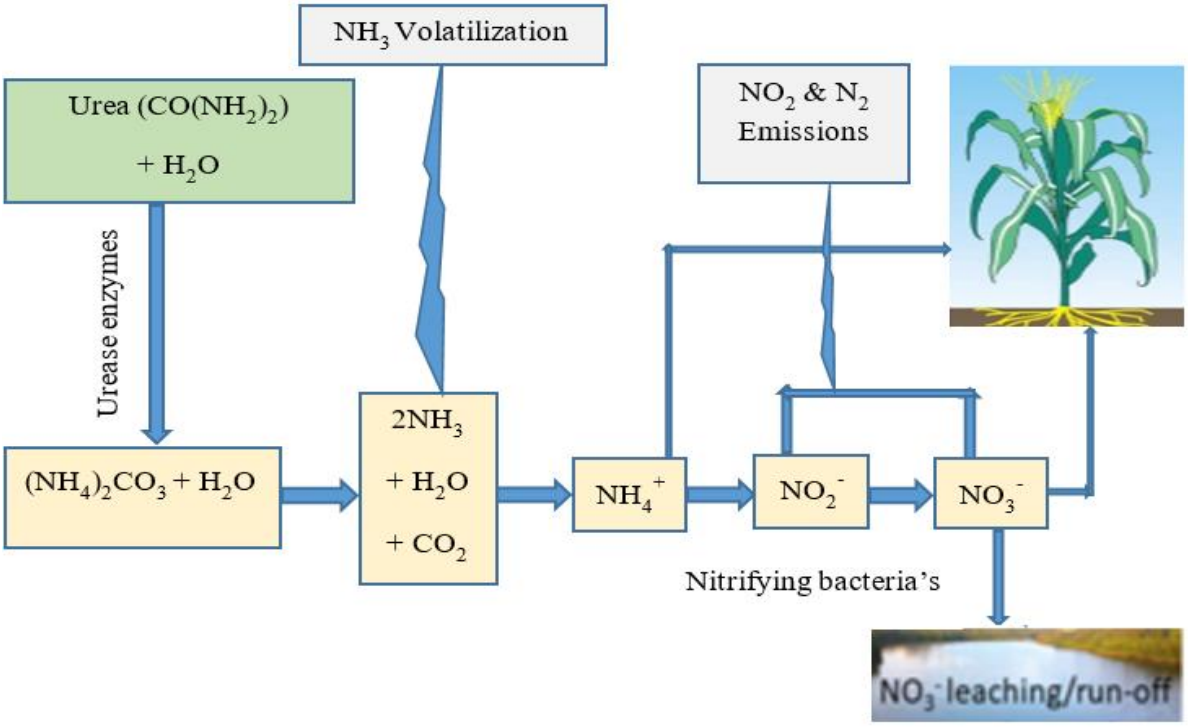

Figure 2.1. The loss of N from urea before the plants use it efficiently

The hydrophilic property urea with a high water affinity comes from its molecular structure, even it soaking up water from humid air. The presence of urease enzyme in the soil with even in a small amount of water causes it to hydrolyze. Urea consists of a carbonyl functional group with two attached amino groups. During hydrolysis the amino groups cleaves off, with each taking up a proton to form NH_3 (g), which is highly volatile or, preferably, can take up additional proton to form NH_4^+ (aq). This process takes approximately one up to four days to complete in normal urea application (Ransom et al., 2020). Therefore, in order to decrease N losses to the atmosphere and water bodies, in order to increase nitrogen use efficiency (NUE) in crops and to maintain a sustainable and healthier environment, the rate of urea hydrolysis needs to be in a controlled manner.

2.4. Slow or Controlled Release Fertilizers (S-CRFs)

Nitrogen use efficiency of plants increases significantly by synchronizing N availability with N demand as much as possible. Therefore, timing the N application to match the maximum uptake by the crop is fundamental to maximizing uptake by the crop and minimizing N losses (Herrera et al., 2016). Slow or controlled-release fertilizers (S-CRFs) were suggested as a vital to enhance the nutrient use performance of plants, and subsequently taken into consideration to address the

troubles because of the increase of world's population. It has been available since the 1950s, although most of the advances in the development of these products were made in the 1980s and 1990s (Mayer, 2010). The whole S-CRFs release progression takes place within three principal stages: permeation of water, dissolution of nutrients, and release of nutrients through the S-CRF system.

Different scholars define “slow release fertilizers (SRF)” and “controlled release fertilizers(CRF)” in different manner. According to Fertahi et al., (2021), SRFs and CRFs are both used to describe the delays of nutrient availability for plant uptake, however to differentiate these two categories, CRFs are generally related to fertilizers coated or encapsulated with different materials. While SRFs consist manures of plants and animals and compost which requires to be decayed by the activity of microorganisms before the nutrients can be released. In addition, CRFs allow a much more controlled rate and duration of nutrient release with semipermeable coatings and hydrophobic encapsulating materials. Whereas for SRFs, the time delay of release in a slow release fertilizer cannot be controlled due to the effectiveness of microbial organisms. Association of American Plant Food Control Officials (AAPFCO) under 57th official publication defines slow release fertilizer as: A fertilizer that retains nutrients for a long time and delays their availability up to a period in which the plants required nutrients, or a fertilizer that supplies the nutrients to the plants for significantly extended periods than a standard fertilizer (rapidly available to the plants) such as urea or ammonium nitrate, potassium chloride or ammonium phosphate. And**,** Lawrencia et al., (2021) said that CRF is a subset of SRF which falls under the category of fertilizer with a physical barrier.

S-CRFs have a lot of advantages in terms of improving the N use efficiency of crops, increasing crop productivity and it reduces consumption of fertilizer, possible to decrease the fertilizer application rate by 20 to 30% of the recommended value to achieve the same yield (Lawrencia et al., 2021). It also reduces ecological, environmental and human health problems, which are caused by volatilization and leaching of nutrients to the atmosphere and to the water bodies (Rajan et al., 2021). However, during the application of controlled release fertilizers, it is better to consider the properties of soil where a fertilizer applied (type, pH, temperature, moisture, microorganisms present in a soil, etc.) and properties such as composition and solubility of the coating or encapsulating materials and coating thickness for CRFs formulated by coating commercial fertilizer with different coating materials.

2.5. Factors Affecting the Application of S-CRFs

2.5.1. Soil Temperature

One of the important factors for the release of nutrients is temperature of soil. At temperatures below 10 ^{0}C, there is no fertilizer release. If the temperature is above 32 ^{0}C, the fertilizer release is excessive (Rajan et al., 2021). An increase in temperature causes to increase the nutrient release rate (Husby et al., 2019). According to Husby et al., (2019), the nutrient release rate was maximum at a temperature between 35 - 40 ^{0}C. It was found that high temperature likely to contribute to high ammonia volatilization loss rates because increasing temperature promotes NH_4^+ conversion to NH_3, NH_3 diffusion rate, urea hydrolysis, and organic N mineralization (X. Liu et al., 2020).

2.5.2. Soil pH

The acidic or alkaline nature of the release medium has a significant effect on the interactions of chemical species in the granule and the diffusion coefficient of the ions (Lawrencia et al., 2021). The availability of nutrients is directly affected by the soil pH. Some nutrients become insoluble when the soil's pH is too low or too high, limiting the availability of these nutrients to the plant root system. Most nutrients are more soluble in acid soils than in neutral or slightly alkaline soils (Feng et al., 2015).

2.5.3. Granule Radius and Coating Thickness

Increasing the radius of the S-CRFs is generally preferred in the interest of economic feasibility. However, there is always an optimum granule size required for the proper distribution of nutrients in the root zone (Lawrencia et al., 2021). The nutrients release decreases as the coating thickness increases. Even thicker coating films were unable to deliver positive results when there were coating flaws and a porous coating film. With an increase in coating thickness, the diffusion coefficient drops. Despite a substantial mean coating thickness and the lowest coefficient of variance of coating thickness, samples with coating defects and highly porous coating films still showed an increase in diffusion coefficient. Therefore, desirable release properties of the controlled release urea require more than just a suitable coating thickness, the urea release rate can't be controlled exactly (Azeem et al., 2016).

2.5.4. Activity of Microorganisms

Biodegradation of S-CRFs is a complex process that involves cascade events controlled by abiotic and biotic stimuli in the environment. The degradation process of biodegradable polymer coatings is described by Ganetri et al., (2021) as follows: The microorganisms colonize the surface of the polymers, secreting enzymes responsible for the hydrolysis of the polymeric bonds generating oligomers, dimers that are disintegrated into monomers. These monomers are then converted to carbon dioxide, water, minerals, and biomass under aerobic conditions, or to carbon dioxide, methane, and humid material in the case of anaerobic biodegradation without leaving any potentially harmful substances. Therefore, the degradation rate of S-CRFs depends on the presence and absence of microorganisms in the soil.

2.6. Mechanisms Followed to Develop S-CRFs

Several possible mechanisms have been used to delay the availability of nutrients or consistent supply of nutrients to the plants for extended time periods. These include semipermeable or impermeable membrane coatings, fertilizers for deep placement such as urea super granules (USG), Urease and nitrification inhibitors, and use of Nano fertilizers.

2.6.1. Fertilizers Coated with Semipermeable or Impermeable Membranes

Within a recent few years, the expansion of coated fertilizers in a speedy manner accounts over 95% of slow released fertilizers (Fu et al., 2018). It is to form a layer or a number of layers of semipermeable or impermeable membranes on the surface of the fertilizer granule to reduce release of nutrients. Different membrane structures have different properties that causes to have various slow release effect. Several semipermeable or impermeable materials have been tested for slow release coatings. These materials are usually separated into two types: organic polymeric materials or inorganic mineral compounds (Beig et al., 2020). Organic materials include polymeric resins and thermoplastic polymers, whereas inorganic mineral based substances such as gypsum, sulfur and bentonite are grouped under the category of inorganic coatings.

Sulfur is an example of impermeable materials. The sulfur sprayed over urea fertilizer act as a barrier and preserves the rain water and water in the soil away from the very soluble urea until cracks or fissures are established in coating by any physical and microbial activity. Coating of urea with sulfur reduces the dissolution rate of the fertilizer granules and reduces the release of

nutrients. However, sulfur coated fertilizers often fail to meet the slow release standards mostly due to high production cost and inconsistent release patterns (Beig et al., 2020; Naz & Sulaiman, 2016). As sulfur coating fertilizers are known by their brittle and relatively easily damaged surface characteristics, it cracks and permitting the water entry which leads dissolution of urea granules prematurely, causing in nutrient loss through leaching (Naz & Sulaiman, 2016). Additionally, elemental sulfur is quite acidic; as such, its use for coating can effect in soil acidification and, accordingly causes N deficiency (Dimkpa, Fugice, et al., 2020; Lawrencia et al., 2021). This acidification might also additionally cause a disorder on other nutrients such as calcium deficiency or magnesium deficiency (G. Liu et al., 2014).

Synthetic polymers are semi-permeable membranes with tiny surface pores. Compared to sulfur, synthetic polymers are chosen because of a reduced tendency for coating disruptions caused by any physical and microbial activities (Naz & Sulaiman, 2016). Moreover, coating polymers are relatively hydrophobic, permitting controlled diffusion of moisture through their variably permeable membranes and thus the N release rates varies with the characteristics of polymer and soil properties such as permeability, composition and thickness of polymer and temperature, pH and moisture of soil.

Synthetic polymers such as polyethylene, polystyrene, polyacrylamide, and polysulfide obtain a promising outcomes with respect to controlled release characteristics. Most of them have a hydrophobic nature, permitting controlled diffusion of moisture through their permeable membranes (Chen et al., 2018). However, these materials could not be used to produce controlled release fertilizer on industrial scale due to augmented cost and non-biodegradability factors. Synthetic polymers may be subject to the deposition of non-biodegradable residues, with potential hazard implications for the environment (Dimkpa, Fugice, et al., 2020). Biopolymers such as starch, cellulose, lignin, vegetable oil, animal and vegetable gum, rosin are known for their relatively cheap price compared to the synthetic polymers and biodegradable in soil and nontoxic (Fertahi et al., 2021), however, they are poor films and weak coating barrier; mostly need**s** modifications (Fu et al., 2018).

2.6.2. Urease and Nitrification Inhibiter

In recent years, mitigation technologies including urease inhibitors and nitrification inhibitors have been explored to reduce emissions and N losses from agricultural fertilizer usage. Urease

inhibitors work by blocking the active site of urease, slowing down urea hydrolysis, and limiting the amount of N lost to the atmosphere as NH_3. Whereas nitrification inhibitors generally work to inhibit bacteria's present in soil such as nitrifying bacteria's, nitrobacter and nitrosomonas, which are responsible for nitrification and ultimately, limit N losses by reducing N_2O emissions, and NO_3^- losses via leaching from soil (Cantarella et al., 2018). Both urease and nitrification inhibitors can effectively reduce N loss and reduce GHG emissions and water pollutions.

According to Cantarella et al., (2018), Urease inhibitors are formulated into solid by coating fertilizer products, or applied separately to the soil primarily to reduce urea hydrolysis by urease enzymes. The most widely used urease inhibitor by far is N-(n-butyl) Thiophosphoric triamide (NBTPT), known commercially as Agrotain, developed by Koch Agronomic Services. Other common urease inhibitors include ammonium thiosulfate (ATS) phenylphosphorodiamide /phenylphosphorodiamide (PPD/PPDA), hydroquinone, and calcium thiosulfate (CTS).

Nitrification inhibitors are a class of chemicals used to slow down the nitrification process by inhibiting nitrifying bacteria that produce the enzyme ammonia monooxygenase (AMO), hydroxylamine oxidoreductase (HAO) and nitric oxide reductase (NOR) (Ruser & Schulz, 2015). The mode of action for most nitrification inhibitors is inhibition ammonia monooxygenase during the first step of nitrification (the oxidation of NH_4^+ to hydroxylamine (NH_2OH) via the enzyme AMO), NH_2OH is then subsequently converted to NO_2^- via the enzyme HAO, and the second step is inhibition nitrobacter nitrification which oxidize NO_2^- to NO_3^- by means of the nitric oxide reductase. Nitrification inhibitors have gained interest as a possible mitigation strategy for lowering N_2O emissions as well as reducing water pollution associated with use of fertilizers. Some examples of nitrification inhibitors include dicyandiamide (DCD) and 3,4-dimethyl-1H-pyrazole phosphate (DMPP), carbon sulfide (CS_2), thioethers, and 2-ethynylpyridine (Byrne et al., 2020). However, Urease and nitrification inhibitors alter the osmotic strength of soil solution. The decreased osmotic shock along with delayed urea hydrolysis might reduce the flush of mineral N (Abalos et al., 2014).

2.6.3. Urea Supper Granular Formulation

The USG fertilizer is manufactured from the physical modification of ordinary urea fertilizer. The International Fertilizer Development Center (IFDC), Muscle Shoals, Alabama 35660, USA, has developed it. Its nature and properties are similar to that of urea but its granule size is bigger and

condensed with some conditions for slow hydrolysis. USG is spherical in shape containing 46% nitrogen which is similar to commercial urea. Average diameter of the granule is 11.5 mm and weight is 1.8 g (Hussain et al., 2017).

According to Sarkar et al., (2021), the application of USG guarantees has the better utilization of nitrogen throughout the growing period of the plant and showed that (10-20) % urea could be saved by the use of USG instead of commercial urea for cabbage and cauliflower. However, USG must be placed deeply to avoid the burn of seeds or plant roots and ammonia volatilization by fast dissolving in paddy soil (L. Liu et al., 2018). The deep placement approach of the USG is labor-exhaustive and time-consuming, which has limited it use in large-scale agricultural manufacturing systems.

2.6.4. Nano Fertilizers

Nano fertilizers are nutrients encapsulated/coated with nanomaterial for the control and slow delivery of one or more nutrients in order to satisfy the imperative nutrient requirements of plants. The process of encapsulation of nutrients with nanomaterials can be performed in three ways; commercial fertilizers coated with a thin layer of nanoparticles; plant nutrients encapsulated in the nanomaterials to formulate a new fertilizer; and prepare nutrients in the form of Nano-emulsion to deliver directly to the plants (Zulfiqar et al., 2019).

Nano fertilizers containing zinc oxide, silicon dioxide and titanium oxide nanoparticles exhibited novel performance characteristics for example improved seed germination and shoot length and healthy seedlings (Madzokere et al., 2020) and reported that use of Nano-fertilizers has resulted in 6 to 17% increase in crop productivity. NFs releases its nutrient either applied alone or in combination with CF at a slow and steady rate for 40 to 50 days while commercial fertilizers do the same in 4 to 10 days only (Seleiman et al., 2021). Accordingly, Seleiman et al., (2021) have reviewed and found that a lot of NFs have been already developed and put the potential role in modern agriculture in terms of growth and development of plants including quality and yield with a little number of dosages compared to commercial fertilizers. Saha et al., (2021) has also reviewed that the applied doses of NFs were varied from 0.05 to 5000 mg/L, which is very lower in amount than CFs and higher nitrogen use efficiency with minimum effects on environmental pollution. However, it is alarming that the ranges of NFs dosage used in different crop production are different. It implies the lacking of information regarding the optimum dosages of NFs for particular

crops. Thus, due to the lack of recommended doses of NFs, the cost of crop production, as well as the plant toxicity, might be increased. The extensive release of nanomaterials into the environment and the food chain may pose a risk to human health (Zulfiqar et al., 2019). High cost of Nano fertilizers, Lack of production and supply of Nano fertilizers in required quantities, limits the wider scale adoption of Nano-fertilizers as a source of plant nutrients. Absence of proper Nano-fertilizer risk management systems and Standardization missing mostly in Nano-fertilizer formulation process were also reported as a limitation of using Nano fertilizers (Saha et al., 2021).

2.7. Advantages and Limitations of the Above S-CRF formulation Mechanisms: Summary

Ultimate grand goal of all the above mechanisms is to keep nitrogen much longer in the soil in the form of NH_4^+ and NO_3^- up to plant's uptake period of time. Since plants use nitrogen from urea in the form of NH_4^+ and NO_3^-. As shown in the Figure 2.2 below, the application of all the above mechanisms on the urea fertilizer helps to reduce urease enzyme and nitrifying bacteria's activity, helps to reduce the loss of nitrogen through ammonia volatilization, nitrous oxide emission, and surface runoff. As a result, applying all those mechanisms on commercial urea fertilizer benefits in increasing nutrient (N) use efficiency of plants; reducing the amount of fertilizer used, and reducing negative environmental and human health impacts.

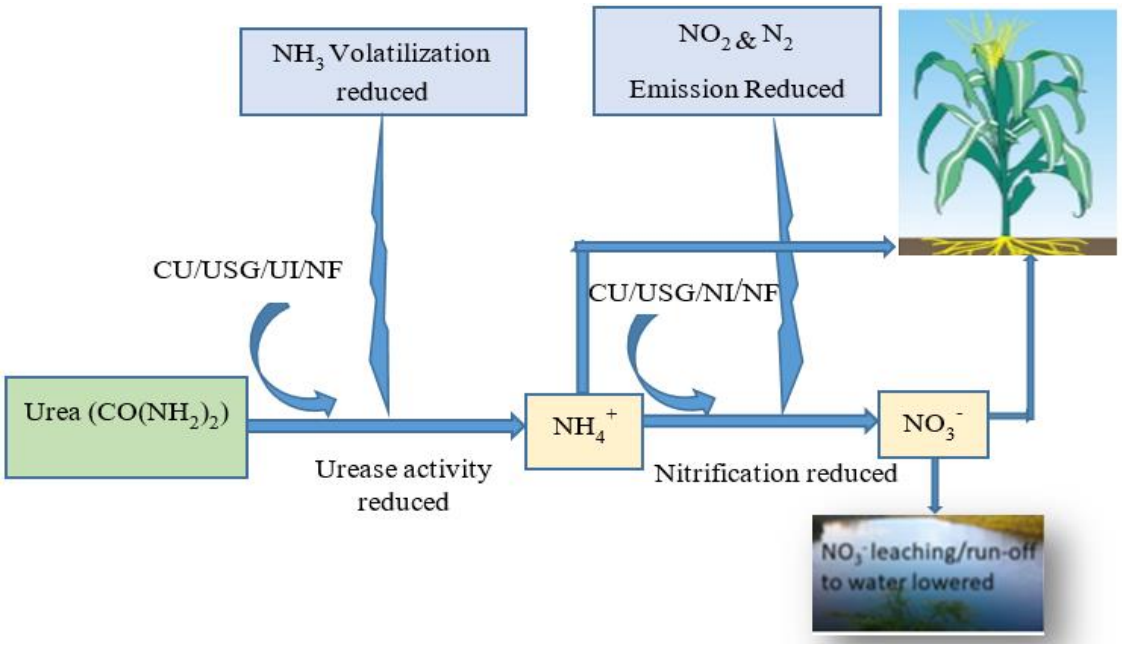

Figure 2.2. Effect of CU, USG, NF, UI, and NI to reduces the N transformation rate

As shown in the tables (i.e. Table 2.2 and Table 2.3) below, although developing of a slow or controlled release fertilizers using the above mechanisms play great role in enhancing nitrogen use efficiency of plants and reducing environmental and health problems, it has its own limitations such as: high processing cost, non-biodegradability and mostly they are still venerable to nutrient loss due to easily cracking nature of coating materials.

Table 2.2. Advantages of using S-CRF formulation mechanisms

Mechanisms	Advantages	Reference
Sulfur coating	➢ S coating of urea could significantly reduce ammonia (NH3) volatilization from soil. ➢ High S-induced N recovery from soil by plants.	➢ **(**Naz, & Sulaiman, 2016) ➢ (Beig, et al. 2020)
Polymer coating	❖ It has a hydrophobic nature, permitting controlled diffusion of moisture through their permeable membrane. ❖ Least affected by soil properties.	❖ **(**Dimkpa, et al. 2020)
Urea super granule	➢ Reduce the ammonia volatilization loss ➢ Reduce the usage of fertilizer in the fields.	➢ (Sarker, et al. 2012)
Urease and Nitrification Inhibiter	❖ Inhibits urease enzymes and microorganisms that causes N losses in the form of N_2O, NO and NH_3. ➢ Reduce burning of seed due to a high concentration NH_4^+ and NO_3^-.	❖ (Abalos et al. 2014) ➢ **(**Cantarella, et al. 2018)
Nano fertilizers	❖ Improves the nutrient-use efficiency and decreasing nutrient loss through evaporation and leaching.	❖ (Seleiman, et al. 2021) ❖ **(**Madzokere, et al. 2021)

Table 2.3. Limitations of using S-CRF formulation mechanisms

Mechanisms	Limitations	Reference
Sulfur coating	➢ High production cost and irregular release pattern. ➢ S is relatively acidic; can result in soil acidification.	➢ **(**Naz, & Sulaiman, 2016) ➢ (Beig, et al. 2020) ➢ **(**Dimkpa, et al. 2020) ➢ (Lawrencia, et al. 2021)
Polymer coating	❖ Highly expensive ❖ Mostly non-degradable ❖ Pollutant ❖ Toxic	❖ **(**Dimkpa, et al. 2020)
Urea super granule	➢ Labour-intensive and time-consuming	➢ (Liu, et al. 2018)
Urease and Nitrification Inhibiter	❖ Decreased osmotic shock along with delayed urea hydrolysis might reduce the flush of mineral N.	❖ (Abalos et al. 2014)
Nano fertilizers	➢ High cost of production ➢ Lack of information regarding the optimum dosages of NFs for particular crops causes to increase crop production cost as well as the plant toxicity.	➢ (Zulfiqar, et al. 2019)

Recently, a number of S-CRFs has been formulated by coating of a fertilizer with different coating materials. It accounts over 95% of slow released fertilizers (Fu et al., 2018). Not only coating of urea with semipermeable and impermeable membranes such as sulfur, gypsum, polymer and lignin, but also mostly formulation of slow released fertilizers using urease and nitrification inhibitor and Nano fertilizers has been performed by coating of urea with urease and nitrification inhibitor materials such as urea coated with N-(n-butyl) Thiophosphoric triamide (NBTPT) inhibitor (Antille et al., 2015; Byrne et al., 2020; Janke et al., 2020; Khan et al., 2014; Sha et al., 2020; Skorupka & Nosalewicz, 2021; Zuki et al., 2020); and with neem oil (Ali et al., 2020; Kumar et al., 2011; Mohanty et al., 2021; Rehman et al., 2021; B. Singh, 2019); and also urea coated with Nano particles (Dimkpa, Andrews, et al., 2020; Jia et al., 2020; Li et al., 2021; Shan

et al., 2021; Umar et al., 2022). However, although coating of a fertilizer with different coating materials reduces the nitrogen loss through leaching and volatilization, in most coated fertilizers, still it has a tendency to loss since, an irregular release of nutrients due to the removal of coating materials by means of any physical, chemical and biological activity occurs. It is also difficult to estimate the thickness of a coating layer that can permit the appropriate amount of nitrogen with the appropriate time to the plants. Figure 2.3 below shows how the nutrient (nitrogen) is verneluable to loss due to its irregular release by the disintegration of coating layers occurs when the coated urea is exposed to water and soil.

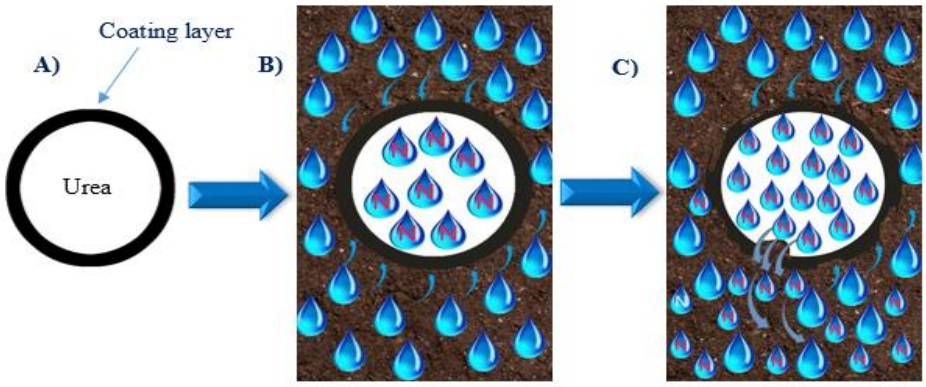

Figure 2.3. Irregular release of nitrogen due to disintegration of coating materials, A) coated urea, B) coated urea exposed to soil and water, C) irregular release of nitrogen (Dimkpa, Fugice, et al., 2020).

In order to solve a problem related to coated urea; to reduces its disintegration, firstly, it is preferable to choose coating materials that take into account their interactions with various soil properties and soil microorganisms, as well as their biodegradability, affinity for urea, permeability property to allow water and urea solution, capability to delay immediate urea escape from the coating surface, and ability to release urea in a way that meets a crop's nutritional needs. Developing of a controlled nitrogen release fertilizer with original industrial grade urea granules at the beginning rather than coating urea with coating materials is the second very important way to solve problems related to coating materials. As shown in the Figure 2.4 below, when urea is encapsulated in a biodegradable matrix, the nitrogen from urea can be released in regular manner. Here in this case synthesizing of urea encapsulated bio-adhesive for a controlled release of nitrogen was conducted by dispersing urea powder into a hydrophobic and bio-degradable adhesive, which

can solve problems related to disintegration of coating materials by means of any physical, chemical and biological activity, can enhance the nitrogen use efficiency of the plants.

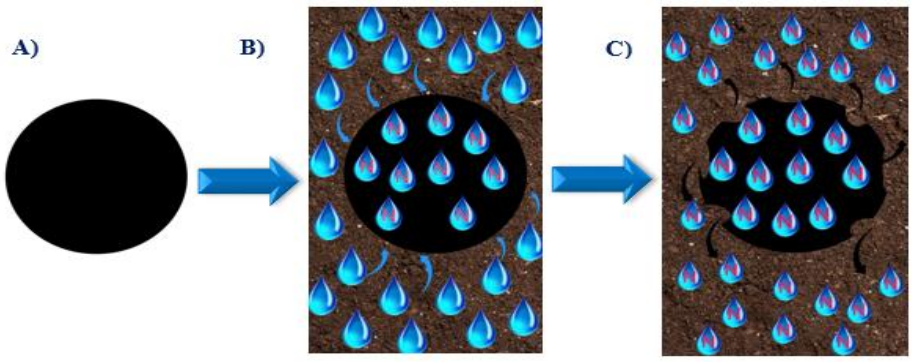

Figure 2.4. The Nitrogen release from the newly formulated fertilizer, A) urea encapsulated in a bio-adhesive, B) when it is exposed to soil &water, C) release of N through degradation (Dimkpa, Fugice, et al., 2020).

Table 2. 4. Matrix materials used for the formulation of slow-release fertilizer with its formulation methods

No	Matrix material + Modifier	Formulation methods	References
1	Natural bentonite + binder: corn starch or hydroxypropyl methyl-cellulose	Melt blending	(Hermida and Agustian, 2019)
2	Montmorillonite clay (bentonite) + hydrophobic/hydrophilic polymer: polycaprolactone or polyacrylamide hydrogel	Melt blending	(Pereira et al., 2015)
3	Gypsum & Sulfur + paraffin; ground magnesium lime	Coating	(Babadi et al., 2015)
4	Phosphogypsum + Paraffin wax + span-80	Coating	(Yu & Li, 2019)
5	Polyvinyl alcohol + biochar	Melt blending	(Chen et al., 2018)
6	Polyurethane + mesoporous silica	Coating	(Li et al., 2016)
7	Polystyrene + Wax; Polyurethane	Coating	(Y.-c. Yang et al., 2012)
8	Bio-based Polyurethane (PU) + Isocyanate, acrylonitrile	Coating	(Bortoletto-Santos et al., 2020)

2.8. Adhesives

Adhesives are a broad category of substances used to hold or bind at least two martials together in a manner that is appropriate for the application (Cui & Liu, 2021). The adhesive must have surface adherence and cohesion to facilitate bonding and it works primarily by the property of adhesion**.** Adhesion is the attraction between two distinct substances brought on by intermolecular interactions. Bonding is the process of joining materials with an adhesive. Different types of material are bonded using a variety of adhesives under various circumstances (Banea & Da Silva, 2009).

2.8.1. Classifications of Adhesives Based on Origin

All adhesives operate by the same basic properties. However, there are several different types of adhesives available, each of which can be differentiated by their particular characteristics and origin. based on their origin adhesives can be classified into natural and synthetic adhesives.

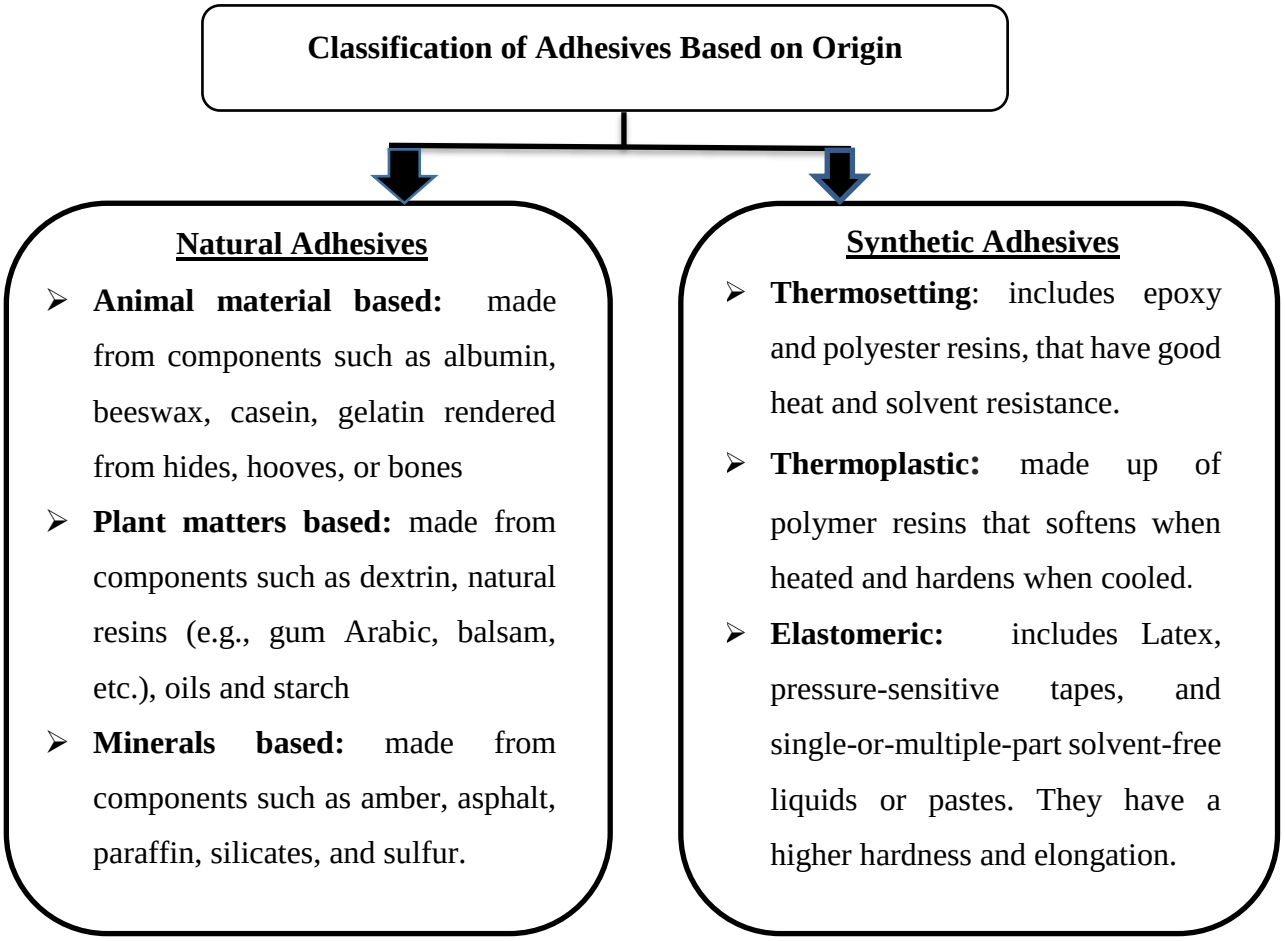

Figure 2. 5. Classification of adhesives based on origin

With the blending of several kinds of polymers and elastomers to create hybrid adhesive formulations, substantial advancements in adhesive technology were made in a short period of time. The focus of recent adhesive technology research has been on elastomers and high-temperature materials. The use of a specific type of microstructural adhesive is an example of the continually expanding applications. Typical synthetic adhesives are epoxies, polyurethanes, cyanoacrylates, polyimides, silicones, acrylics, polyamides, cyanoacrylates, polyvinyl acetate (PVA), nitrile, neoprene (Technology et al., 2018).

Although, these types of adhesives offer greater bond strengths and durability, as well as provide more options for customization they are costlier than natural adhesives due to uncertainty in the availability of petrochemicals and their unusual price hike posed an adverse effect on synthetic adhesive technology. In such a restrictive situation, the replacement of the petrochemical-based adhesive materials by adhesives based on renewable resources become a necessity. Proteins, natural rubber and polysaccharides, especially starch, natural gums and cellulose, are all renewable polymers that have been used as adhesives in the past (Heinrich, 2019).

2.9. Bio-Adhesive Polysaccharides

An elaborate type of carbohydrate derivative known as a polysaccharide contains chains of mono saccharide subunits linked together by an intermediate connection (Gopinath et al., 2018). Many types of composites have lately been created using polysaccharide biopolymer materials, which are abundant in nature and have great structural qualities (Bealer et al., 2020). Their prevalence is documented in a good manner in all organisms, viz. animals, plants, fungi, and bacteria. The fundamental structural features of polysaccharides showing adhesive behavior specially contain excessive molecular weight and polar functional groups.

The polysaccharides with polar and hydrogen bonding functional groups, ethers, hydroxyls, and carboxylates, shows a higher adhesion to wood and metals that are large surface strength adhered. The hydroxyl and carboxylate groups additionally used as possible sites for chemical change and cross-linking with the purpose to enhance adhesive behaviour. These groups also upkeep noncovalent inter and intra-chain interactions and promote adhesion. Note that the large molecular weight of those macromolecules increases their mechanical strength. The best known

polysaccharides for adhesive development are starch, chitosan, pullulan, gum acacia (or known as Gum Arabic), and some bacterial exopolysaccharides (Gopinath et al., 2018).

2.10. Gum Acacia

A complex polysaccharide exudate generated from the stem and branches of acacia trees is called gum acacia (GA), and it is organic, biocompatible, and biodegradable. There are greater than one thousand species of the gum acacia (T. H. Musa et al., 2021). However, from those species, only the acacia senegal and acacia seyal are used for products that can be used for marketable purposes (H. H. Musa et al., 2019). Due to its low tannin content, Acacia sensgal offers the highest level of satisfaction, and its gum contains a variety of GA market products (T. H. Musa et al., 2021). Due to their ability to produce gels and stabilizing qualities, natural gums are being employed more and more in a variety of technological domains. Acacia gum is the most well-known and widely utilized natural gum in the world, being employed both domestically and abroad during the manufacturing process. It can be used for a wide range of applications (Gafar & Abdel-Kader, 2020). It can be used as filler with a few changes in its structural behavior for reducing the gas and moisture movement thru the films. The gas and moisture movement system is described using permeability, diffusion, and solubility coefficients. As it becomes hydrophobic after some modification (Katiyar & Tripathi, 2019), it is used to reduce (decrease) the release kinetics of nutrients.

Table 2.5. Applications of gum acacia

No.	Applications area	Reference
1	❖ As binder in water color paint, photography, production of emulsion house paint, formulation of paracetamol tablets and so on.	❖ (Qi et al., 2019) ❖ (Kora, 2021) ❖ (Abdelrahman et al., 2021)
2	➢ As stabilizer, emulsifier and thickening agent in foods.	➢ (Sulieman, 2018) ➢ (Barak et al., 2020) ➢ (Salarbashi et al., 2021)
3	❖ As crystallization inhibitor to restrict crystallization of sugar	❖ (Chezanoglou & Goula, 2021)

4	➢ As a composting and blending (mixed with other polymers or materials to form a blend or composite)	➢ (Kalita et al., 2021) ➢ (Amalraj et al., 2020)
5	❖ In preparing nanoscale formulations or in microencapsulation of substances (either in gel, powder, or liquid forms)	❖ (Razavi et al., 2021) ❖ (Reque & Brandelli, 2021) ❖ (McClements & Öztürk, 2021)

2.10.1 Physio-Chemical Properties of Gum Acacia

When fresh, gum acacia is an amber-colored, amorphous, highly viscous substance that becomes solid upon contact with the atmosphere. Depending on the variety of acacia trees, it can also be a light shade of red, yellow, or brown. It is non-toxic, tasteless and odorless, soluble in water, and produces a homogeneous colloidal and colorless system. Only in harsh conditions do acacia plants yield gum (i.e., lack of moisture, poor nutrition, and high temperatures (Mohammed, 2017).

Figure 2.6. Raw gum acacia

Gum acacia is a complex mixture of polysaccharides and glycoproteins with a large molecular weight (350–850 kDa) and contains minerals (such as potassium, magnesium, and calcium) in addition to galactose (44%), rhamnose (13%), glucuronic acid (16%), and arabinose (27%) residues (T. H. Musa et al., 2021). Additional gum Arabic physical characteristics that have been found as quality indicators include moisture, total ash, volatile matter, and internal energy. Gum acacia is a complex blend of hydrophilic carbohydrate and hydrophobic protein components, and

the critical amounts of foreign matter, acid insoluble matter, salts of calcium, potassium, and magnesium are determined by the total ash content (Mohammed, 2017).

Table 2.6. International specifications of quality parameters of gum acacia Property Range (Mohammed, 2017)

Properties	Values
Ash Content	(2-4)%
Moisture Content	(13-15)%
Internal energy	(30-39)%
Volatile matter	(51-65)%
Nitrogen content	(0.26-0.39)%

Gum Acacia physicochemical responses can be handled depending on the balance of hydrophilic and hydrophobic interactions. Gum acacia functional properties are closely related to its structure, for example its solubility, viscosity, degree of interaction with water and oil in an emulsion, microencapsulation ability depends on its structure (Mohammed, 2017).

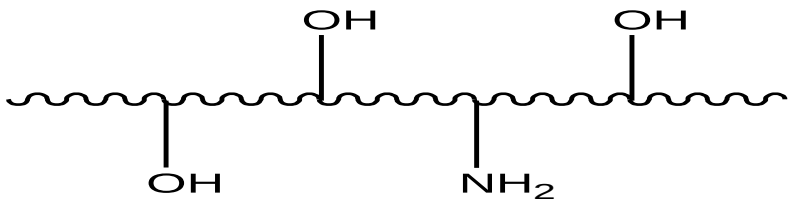

Figure 2.7. Molecular structure for Gum acacia

2.11. Lactic Acid

The organic acid lactic acid, sometimes known as "milk acid," has the chemical formula of: $CH_3CH(OH)COOH$. 2-hydroxypropanoic acid is the official name given by the International Union of Pure and Applied Chemistry (IUPAC). It has a carboxylic acid and hydroxyl functional group in its - hydroxyl acid. Lactic acid (LA) is a chemical building block that can be produced biotechnologically from agricultural waste, byproducts, and residues and used to make more LA polymers that are biodegradable and biocompatible (Castillo Martinez et al., 2013).

It is a crucial component of the bio-renewable economy. It has a wide range of applications in food, pharmaceutical, cosmetics, and chemical industries, it is currently the most extensively used organic acid. It can be used as neutralizers, solvents, and cleaning agents employed to make biodegradable polymers with medicinal applications (Komesu et al., 2017). Polymers of lactic acids are biodegradable and their degradation can be controlled by adjusting the composition, and the molecular weight, as a result they are used for a control drug or nutrient releases.

2.11.1. Physio-Chemical Properties of Lactic Acid

Lactic acid (2-hydroxypropanoic acid) is an organic acid widely distributed in nature. The monomer, lactic acid (LA), is the smallest optical active organic compound found in nature. Due to the presence of a chiral carbon, LA occurs in the two optical isomers, L (+) and D (-) (Castillo Martinez et al., 2013), as shown in Figure 2.8 below. The chemical performances of lactic acid depends on its physio chemical properties such as its acidic behavior in aqueous medium, and bi-functional reactivity related to the presence of a carboxyl and a hydroxyl group, which offers it awesome reaction versatility (Castillo Martinez et al., 2013).

Isomer D (-) Isomer L (+)

Figure 2. 8. Molecular Structure of D (-) and L (+) isomers of the lactic acid

Table 2.7. Physiochemical properties of lactic acid (Ameen, 2017)

Properties	Description
Empirical Formula	$C_3H_60_3$
Chemical Name	2-hydroxypropanoic acid
Compound name	Lactic Acid
Taste	Mild Acid Taste
Dissociation Constant, Ka	1.38×10^{-4}

Molecular weight	90.08 g/mol
Boiling Point	122^0C
Melting point	17 ^{0}C
Specific gravity	1.2
Appearance	Colorless and syrupy liquid

2.12. Oligomers

In contrast to polymers, which can theoretically include an endless number of monomers, oligomers are molecular complexes of molecules that only contain a small number of repeating units. For example, the oligomers dimers, trimers, and termers are made up of two, three, and four monomers, respectively (Schneider et al., 2018). Oligomerization is the process of transforming a monomer or a combination of monomers into an oligomer. An oligomerization by chain reaction is carried out in the presence of a large amount chain-transfer agent, so that the end groups are essentially fragments of the chain-transfer agent, is termed in to oligomerization (Ambrosio-Martín et al., 2015). Lactic acid oligomers are formed from lactic acid, a renewable material produced by fermentation of sucrose or glucose. Lactic acid-based oligomers are totally natural and fit nicely within the parameters of green chemistry due to their synthesis process and origin. In the case of lactic acid, since the molecule is bi-functional (i.e. a hydroxyl acid), it will be the only reagent of the poly-condensation. The poly-condensation reaction of lactic acid leads to linear chains of oligomers with an average molecular weight that depends on the process conditions. Lactic acid oligomers are currently used in the following added value domains, polymerization or copolymerization of new and existing polymers; replacement of waxes, oils, and oligomers already used in the formulation domain; and synthesis of graft copolymer for various applications.

2.13. Poly (Lactic acid) Graft Copolymers

In order to obtain desirable physical, chemical, and biological qualities, polysaccharides have undergone significant modifications. There are numerous techniques to modify polysaccharides, including grafting polymeric chains, derivatization of functional groups, etherification, hydrolytic breakdown and oxidative degradation (Tripathi & Katiyar, 2018). Grafting is one of the promising methods for polymer modification that has recently attracted by a lot of researcher's interest. The investigation of poly (lactic acid)-based graft copolymers for their applications in many fields has undoubtedly received more interest in recent years. These graft copolymers have undergone

extensive analysis using a variety of monomers and polymers, such as chitosan, cellulose, gum acacia, starch, polyethylene glycol, vinyl-based polymers, lignin, dextran, methyl methacrylate, maleic anhydride, and graphene oxide the backbones has connected to its polymeric sideway chains (the grafts) of various chemical nature, mostly distributed randomly (Maharana et al., 2015).

CHAPTER THREE

3. MATERIALS AND METHODS

3.1. Materials and chemicals

Materials/ Equipment's

For the synthesis and characterization of lactic acid oligomer grafted gum acacia (LAO-g-GA) as well as to encapsulate urea into a LAO-g-GA, and to analyze its physiochemical properties different materials/ equipment's such as, analytical balance, water bath, pH meter, spatula, boll mill, hot plat, sieve, measuring cylinder, beaker, fine mesh cloth, copper wire, temperature controlled reactor/oven, and mixer were used. And instruments such as FTIR, NMR, ABBE Digital Refractometer, and Automatic Kjeldhal Analyzer were also used for analysis purposes.

Chemicals

Commercial urea granule (1-4 mm in size) with nitrogen content of around 46% was obtained from governmental fertilizer distributers, Ethiopia. The reagents which were used to synthesis a lactic acid oligomer grafted gum acacia (i.e., degradable monomer (lactic acid) with 88% quality and gum Arabic) were purchased from a local market, other chemicals such as sodium phosphate dibasic, sodium bicarbonate, sodium carbonate, citric acid and solvents such as chloroform and deionized water was used from the laboratory.

3.2. Methods

3.2.1. Experimental Design for Synthesizing a bio-based adhesive

Design Expert® version 11.1.0.1 software was used for randomized design of the experiment, and analysis of variance (ANOVA) was used to study the statistical significance of the experimental data's. In the experimental design, 3 factors (i.e. reaction temperature, reaction time and GA to LA mixing ratio) with 2 levels were selected to study their effects on the grafting efficiency of synthesized bio-based adhesive (Lactic acid oligomer grafted gum acacia) itself and on the percent of urea release rate in water after the same amount of urea powder (75%) was encapsulated in each synthesized lactic acid oligomer grafted gum acacia. The levels of each factor are tabulated in the following Table 3.1, below, and the levels of factors were valued based on the preliminary experiment results, illustrated in Appendix-1.

Table 3.1. Levels for each factor.

S.No	Factor	Unit	Level	
			Low	High
1	Reaction temperature	^{0}C	165	195
2	GA to LA Mixing ratio	w/w%	8.3	12.5
3	Reaction time	hrs.	1.5	2.5

3.2.2. Synthesis of Lactic Acid Oligomer Grafted Gum Acacia (LAO-g-GA)

During the synthesis of a bio-based adhesive (LAO-g-GA), a desired amount of lactic acid and gum acacia (according to design experiment) was initially taken into reactor vessel (beaker) and mixed using spoon. The vessel containing a mixture of lactic acid and gum acacia was introduced into a temperature controlled reactor/oven by adjusting reaction time and reaction temperature on a fixed value, then poly-condensation reaction was conducted through convectional heating system. Accordingly, LAO-g-GA was synthesized after the completion of the reaction. The experiment run was repeated by varying the values of those factors to do a desired number of experiments. Finally, the synthesized LAO-g-GAs were kept for further characterization.

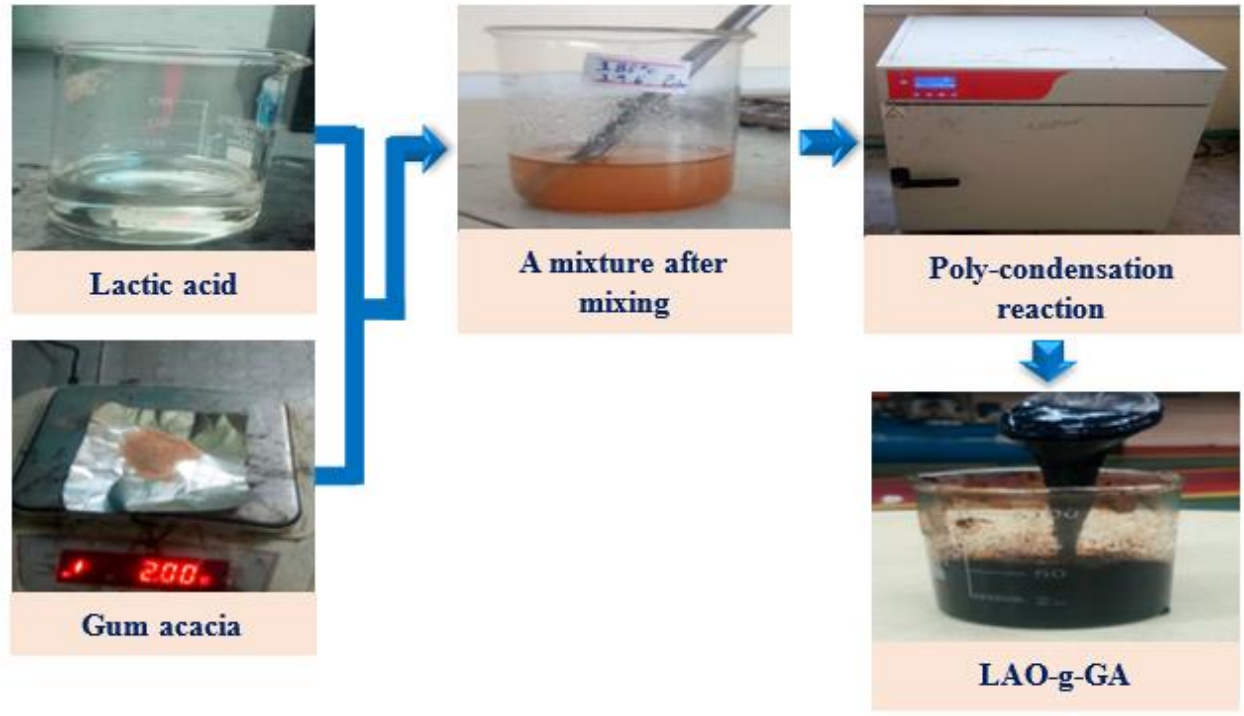

Figure 3.1. Poly-condensation reaction process to synthesis LAO-g-GA copolymer

3.2.3. Synthesis of Lactic Acid Oligomers (LAO)

Lactic acid oligomer (LAO) was synthesized by a poly-condensation reaction. Oligomerization of lactic acid through poly-condensation was performed using a convectional heating system in the absence of any catalyst simply by removing water from 88wt% aqueous solution of LA at temperatures of 165 ^{0}C for 2.5hrs.

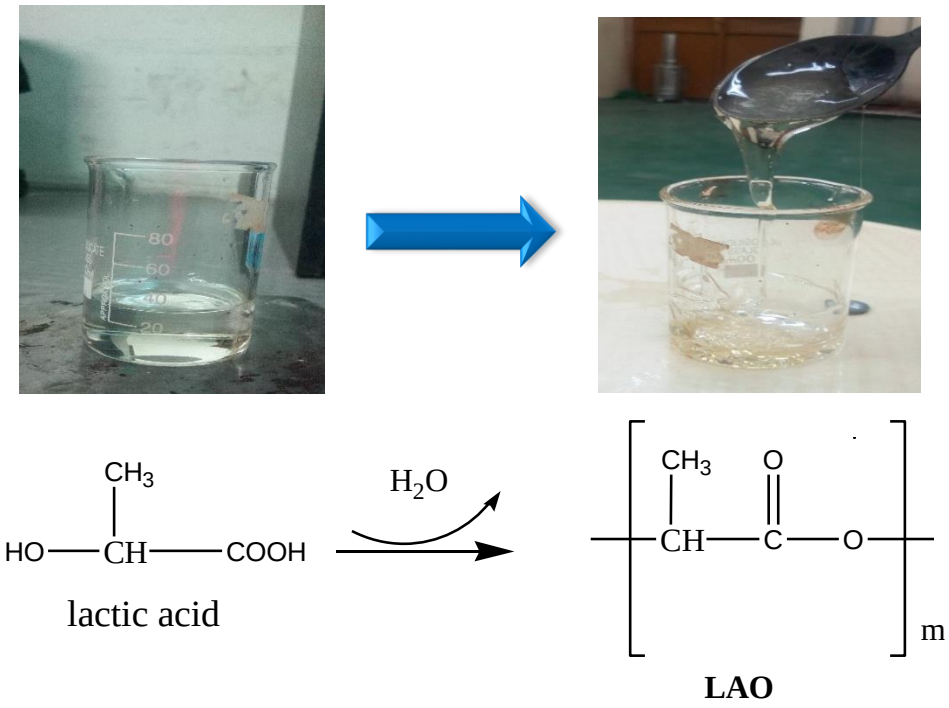

Figure 3.2. Production scheme of LAO

3.3. Characterization of Synthesized Bio-Adhesive

3.3.1. Solubility and Grafting Efficiency

The solubility of a LAO-g-GA was evaluated by dissolving it into chloroform with the concentration of 20 mg/ml at 25 °C and the solutions were shaken for 10 minutes by using shaker (Tripathi & Katiyar, 2018) as shown in the Figure 3.3 below. The solutions were filtered and then the residual weight was calculated by subtracting the initial weight of the filter paper from a measured weight of a filter paper with dried residue. And in the experimental determination of the grafting efficiency of each synthesized LAO-g-GAs, firstly the weights of raw materials before they undergo a chemical reaction and the weight of grafted copolymer (after poly-condensation reaction) were measured separately using analytical balance. Finally, the grafting efficiency and

percentage solubility of a bio adhesive was determined using the following equations (Tripathi & Katiyar, 2018).

$$\text{Grafting efficiency(GE\%)} = \frac{W1 - W0}{W2} * 100 \ldots\ldots\ldots\ldots\ldots\ldots (1)$$

$$\text{Percentage solubility (SP\%)} = \frac{W4 - W3}{W4} * 100 \ldots\ldots\ldots\ldots\ldots\ldots\ldots . (2)$$

Where, W_0: weight of neat gum; W_1: total weight of synthesized grafted copolymer; W_2: weight of lactic acid; W_3: weight of residue remains on the filter paper; W_4: total weight of grafted copolymer dissolved in a chloroform.

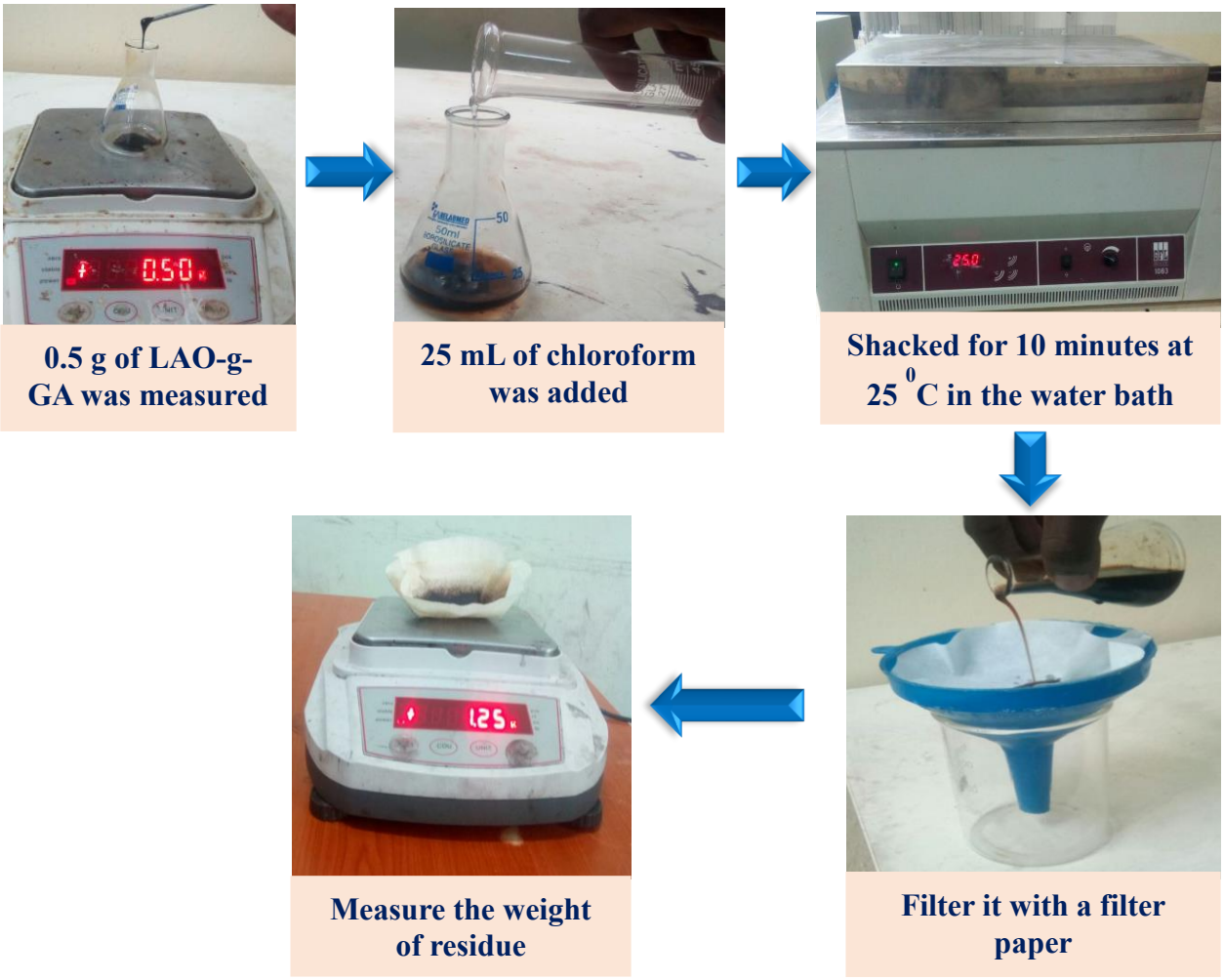

Figure 3.3. Solubility testing procedure for a synthesized LAO-g-GA

3.3.2. Contact Angle Measurement

The contact angle produced between the water droplet and the LAO-g-GA that comes into contact is usually used to explain the surface hydrophobicity behavior of LAO-g-GA. Contact angle measurement was simply carried out by adapting the method listed in Le & Nguyen, (2020). The synthesized LAO-g-GA was sprayed on a clean dry glass slide (2.5 x 10 cm). The glass sheet was dried for 3hrs at room temperature. A drop of water was then drop on the surface of the glass sheet, the drop image was photographed, and the contact angle of the water drop was measured using image-j software application.

3.3.3. FTIR and NMR Analysis for the Synthesized LAO-g-GA

FTIR analysis: The existence of the expected functional groups and the grafting of LAO on the backbone of GA were further confirmed by using FTIR spectroscopic machine. The attenuated total reflectance FTIR with model name of FTIR-6600 type A and serial number A013861790 in the range of 4000 to 400 cm^{-1} was used.

NMR Analysis: The idealized chemical structure and the grafting of LAO on the GA backbone was also analyzed by ^{1}H NMR characterization. Before the analysis, the samples were dissolved in deuterated chloroform ($CDCl_3$), filtered with a 0.25μm filter, and transferred to 5 mm diameter NMR tube.

3.4. Encapsulation of Urea into a Synthesized LAO-g-GA

Commercial urea granule 1-4 mm in size was firstly grinded using ball mill grinder at 350 rpm for 15 minutes, and sieved to obtain a powder with a size of about 35 mesh sieve as shown in Figure 3.4 below. Urea encapsulated lactic acid oligomer grafted gum acacia (U-e-LAO-g-GA) was then formulated by dispersing urea powder into a LAO-g-GA synthesized according to method 3.2.2 above. There was a continuous mixing for about 10 minutes at a temperature of 50 ^{0}C to disperse it uniformly. The mixing temperature was selected from the preliminary experiment. The heated semisolid mixture was then pelletized using a palletizing machine. Finally, the U-e-LAO-g-GAs were prepared for final product characterization. The overall process to formulate a U-e-LAO-g-GA is shown in the Figure 3.5 below.

Figure 3.4. Urea powder preparation

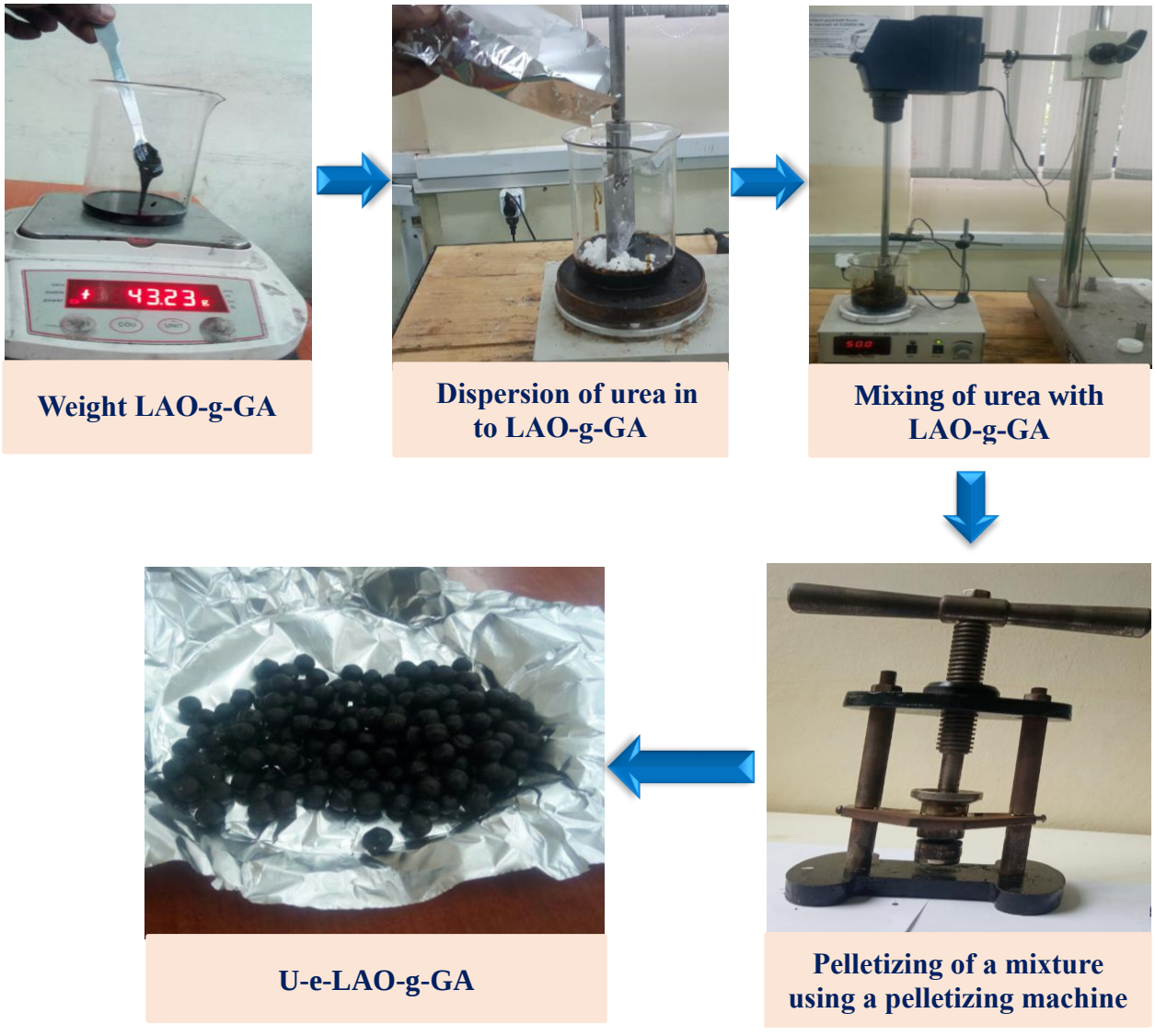

Figure 3.5. Overall process for the formulation of U-e-LAO-g-GA

3.5. Characterization of U-e-LAO-g-GA

3.5.1. Effect of LAO-g-GA Synthesizing Factors on the Urea Release Rate

The urea release rate from the U-e-LAO-g-GA**s** was performed in a deionized water. In order to investigate the effect LAO-g-GA synthesizing factors (i.e. reaction time, reaction temperature and gum acacia to lactic acid mixing ratio) on the urea release rate, 10 grams of each U-e-LAO-g-GA**s** that have the same amount of urea concentration (75 % urea) were placed in a fine mesh cloth bags and immersed into 100 mL of distilled water in a glass beaker, properly covered at room temperature. The bags were attached to a copper wire. After 3hrs of incubation, the samples were carefully taken out using the pre-attached copper wire and the solutions were shacked very well. Then by taking 20 mL solution from each beaker, the refractive index of each sample was measured using ABBE Digital Automatic Refractometer (Affendi et al., 2020; Jintakanon et al., 2008; Taha et al., 2016; L. Zhang et al., 2022). The amount of urea released into a deionized water from each U-e-LAO-g-GA was then determined using the standard calibration curve (a correlation between refractive index and concentration of pure urea), illustrated in Appendix-3. This was done in duplicate for each individual sample. After calculating the concentration of urea released into a deionized water using the standard calibration curve, the percent of urea released was finally calculated using the equation (3) below (Silva et al., 2021).

$$\text{Urea released } (\%) = \frac{Mn}{M} * 100\% \text{.....(3)}$$

Where Mn is the concentration of urea released within a given time interval (i.e. after 3hrs of incubation for this test) of the experiment and M is the final concentration released in the experiment.

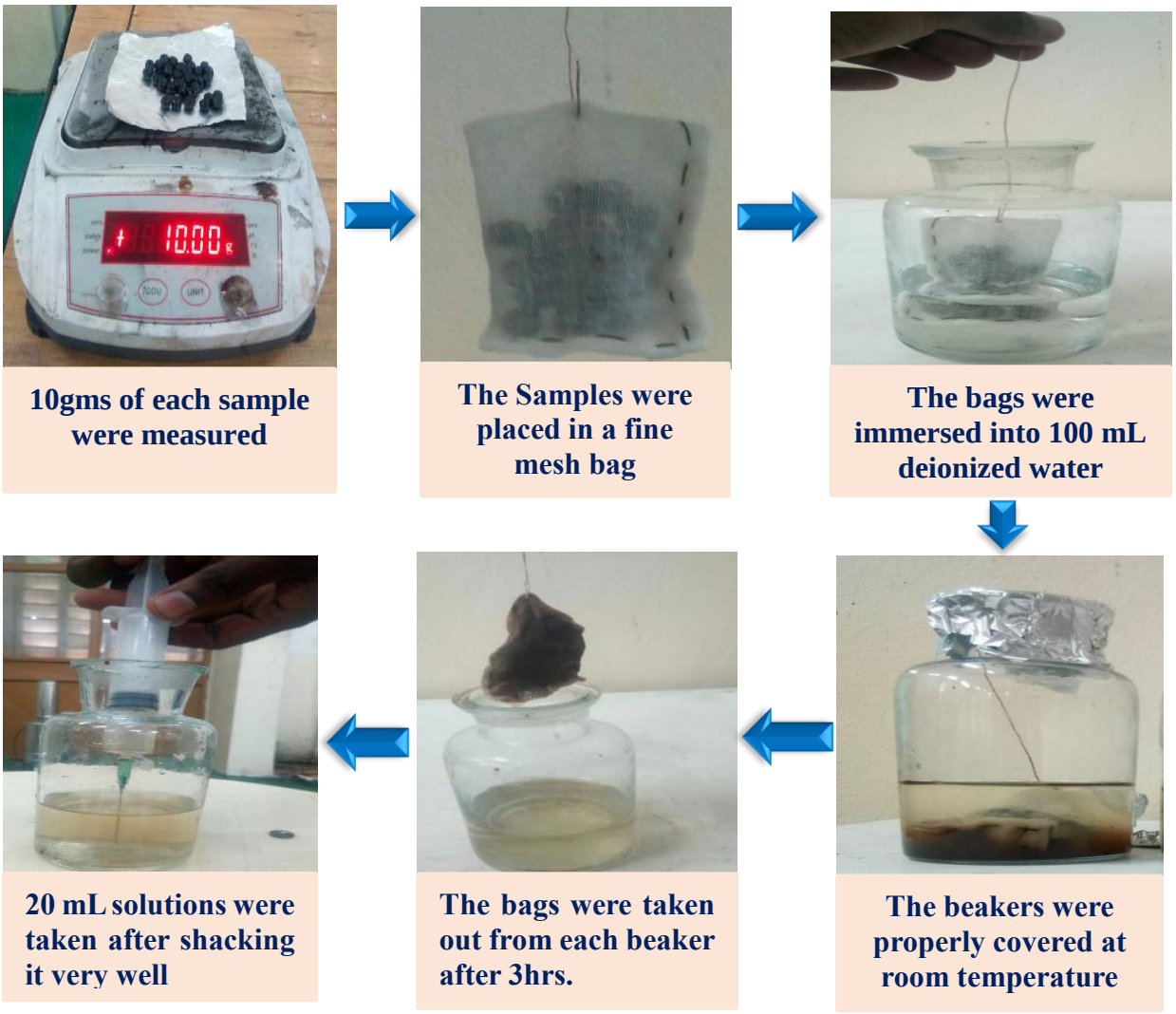

Figure 3.6. The process of preparing solutions to measure its refractive index

3.5.2. Effect of pH, Temperature, and Urea Concentration on the Urea Release Rate

The effect of pH, temperature, and urea concentration on urea release rate was determined by varying the values of those parameters on the three selected U-e-LAO-g-GAs, which were selected from the urea release rate results of method 3.5.1, based on their release rate quality (i.e. highly released, medium released, and low released) after 3hrs incubation in a deionized water. The urea release rate determination process is similar to method 3.5.1. In order to evaluate the effect of temperature on the urea release rate, the glass beakers that contain 100 mL deionized water were placed at different temperature conditions (i.e., 25 ^{0}C, 35 ^{0}C, and 45 ^{0}C) in the water bath. The three selected U-e-LAO-g-GAs (10 g for each) that have the same amount of urea concentration (75%) were placed into a fine mesh cloth bags, and immersed into the glass beakers separately and

properly covered. The cloth bags that contain the samples were then taken out from the glass beakers at a certain time interval (i.e., at 1, 3, 5, 7, 9, 11, 13, 15, 17, 19, 21, and 23hrs) using the pre-attached copper wire and the solutions in each individual beaker were shacked very well. Finally, by taking 20 mL of solutions from each beaker, the refractive index was measured using ABBE Digital Automatic Refractometer. Then the amount of urea released into a deionized water from each sample at different time interval was calculated using the standard calibration curve equation and the urea release rate from each sample was then calculated using equation (3), above. And the effect of pH on the urea release rate determination process was similar to the temperature effect evaluation process except instead of using a deionized water as a medium, it uses three different buffer solutions (i.e. pH 4, pH 7, and pH 10) and it was conducted at room temperature. And the time of incubation in which the samples were taken out extends with 2hrs interval until the high released sample reach's its equilibrium condition (29hrs) (i.e., at 1, 3, 5, 7, 9, 11, 13, 15, 17, 19, 21, 23, 25, 27, and 29hrs). Likewise, the effect of urea concentration on the urea release rate of these synthesized U-e-LAO-g-GAs was determined by varying only the amount of urea encapsulated in each of the three selected LAO-g-GAs (i.e. 70%, 75% and 80% urea concentration) at a medium of pH 7 and at room temperature. Here, the time of incubation in which the samples were taken out extends up to 25hrs (the high released sample reaches equilibrium) (i.e., at 1, 3, 5, 7, 9, 11, 13, 15, 17, 19, 21, 23 and 25hrs). All the experiments were done in duplicate and the average values were taken.

3.5.2.1. Preparation of Buffer Solutions

During the effect of pH on the urea release rate determination process, three buffer solutions at pH 4, 7, and 10 were prepared according to Dórame-Miranda et al., (2018), pH 4 solution was prepared by mixing 395 mL of 0.2 M sodium phosphate dibasic and 615 mL of 0.1 M citric acid within 2 L of deionized water. pH 7 solution was prepared by mixing 872 mL of 0.2 M sodium phosphate dibasic and 130 mL of 0.1 M citric acid within 2 L of deionized water. And buffer solution pH 10 was prepared by mixing 50 mL of 0.1 M sodium bicarbonate and 50 mL of 0.1 M sodium carbonate within 2.25 L of deionized water.

3.5.3. Urea Release Rate Test in Soil

The urea release rate test in soil was carried out according to Xiaoyu et al., (2013) by burying a U-e-LAO-g-GA in soil at room temperature. To conduct the urea release rate in the soil, plastic bottles, which have a hole with the same size at the bottom were prepared for each of the three selected U-e-LAO-g-GAs and for a pure urea. Each individual plastic bottles were filled with a cleaned sand up to 10 cm depth, and in order to reduce the entry of soil into the leachate, a fine mesh cloth was placed over the sand before 400 g soil having 20% moisture content was poured over. 10 g of each U-e-LAO-g-GA (each contain 75% urea concentration) and 7.5 g of pure urea were placed in the fine mesh cloth bags separately and then buried in the prepared plastic bottles 5 cm under soil. At different time intervals of incubation (i.e., at 1, 5, 10, 15, 20, 25, and 30 days), 200 mL of deionized water was poured slowly over the prepared bottles and the leachate was collected at the bottom of each plastic bottles. The percent of urea released in each incubation time was then determined by measuring the refractive index of leachates using ABBE Digital Automatic Refractometer and then the urea release rate (%) was calculated using equation (3) above.

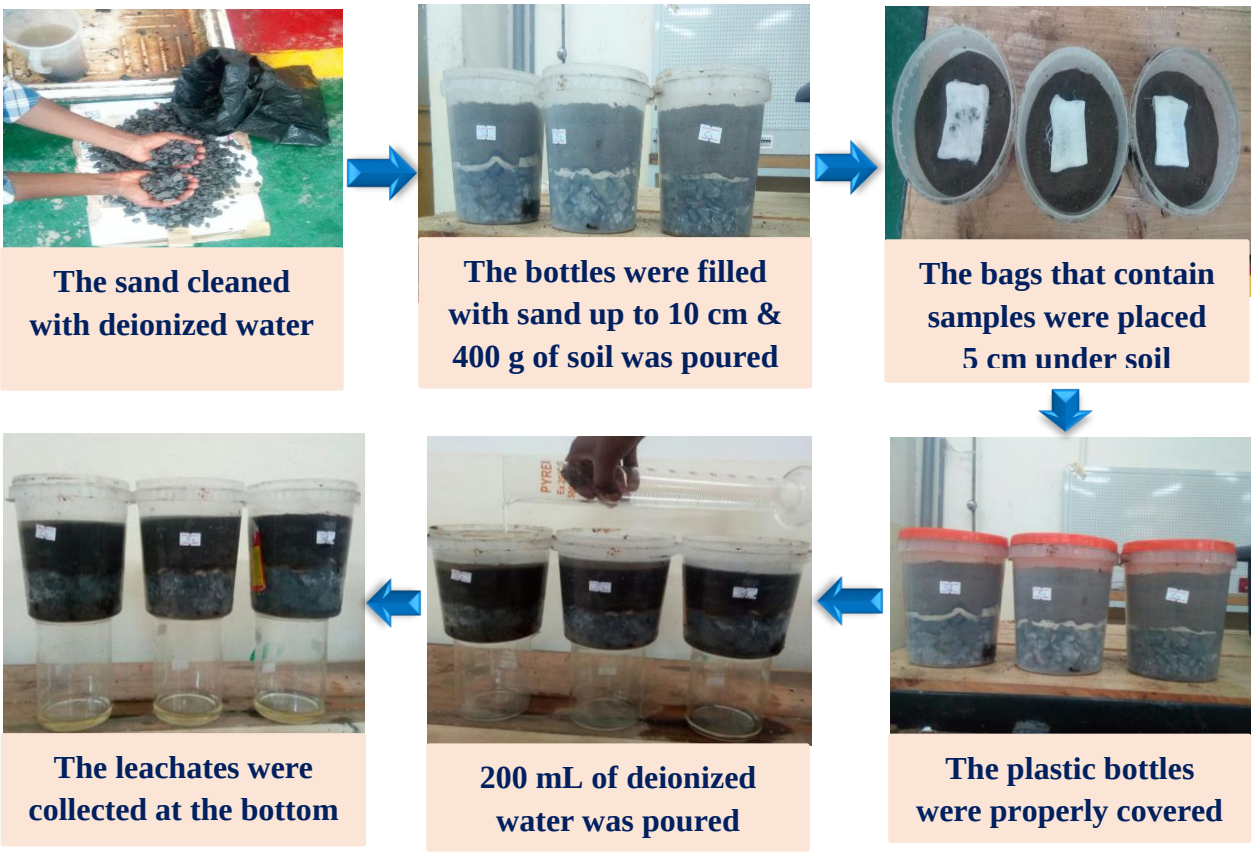

Figure 3.7. Experimental procedure to detrmine urea release rate of samples in soil

3.5.4. Soil Degradation Rate Test

In order to study the biodegradability of a U-e-LAO-g-GA, soil degradation test of the three selected U-e-LAO-g-GAs relative to commercial urea fertilizer was carried out. For each U-e-LAO-g-GA and commercial urea fertilizer, an individual plastic bottle was prepared and filled with 400 g soil. During the incubation, the soil moisture was maintained 20%. To conduct the experiment, 2 g of each U-e-LAO-g-GAs and commercial urea fertilizer were placed in the fine mesh cloth bags (5 x 6 cm size) to prevent loss of samples and then buried 5 cm under the soil surface contained in a plastic bottles. The soil degradation test was studied for 25 days of incubation in soil by recording the weight loss from each U-e-LAO-g-GAs and commercial urea fertilizer. At every certain time interval (1, 3, 5, 7, 9, 11,13 ,15, 17, 19, 21, 23 and 25 days), the samples were dug out, cleaned, and dried for 2hrs at room temperature. Then the dried samples were weighed, and their percentage of degradation were determined by using the equation (4) below (Llive et al., 2020). The experiment was replicated twice and the average value was taken.

$$\text{Degradation}(\%) = \frac{(W1-W2)}{W1} * 100 \ldots\ldots\ldots\ldots\ldots\ldots\ldots\ldots (4)$$

Where, W_1 and W_2 are the weights (g) of the dried samples before and after the soil burial, respectively.

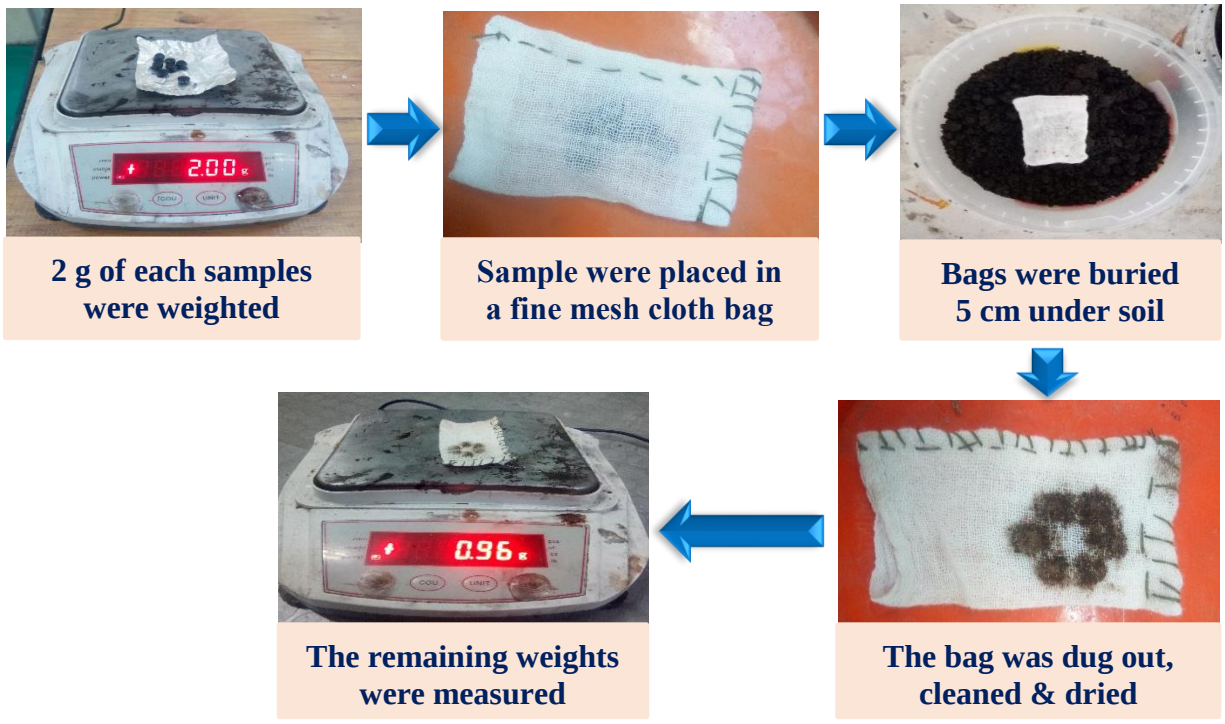

Figure 3.8. Soil degradation test process of U-e-LAO-g-GAs and commercial urea

3.5.5. Studding the Nitrogen Release Rate and Its Release Kinetics Behavior

The experimental procedure done for preparing a solution to determine the nitrogen release rate in water was similar to the urea release rate determination procedure discussed in 3.5.1 above. U-e-LAO-g-GAs (10 g from each sample) that have the same urea concentration (75% urea) were placed in a fine mesh cloth bags attached to a copper wire and completely immersed into 100 mL of pH 7 aqueous medium in glass beakers separately and properly covered at room temperature. Then at different time intervals (i.e., at 1, 2, 3, 4, 5, 10, 15, 20, and 25hrs) the cloth bags which contains samples were taken out using the attached copper wire and the solution were shacked very well. Finally,10 mL solution were taken from each sample and the total nitrogen content was determined by using Kjeldahl method (Zhao et al., 2021). The experiment was done in duplicate. The total nitrogen release rate from each individual sample at different time interval was then calculated using the equation (5) below (Ding et al., 2016).

$$\text{Nitrogen release rate (\%)} = \frac{C*V}{M} * 100\% \text{.....(5)}$$

Where C is concentration of nitrogen in leachate (g/mL) obtained from Kjeldahl method, V is the leachate volume in each sampling (mL), and M is total nitrogen present in a fertilizer (g).

And the release kinetics behavior of those U-e-LAO-g-GAs were evaluated using the following four different model equations (Adebayo et al., 2021).

a. Korsmeyer-Peppas

$$\frac{Mt}{M\infty} = K_i t^n \text{……...……(6)}$$

Where K_i**,** t, and n are diffusion content, time and diffusion exponent indicative of the release mechanism respectively**.** Mt/M∞ is the fraction of urea released at time t. The n value is used to characterize different release mechanisms.

b. Higuchi kinetic model

$$Qt = K_H t^{1/2} \text{…….. (7)}$$

c. Zero order kinetic model

$$Qt = K_o t \text{ ……...……. (8)}$$

d. First order model

$$Qt = Q_o e^{-kt} \ldots\ldots\ldots\ldots\ldots\ldots\ldots\ldots\ldots\ldots\ldots\ldots (9)$$

Where Qt is the amount of nutrient release at time t, Qo**,** is the amount of nutrient initially in the formulated fertilizer, t is the time, K_H is the Higuchi dissolution constant, Ko and K is the zero order and first order release constant respectively**.**

CHAPTER FOUR

4. RESULT AND DISCUSSIONS

The features of LAO-g-GA, from which U-e-LAO-g-GA was synthesized for a controlled dissolution rate, greatly affects the physiochemical characteristics of the synthesized U-e-LAO-g-GA. Therefore, it is better to examine the fundamental properties of LAO-g-GA before studying directly the characteristics of U-e-LAO-g-GA, especially those features which are directly related to the target of its application (i.e., controlling the urea release rate) such as the grafting efficiency, solubility, and hydrophobicity of LAO-g-GA. In this chapter, the effect of different LAO-g-GA synthesizing factors (i.e., reaction temperature, reaction time & GA to LA mixing ratio) on its grafting efficiency, and on the urea release rate after urea encapsulation was discussed in detail. And the effect of grafting efficiency on its solubility and hydrophobicity was also briefly conferred, which was a great input to control the dissolution rate of the final product (U-e-LAO-g-GA). The effect of different parameters such as pH, temperature and urea concentration on the urea release rate of a U-e-LAO-g-GA and other supporting characteristics such as FTIR and NMR analysis's of a LAO-g-GA, urea release rate in soil, soil degradation rate test, the effect of urea concentration on its degradation rate, total nitrogen release rate in water and its release kinetics behaviour tests of a U-e-LAO-g-GA were also discussed in detail.

4.1. Characterization of a Bio Adhesive

4.1.1. The Reaction Mechanism During the Synthesis of LAO- g-GA

During the synthesize of LAO-g-GA copolymer, when a mixture of LA and GA was placed in an oven at a certain temperature, a poly-condensation reaction process was performed through convectional heating system. During the poly-condensation reaction, the heating system causes to remove the small polar molecules of water and free radicals were generated on the functional groups of the polysaccharide GA backbone as well as on the LAO functional groups. LAO was grafted on the backbone of GA i.e., the LAO was attached and added up on the produced free radical active sits of GA backbone. The free amino groups which causes to take place a reaction with the reducing end groups of LAO molecules was functional groups in proteins of GA (Tripathi, 2016). Schematic representation for the synthesis of LAO-g-GA copolymer was given in Figure 4.1 below.

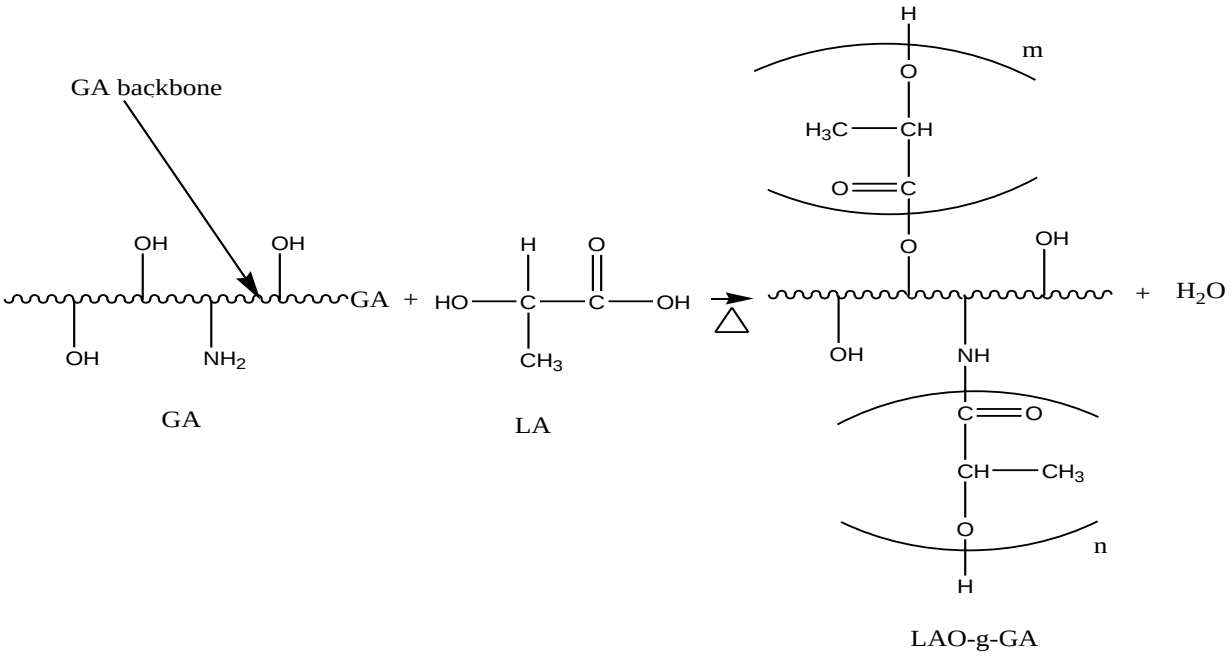

Figure 4.1. Schematic representation for the synthesis of LAO-g-GA copolymer

The expected interactions between lactic acid oligomers (LAO) and GA, the grafting of LAO on the backbone GA to form LAO-g-GA was confirmed by doing the FTIR and NMR analysis. However, since it is difficult and time consuming to conduct the FTIR and NMR analysis and other physiochemical characterizations of all synthesized LAO-g-GAs, firstly, it is better to evaluate the statistical analysis for the experimental design results to select LAO-g-GAs for further characterizations.

4.1.2. Statistical Analysis for Experimental Design Results

The Design Expert 11.1.0.1 program was used with box Behnken method having 17 runs in the regression analysis and analysis of variance (ANOVA). The statistical software program analysis was done in order to identify the interaction effects of independent variables on the grafting efficiency of LAO-g-GA, and on its urea release rate after urea encapsulation. And also, it was used to identify the relationship between the two responses (i.e., grafting efficiency and urea release rate). The model equations, which was used to identify the relative impacts of each factor on the responses was also generated from the statistical software program.

Most plants need the essential nutrient nitrogen throughout their lives, and also nitrogen demand usually increases as plant size increases. Therefore, since different crops have different lifetime, different plants need the essential nutrient (N) from urea for different length of time. And since

different plants have different size, the amount nitrogen required for their growth differs from plant to plant although they have the same lifetime. There is also a differences among species and within genotypes of species in their abilities to absorb and utilize available N from soil in soil plant systems (Olson & Kurtz, 2015). As a result, controlling the dissolution rate of urea in water is very important to deliver the essential nutrient nitrogen properly to the plants. Here in the U-e-LAO-g-GA, the control system was done by controlling the grafting efficiency of LAO on the backbone of GA as shown in the schematic representation of Figure 4.2 above.

The Box-Behnken design in the response surface optimization method along with grafting efficiency (%) and urea release rate (%) as response variable is given in Table 4.1 below. The influence of grafting efficiency of LAO-g-GA on the urea release rate of U-e-LAO-g-GA was clearly illustrated in the Table 4.1, i.e., as the grafting efficiency of LAO-g-GA increase the percent of urea released from U-e-LAO-g-GA decreases. This is due the fact that the increased in grafting efficiency implies a large number of polar hydrophilic GAs were replaced by a hydrophobic ester groups of LAO, causes to enhance the hydrophobicity of LAO-g-GAs (Tripathi, 2016). As result, when the hydrophobicity of LAO-g-GA increases its solubility in water decreases. And the water was expected to penetrate into the U-e-LAO-g-GA through the small gaps between LAO-g-GA molecular chains as well as through the LAO-g-GA surface, and the urea in a U-e-LAO-g-GA is released into deionized water. At high grafting efficiency, the gap between the molecular chains decreases and the surface strength of LAO-g-GA becomes comparable with the water pressure in the penetrating zone, as a result, the amount of water penetrated into the U-e-LAO-g-GA decreases, implies the urea released out from the U-e-LAO-g-GA decreases. However, at low grafting efficiency, the gap between the molecular chains increases and the surface strength of the LAO-g-GA becomes weaken, the water can enter through the gap as well as through its surface easily, consequently, the urea released from the U-e-LAO-g-GA increases (Niu & Li, 2012).

As shown in the Table 4.1, below, the highest grafting efficiency (66.12%, i.e., the average of 5 repeated experimental results), and the lowest urea release rate (15.3%, i.e., the average of 5 repeated experimental results) was achieved at 180 ^{0}C reaction temperature, 2hrs.' reaction time, and 10.4 w/w% of GA to LA mixing ratio. And the lowest grafting efficiency (41.5%) and the highest urea release rate (37.1%) was obtained at 165 ^{0}C reaction temperature, 2hrs.' reaction time, and 8.3 w/w% of GA to LA mixing ratio.

Table 4.1. Box Behnken arrangement and responses (i.e., grafting efficiency & urea release rate)

Std.	Run	Factors			Responses	
		Reaction Temperature (^{0}C)	Reaction time(hrs.)	GA to LA Mixing ratio(w/w%)	Grafting efficiency (%)	Urea released (%)
8	1	195	2	12.5	59.3	18.5
16	2	180	2	10.4	65.6	15.6
9	3	180	1.5	8.3	43.4	35.2
1	4	165	1.5	10.4	49.6	25.6
6	5	195	2	8.3	47.5	28.7
3	6	165	2.5	10.4	53.2	22.4
10	7	180	2.5	8.3	45.3	31.3
7	8	165	2	12.5	57.2	19.4
11	9	180	1.5	12.5	55.3	21.7
12	10	180	2.5	12.5	63.5	16.5
14	11	180	2	10.4	66.4	15.1
4	12	195	2.5	10.4	61.4	17.6
5	13	165	2	8.3	41.5	37.1
15	14	180	2	10.4	66.1	15.5
2	15	195	1.5	10.4	51	23.7
13	16	180	2	10.4	66.7	14.9
17	17	180	2	10.4	65.8	15.4

The grafting efficiency of LAO-g-GA can be controlled by controlling its synthesizing factors (i.e. reaction time, reaction temperature and GA to LA mixing ratio), and since the urea release rate is inversely proportional to the grafting efficiency, therefore, the release rate of urea from U-e-LAO-g-GA into a deionized water can be controlled properly by controlling simply the grafting efficiency of LAO on the backbone of GA.

The response surface optimization method is also used to establish a mathematical model, and the response surface quadratic polynomial regression simulation equation is obtained by multiple regression fitting on the test data's as follows:

$$R1 = 66.12 + 2.21A + 3.01B + 7.20C + 1.70AB - 0.975AC + 1.58BC – 6.41A^2 – 5.91B^2 – 8.33C^2 \ldots (9)$$

$$R2 = 15.3 – 2.00A – 2.30B – 7.03C – 0.725AB + 1.88AC - 0.325BC + 3.39A^2 + 3.64B^2 + 7.24C^2 \ldots (10)$$

Where, R1 and R2 are the grafting efficiency of a synthesized LAO-g-GAs, and present of urea released from the U-e-LAO-g-GAs after 3hrs of incubation in a distilled water, respectively. Whereas, A, B, and C are the corresponding coded variable levels of the reaction temperature, reaction time and GA to LA mixing ratio, respectively.

The above equations in terms of coded factors can be used to make predictions about the responses for given levels of each factor. The coded equations are useful for identifying the relative impact of the factors on the responses by comparing the factor coefficients. The signs of coefficients represent the positive and negative effects of each independent variable on the responses of the system.

4.1.3. Analysis of Variance

Statistical testing of the model was performed by the analysis of variance (ANOVA), which is used to identify the statistical significance of the experimental data's, and the results for the coded variable levels are shown in Table 4.2 below.

Table 4.2. Analysis of variance (ANOVA) for Grafting efficiency (%) and urea released (%)

A) ANOVA for response surface quadratic models of grafting efficiency (%)

Source	Sum of Squares	df	Mean Square	F-value	p-value	
Model	1234.10	9	137.12	251.57	< 0.0001	Significant
A-Reaction temperature	39.16	1	39.16	71.85	< 0.0001	
B-Reaction time	72.60	1	72.60	133.20	< 0.0001	
C-Mixing ratio	414.72	1	414.72	760.85	< 0.0001	
AB	11.56	1	11.56	21.21	0.0025	

AC	3.80	1	3.80	6.98	0.0334	
BC	9.92	1	9.92	18.20	0.0037	
A^2	173.00	1	173.00	317.39	< 0.0001	
B^2	147.07	1	147.07	269.81	< 0.0001	
C^2	292.51	1	292.51	536.65	< 0.0001	
Residual	3.82	7	0.5451			
Lack of Fit	3.03	3	1.01	5.12	0.0742	not significant
Pure Error	0.7880	4	0.1970			
Cor Total	1237.92	16				

B) ANOVA for response surface quadratic models of urea released (%)

Source	Sum of Squares	df	Mean Square	F-value	p-value	
Model	841.93	9	93.55	541.18	< 0.0001	Significant
A-Reaction temperature	32.00	1	32.00	185.12	< 0.0001	
B-Reaction time	42.32	1	42.32	244.83	< 0.0001	
C-Mixing ratio	394.81	1	394.81	2284.0	< 0.0001	
AB	2.10	1	2.10	12.16	0.0102	
AC	14.06	1	14.06	81.35	< 0.0001	
BC	0.4225	1	0.4225	2.44	0.1619	
A^2	48.32	1	48.32	279.52	< 0.0001	
B^2	55.71	1	55.71	322.30	< 0.0001	
C^2	220.55	1	220.55	1275.9	< 0.0001	
Residual	1.21	7	0.1729			
Lack of Fit	0.8700	3	0.2900	3.41	0.1333	not significant
Pure Error	0.3400	4	0.0850			
Cor Total	843.14	16				

The Model F-value of 251.57 and 541.18 in the ANOVA table of responses, grafting efficiency (%) and urea released (%), respectively, implies the model is significant. There is only a 0.01% chance for both responses that an F-value this large could occur due to noise.

P-values less than 0.0500 indicate model terms are significant. In this model, A, B, C, AB, AC, A^2, B^2, C^2 are significant model terms in both responses, grafting efficiency (%) and urea released (%). However, BC is significant only in grafting efficiency. As it is shown in the ANOVA tables above, the p- value of the reaction time, reaction temperature and mixing ratio ($p < 0.0001$) in both responses indicates that all factors have a high significant effect in determining the model. Values greater than 0.1000 indicate the model terms are not significant. If there are many insignificant model terms (not counting those required to support hierarchy), model reduction may improve your model. Here most of the model terms are significant in both responses, thus model reduction is not required.

The Lack of Fit F-value of 5.12 and 3.41 in the grafting efficiency and in the urea released respectively implies Lack of Fit is not significant relative to the pure error. there is a 7.42% and 13.33% chance for grafting efficiency and urea released, respectively, that a Lack of Fit F-value this large could occur due to noise.

Table 4.3. Fit Statistics.

A) Fit statistics for grafting efficiency (%)			
Std. Dev.	0.4158	R^2	0.9986
Mean	22.01	Adjusted R^2	0.9967
C.V. %	1.89	Predicted R^2	0.9829
		Adeq Precision	67.5031

B) Fit Statistics for urea released (%)			
Std. Dev.	0.7383	R^2	0.9969
Mean	56.40	Adjusted R^2	0.9930
C.V. %	1.31	Predicted R^2	0.9599
		Adeq Precision	44.3847

The Predicted R^2 values in both responses, 0.9829 in grafting efficiency (%), and 0.9599 in urea released (%) are in reasonable agreement with the Adjusted R^2 values of 0.9967 and 0.9930 respectively; i.e. the difference in Predicted R^2 and Adjusted R^2 is less than 0.2 in both responses. And the lower coefficient of variation (C.V. = 1.89 % for grafting efficiency (%), and 1.31 % for

urea released (%)), indicated that the high precision and reliability of the experiment. In both responses, grafting efficiency (%) and urea released (%), the compression between the actual and predicted process efficiency, indicates that the predicted data's were in a good agreement with the actual data's (Figure 4.2a and b). Therefore, the regression model can be used to predict the grafting efficiency (%) of the synthesized adhesive and the urea released (%) into the deionized water accurately.

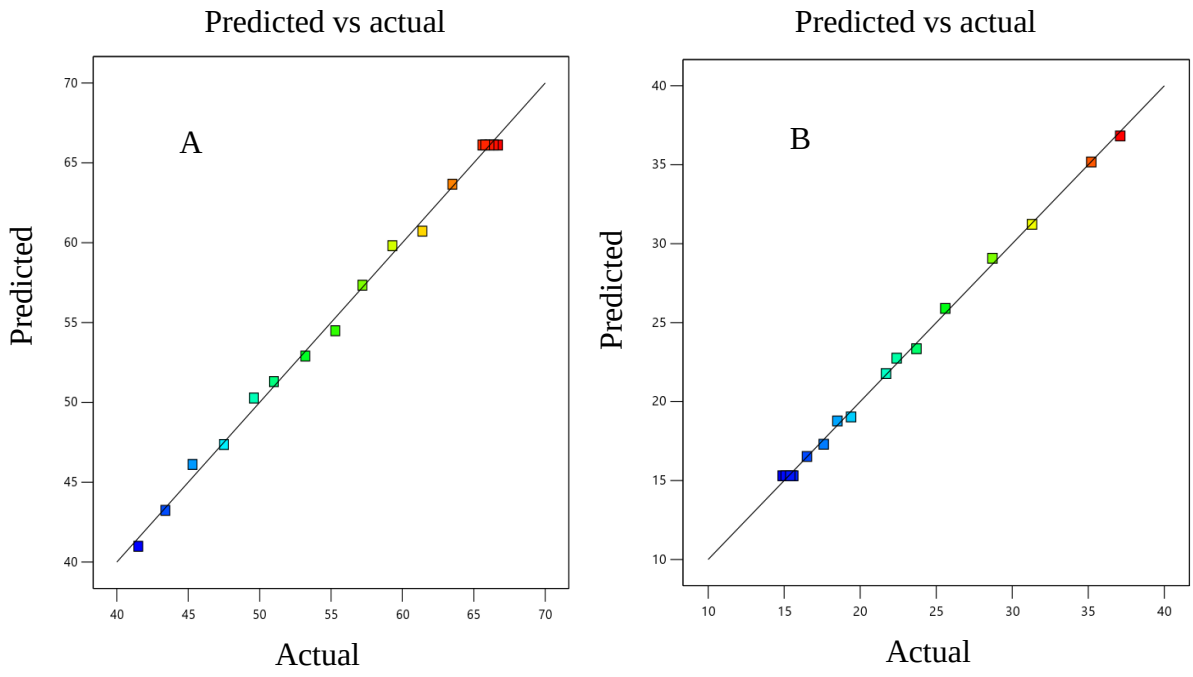

Figure 4.2.Relationship between predicted and actual responses. A) for grafting efficiency (%) B) for urea released (%)

Another useful statistic here was the one labeled "Adeq Precision''. This is a kind of signal to noise ratio that measures the ratio of the range of variation in the predicted response to an estimate of the standard error of the predictions and is obtained by subtracting the minimum predicted value from the maximum predicted value and then dividing by the average standard deviation of a prediction. A high value indicates that the variation that we are observing is large in relation to the underlying uncertainty of the fitted model. With respect to the above model, the ratios 67.503 and 44.385 in responses grafting efficiency (%) and urea released (%) indicates an adequate signal. This model can be used to navigate the design space, since a ratio greater than 4 is desirable.

4.1.4. The Effect of Interaction Between Independent Variables on the Grafting Efficiency and Urea Release rate

4.1.4.1. Effect of Interaction Between Reaction time and Reaction temperature on the Grafting efficiency and Urea Release Rate.

The response surface curves and contour plots were plotted to understand the interaction effects of LAO-g-GA synthesizing factors on the values of responses, grafting efficiency (%) of synthesized LAO-g-GA itself and urea release rate (%) of the U-e-LAO-g-GA after three hours of incubation in water.

As shown in Figure 4.3a below, when the GA to LA mixing ratio is constant (10.4 w/w%), the increase in reaction time and reaction temperature of GA and LA poly-condensation reaction clearly influences the grafting efficiency of LAO on the backbone of GA in a positive manner up to it reaches its maximum value (66.7%) at a reaction temperature of 180 ^{0}C and reaction time of 2hrs, then it starts to decline and reaches 61.4% at 195 ^{0}C reaction temperature and 2.5hrs reaction time. This is due to, when the reaction temperature and the reaction time increases, the propagation of grafting chains takes place at faster rate due to availability of more active sites, which accounts for higher grafting. However, when the reaction temperature and the reaction time further increased above 180 ^{0}C and 2hrs, respectively, the mutual destruction of growing chains might occur which causes to have lower value of grafting efficiency (Mishra et al., 2015). Whereas, as illustrated in the Figure 4.3b below, in the lower stage, the interaction of reaction time and reaction temperature influences the urea release rate into a deionized water negatively. The urea release rate decreases from 25.6% at a reaction temperature of 165 ^{0}C and 1.5hrs reaction time, up to its minimum value 14.9% at a reaction temperature of 180 ^{0}C and 2hrs of reaction time. Then when the reaction time and reaction temperature further increases, the urea release rate gradually increases, and reaches 17.6% at 195 ^{0}C reaction temperature and 2.5hrs reaction time. The decrease of urea release rate in the first stage is due to the increase in grafting efficiency, from the model graph it is observed that, the grafting efficiency increases the percent of urea released from U-e-LAO-g-GA decreases. Consequently, the gradual increase in urea release rate after 180 ^{0}C reaction temperature and 2hrs reaction time is due to the growing chains of LAO-g-GA copolymer starts to degrade with high temperature and long reaction time, which leads to decreasing the quality of LAO-g-GA and lacks its wettability, causes to decrease even its urea encapsulating capacity.

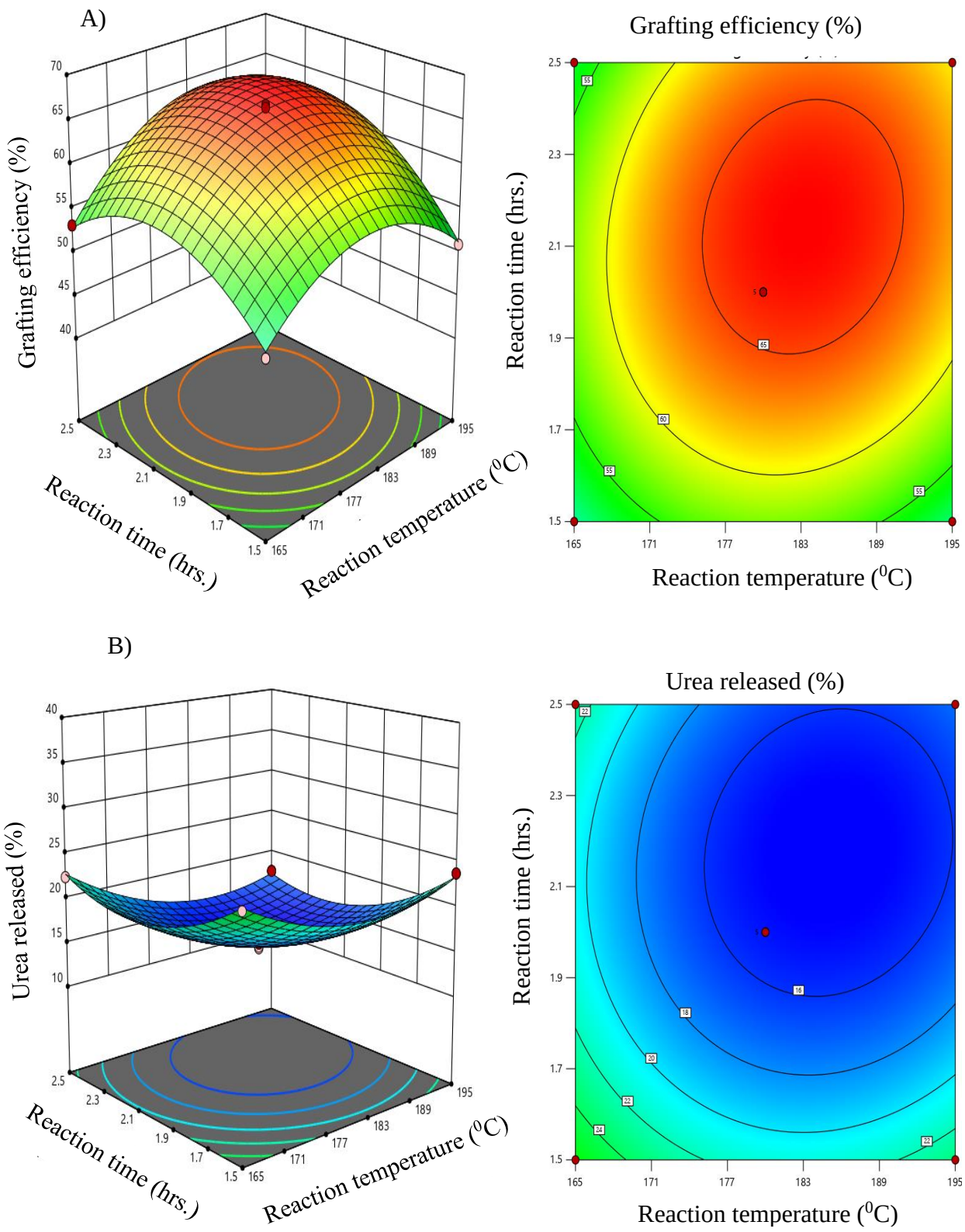

Figure 4.3. Response surface plot shows the effect of the interaction of reaction time and reaction temperature on: A) grafting efficiency, B) urea release rate

4.1.4.2. Effect of Interaction Between Mixing Ratio and Reaction temperature on the Grafting Efficiency and Urea Release Rate

As shown in Figure 4.4a below, when the reaction time is constant (2 hrs.), the increase in GA to LA mixing ratio and reaction temperature of GA and LA poly-condensation reaction clearly influences the grafting efficiency of LAO on the backbone of GA in a positive manner up to its maximum value (66.7%) at 180 ^{0}C reaction temperature and 10.4 w/w% GA to LA mixing ratio. However, when the GA to LA ratio and reaction temperature further increases above 10.4 w/w%, and 180 ^{0}C, respectively, the grafting efficiency starts to decline, and reaches 59.3% at 12.5 w/w% GA to LA mixing ratio and 195 ^{0}C reaction temperature. Whereas, the interaction of GA to LA mixing ratio and reaction temperature influences the urea release rate into deionized water in an opposite manner to that of the grafting efficiency. As discussed earlier, when the grafting efficiency is increased the urea released rate decreases and vice versa. As shown in the Figure 4.4b below, at lower reaction temperature and GA to LA mixing ratio, 165 ^{0}C and 8.3 w/w %, respectively, the urea released was maximum (37.1%), then, when the reaction temperature and GA to LA mixing ratio starts to increase, consequently the urea release rate gradually decreases and reaches a minimum value (14.9 %) at 180 ^{0}C reaction temperature and 10.4 w/w % GA to LA mixing ratio. When the reaction temperature and GA to LA mixing ratio further increases above 180 ^{0}C and 10.4w/w%, respectively, the urea release rate (%) gradually increases, and reaches 18.5% at 195 ^{0}C reaction temperature and 12.5 w/w% GA to LA mixing ratio.

This is because, in the first stage the increase in the GA content with increase in reaction temperature means preparing a number of GA active sites for the attachment of LAO, which leads the increase in grafting efficiency and causes to have a decrease in urea release rate. However, a further increase in reaction temperature causes to degrade the growing chains of LAO-g-GA, and further increase of GA leads to shortage in the availability of LAO for chain propagation (Tripathi & Katiyar, 2018), causes a decrease in grafting efficiency and increase in urea release rate.

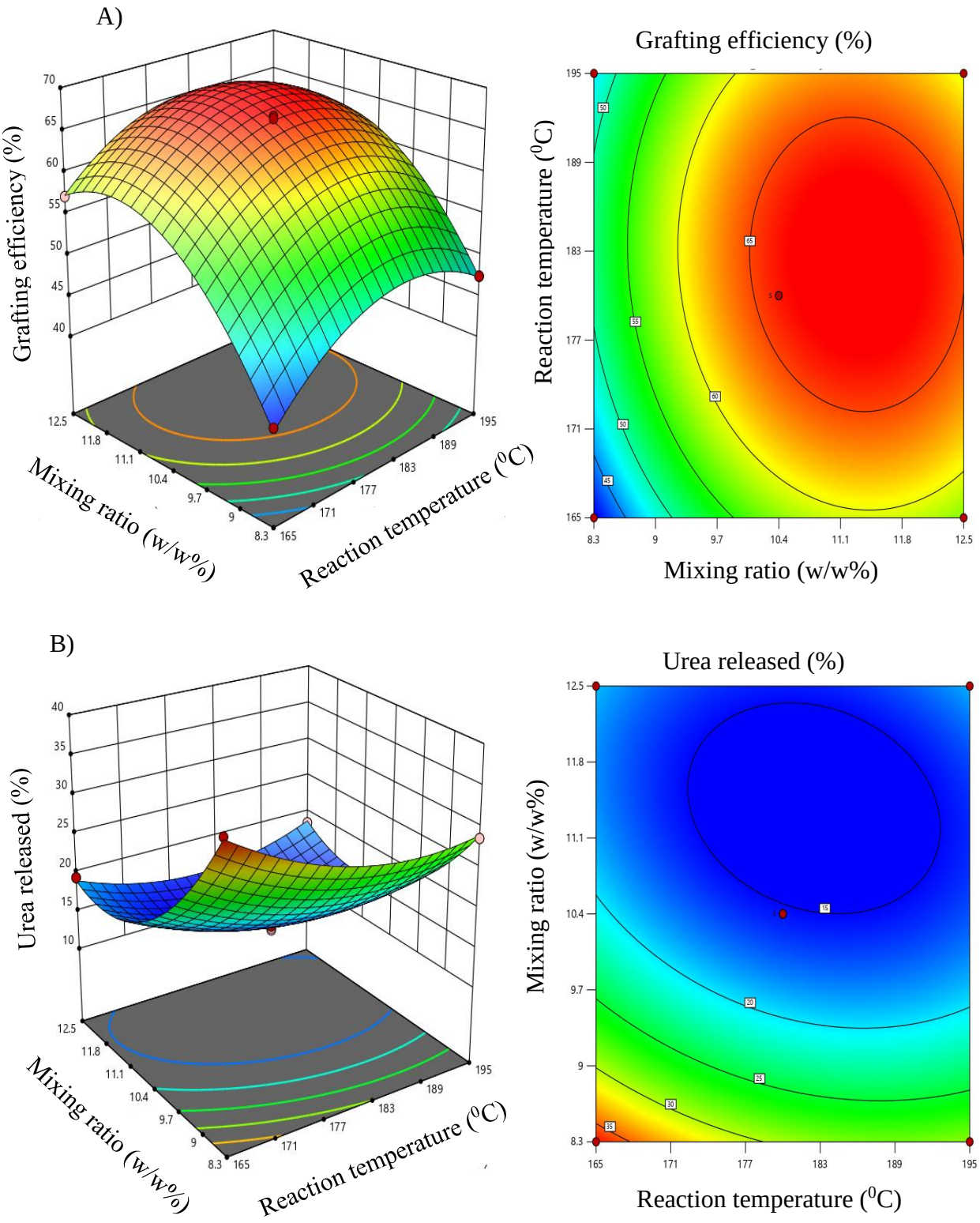

Figure 4.4. Response surface plot shows the effect of the interaction of mixing ratio and reaction temperature on: A) grafting efficiency, B) urea release rate.

4.1.4.3. Effect of Interaction Between Mixing Ratio and Reaction time on the Grafting efficiency and Urea Release Rate.

Similar to the above interaction effects, when the reaction temperature is constant (180 ^{0}C), at the lower stages, the interaction between the GA to LA mixing ratio and reaction time affects the grafting efficiency positively while negatively affecting the urea release rate. However, when reaction time and the GA to LA mixing ratio rises, grafting efficiency declines, and the urea release rate gradually increases. As shown in the Figure 4.5a below, when the GA to LA mixing ratio and reaction time of GA and LA poly-condensation reaction increases, the grafting efficiency of LAO on the backbone of GA increases, and reaches its maximum value (66.7%) at 10.4 w/w% GA to LA mixing ratio and 2hrs reaction time, then it gradually starts to decline and reaches 63.5% at 12.5 w/w% GA to LA mixing ratio and 2.5hrs reaction time. Whereas as shown in the Figure 4.5b, when the GA to LA mixing ratio and reaction time increases, the urea release rate into a deionized water decreases from 35.2% at 8.3 w/w% GA to LA mixing ratio and 1.5hrs reaction time to its minimum value (14.9%) at 10.4 w/w% GA to LA mixing ratio and 2hrs reaction time. Then further increase in mixing ratio and reaction time above 10.4% and 2hrs, respectively, the urea release rate gradually increases and reaches 16.5% at 12.5 w/w% mixing ratio and 2.5hrs reaction time. This is due to, as the GA content and reaction time of a poly-condensation reaction increases, the amount of polar water removed from the functional groups of GA backbone increases and much free radical active sits were generated on the GA backbone for the attachment of LAOs, causes to increase the grafting efficiency and decrease in urea release rate. While further increase in GA content leads to shortage in the availability of LAO for chain propagation and further increase in reaction time also causes to degrade the growing chains of LAO-g-GA, leads to decrease in the grafting efficiency and increase in the urea release rate.

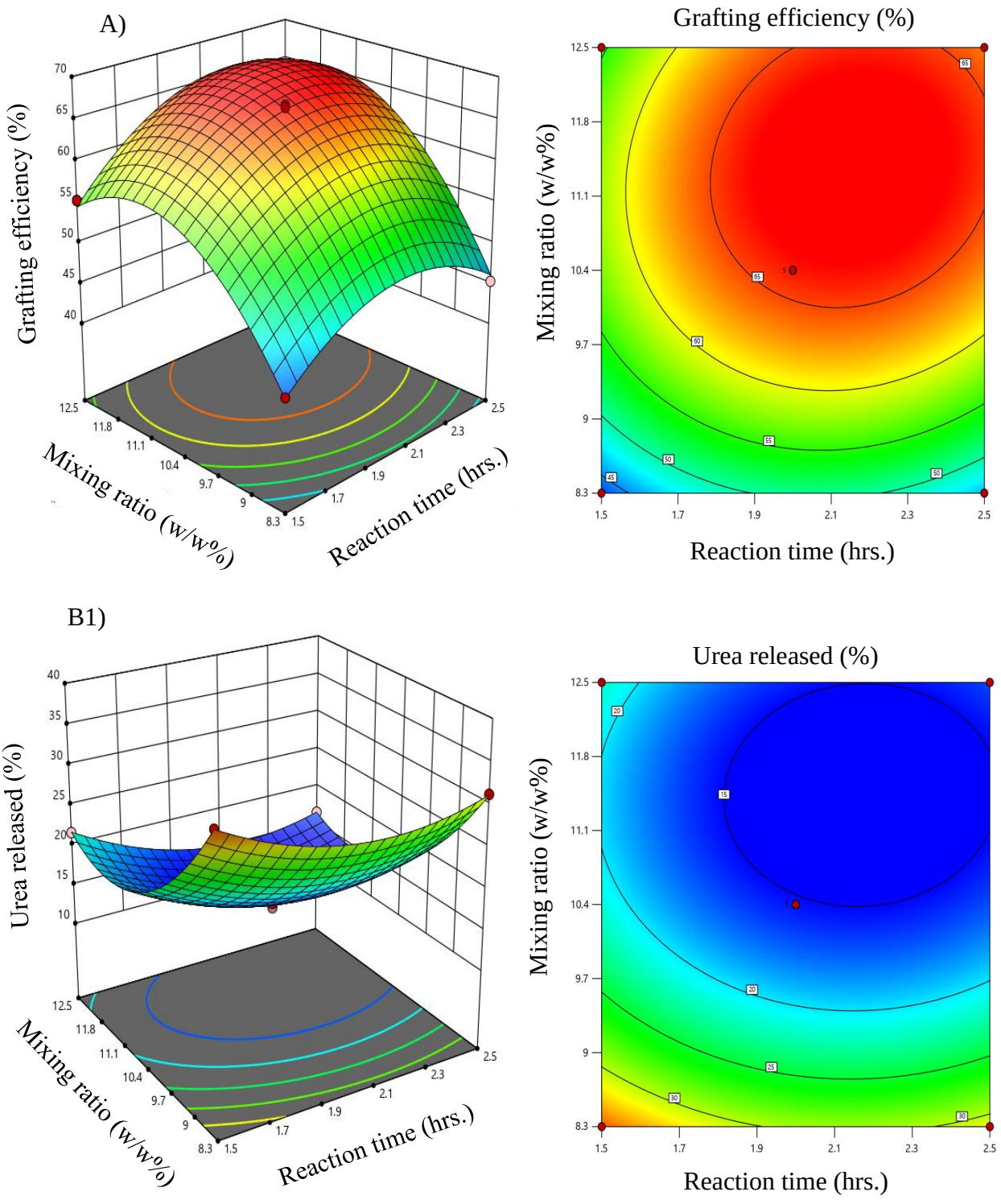

Figure 4.5. Response surface plot shows the effect of the interaction of GA to LA mixing ratio and reaction time on: A) grafting efficiency, B) urea release rate

Selection of the Three Samples for Further Characterization

The solubility test, hydrophobicity test and FTIR and NMR analysis for the synthesized LAO-g-GAs; and FTIR analysis for U-e-LAO-g-GAs; the effect of pH, temperature, and urea concentration on the urea release rate; the urea and urea release rate in soil; the soil degradation rate test; the total nitrogen release rate in water and its nitrogen release mechanism with different kinetic models were studied only for the three selected U-e-LAO-g-GAs, which were selected from the urea release rate results shown in Table 4.1 above, based on their release rate quality (i.e. high, medium, and low), after 3hrs incubation in a deionized water. Those selected U-e-LAO-g-GAs and their corresponding LAO-g-GAs before urea encapsulation were coded in the Table 4.4 below.

Table 4.4. The three selected samples based on their urea release rate.

Sample code before urea dispersion	Sample code after urea encapsulation	Reaction temperature (^{0}C)	Reaction time (hrs.)	GA to LA mixing Ratio (w/w %)	Urea released (%)
LAO-g-GA(h)	HRU-e-LAO-g-GA	165	2	8.3	37.1
LAO-g-GA(m)	MRU-e-LAO-g-GA	165	2.5	10.4	22.4
LAO-g-GA(l)	LRU-e-LAO-g-GA	180	2	10.4	15.3

4.1.5. Solubility and Hydrophobicity Test for LAO-g-GAs

The solubility and hydrophobicity tests for the synthesized LAO-g-GAs (i.e., LAO-g-GA(h), LAO-g-GA(m), and LAO-g-GA(l)) were evaluated as shown in Table 4.5 below. The solubility was performed in chloroform and the hydrophobicity was determined by doing the contact angle measurement. The contact angle values have direct proportionality with the hydrophobicity of the adhesives (Riveiro et al., 2018). The experimental results exhibits that the hydrophobicity and percentage solubility of LAO-g-GAs in chloroform were influenced in a positive manner with its grafting efficiency. As shown in the Table 4.5 below, the contact angle value and percentage solubility in chloroform increases with the increase in grafting efficiency, this is due to the fact that, in a highly grafted LAO-g-GAs, a large number of hydrophilic polar groups of GA were replaced by a hydrophobic ester groups of LAO, causes to enhance the hydrophobicity of LAO-g-GAs (Tripathi, 2016). This means that the polar groups on the GA backbone's surface were

replaced during the grafting process, giving the LAO-g-GA a more hydrophobic appearance. At the same time, during the modification of gum acacia (water soluble), when more polar groups of gum acacia were converted into non polar long carbon chain ester groups, by like dissolves like principle the LAO-g-GA that have large number of non-polar groups becomes more soluble in a non-polar solvent chloroform.

Table 4.5. Solubility and contact angle value for LAO-g-GAs

Sample code	Grafting efficiency (%)	Urea released (%)	Solubility (%) In chloroform	Contact angle (^{0})
LAO-g-GA(h)	41.5	37.1	57.6 + 1.8	39^0
LAO-g-GA(m)	53.2	22.4	69.8 + 3.4	67^0
LAO-g-GA(l)	66.12	15.3	77.5 + 2.3	79^0

During the contact angle measurement, if the contact angle is greater than 60^0, the surface has a hydrophobic nature; while if it is less than 60^0, the surface corsponds to a hydrophilic nature (Fertahi et al., 2020). As shown in the figure 4.6 below, the two LAO-g-GAs, coded by LAO-g-GA(m), and LAO-g-GA(l) shows a hydrophobic nature by having the contact angle value of 67^0 and 79^0, respectively. Whereas, the contact angle value (39^0) for the LAO-g-GA(h) indicats, it has a hydrophilic nature.

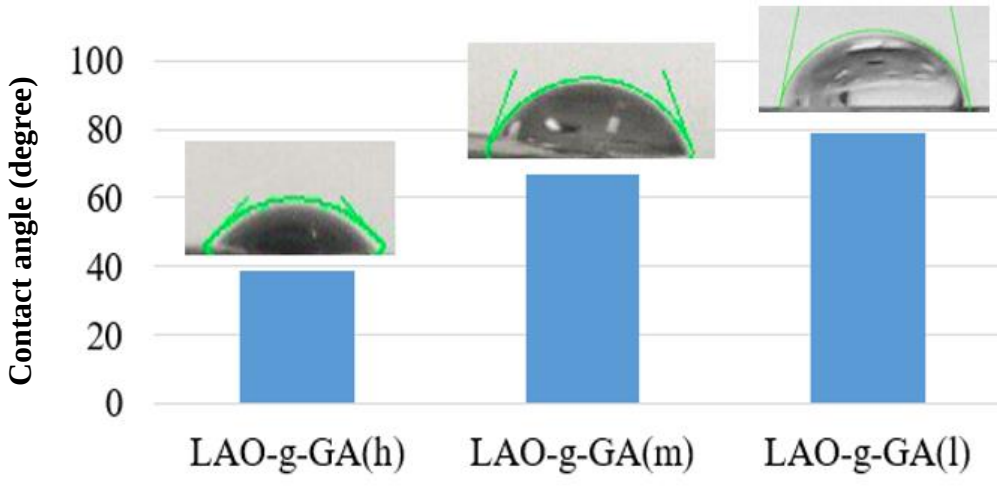

Figure 4.6. Contact angle measurement for LAO-g-GAs

4.1.6. FTIR Analysis for Synthesized LAO-g-GAs, LAO and Pure GA

FTIR analysis was performed to investigate intermolecular interaction and to predict the possible changes in the grafted samples. As shown in the Figure 4.7 below, the peaks 1133 cm-1, 1207 cm-1, 1047 cm-1, 1096 cm-1 confirmed the –C-O- stretching and the peaks at the wavenumber around 870 cm-1 and 1750 cm-1attributes to the bond of -C-C- and –C=O- stretching, respectively, in LAO and in all LAO-g-GAs (i.e. LAO-g-GA(h), LAO-g-GA(m), and LAO-g-GA(l)) (Tripathi & Katiyar, 2018). The peak at the wavenumber around 1632 cm-1 in the three LAO-g-GAs and in the LAO shows N-H deformation (Niu & Li, 2012)**.** The methyl groups -CH- or -CH_3 stretching vibration modes are appearing at the wavenumber around 2992 cm-1, and -CH- or -CH_3 bending at the wavenumbers around 1378 cm-1 and 1454 cm-1 in all samples (Kaavessina et al., 2021).

A broad vibration was observed at 1024 cm-1 in pure GA which is the finger print spectra of carbohydrates present in a sample. It was also observed that the peak at 3538 cm-1 of LAO was shifted to 3518 cm-1**,** 3473 cm-1, and 3434 cm-1 in LAO-g-GA graft copolymers of LAO-g-GA(h), LAO-g-GA(m), and LAO-g-GA(l), respectively, indicates the LAO chains were grafted on the backbone at O-H and N-H functional groups of GA (Tripathi, 2016)**.** In here, the observed reduction in intensity from LAO to LAO-g-GA(h), LAO-g-GA(m), and LAO-g-GA(l), respectively, is due to the consumption of O-H and N-H groups in the reaction (Tripathi & Katiyar, 2018)**.** And the increase in intensity from LAO to LAO-g-GA(h), LAO-g-GA(m), and LAO-g-GA(l), respectively, at wavenumber 1750 cm-1 also indicates formation of long chain –C=O- groups of LAO-g-GA due to grafting of LAO on the backbone of GA, implies the O-H and N-H functional groups of LAO were replaced by –C=O- groups during the grafting of LAO on the GA backbone. In order to justify the reduction in intensity of O-H and N-H groups, and the increase in intensity of –C=O- groups, the intensity ratio of O-H and N-H to –C=O- was done for each individual samples. The intensity ratio of O-H and N-H to –C=O- 0.576, 0.733, 0.959, and 1.221 for LAO, LAO-g-GA(h), LAO-g-GA(m), and LAO-g-GA(l), respectively, indicates there was a consumption of O-H and N-H groups and formation of –C=O- during the increase in grafting efficiency.

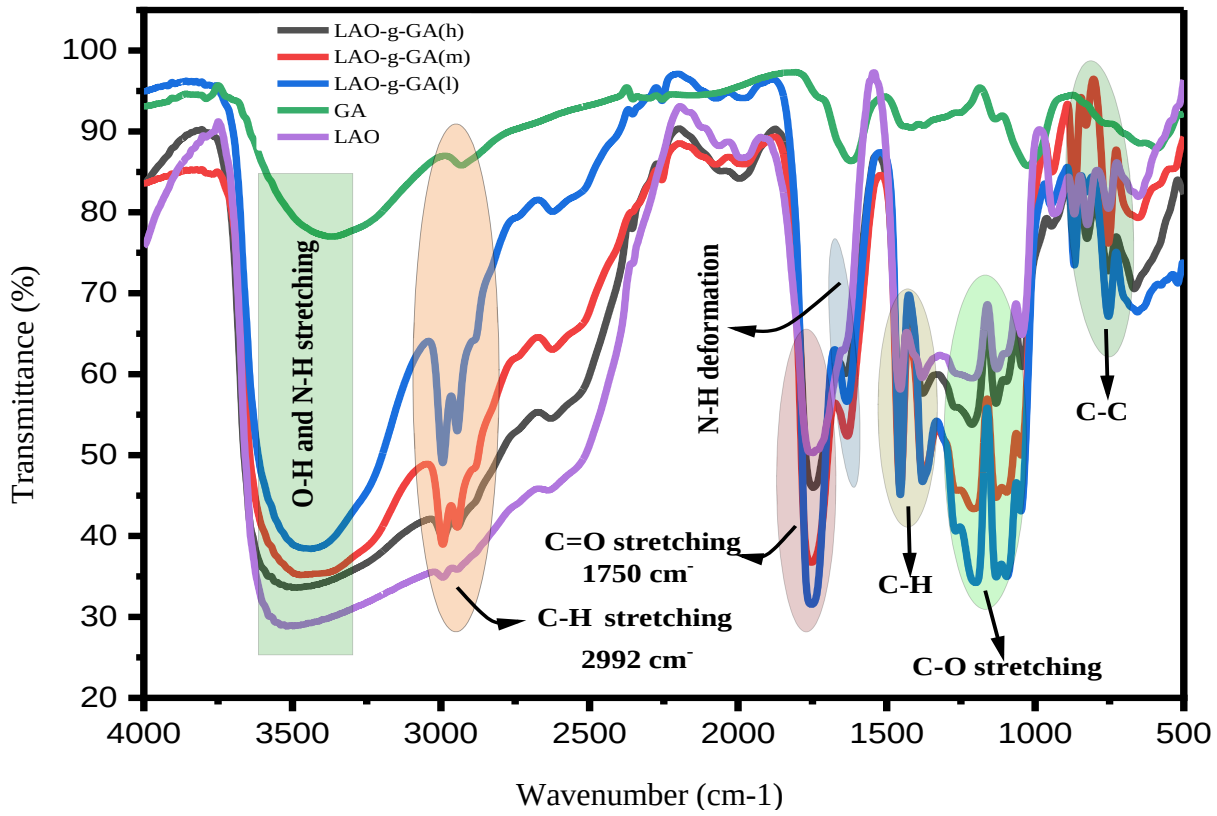

Figure 4.7. FTIR result for the three synthesized LAO-g-GAs, GA and LAO.

4.1.7. Nuclear Magnetic Resonance (NMR) Analysis

The 1H-NMR spectra for LAO and for the two selected samples LAO-g-GA(h) and LAO-g-GA(l) have been presented in Figure 4.9 a, b and c below. The peaks observed at around 1.55, 4.36, 5.15, and 6.77 ppm of LAO were due to the methyl protons (-CH_3) of the LAO side chain (1), terminal –C(CH3)H group (2), –CH- hydrogen of lactyl moiety (3), and –OH (4) group, respectively. The observed reduction of intensity at 4.36 ppm of terminal –C(CH3)H group (3) in the graft copolymers(i.e., LAO-g-GA(h) and LAO-g-GA(l)) confirms that there is a partial grafting of LAO on the –O-H and –N-H functional groups of the GA backbone (Tripathi & Katiyar, 2018). Furthermore, shift in the peak intensity was observed from 6.77 ppm of LAO to 6.64 ppm of LAO-g-GA(h) and 6.07 ppm of LAO-g-GA(l), indicates grafting at groups owing to partial consumption of the groups. As shown in the figure, there is also the reduction in intensity at –OH (4) group starting from LAO to LAO-g-GA(h) and then to LAO-g-GA(l), respectively, confirms the consumption of –O-H functional groups during the grafting of LAO on the GA backbone.

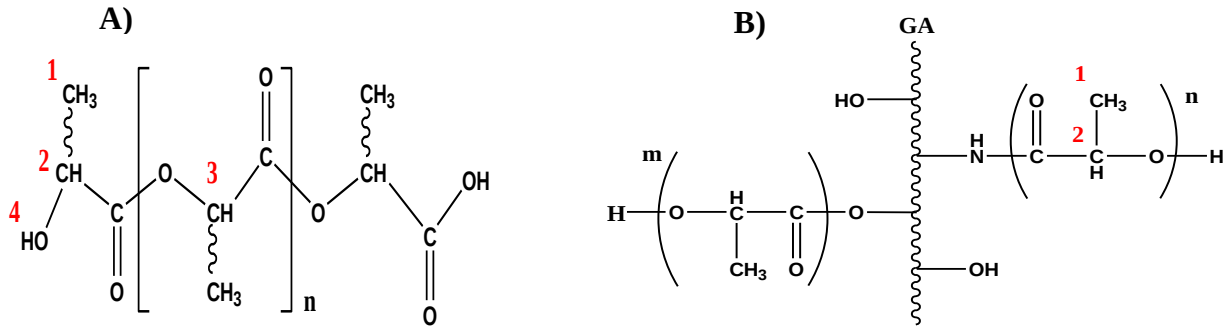

Figure 4.8. Molecular structure for: A) LAO and B) LAO-g-GAs

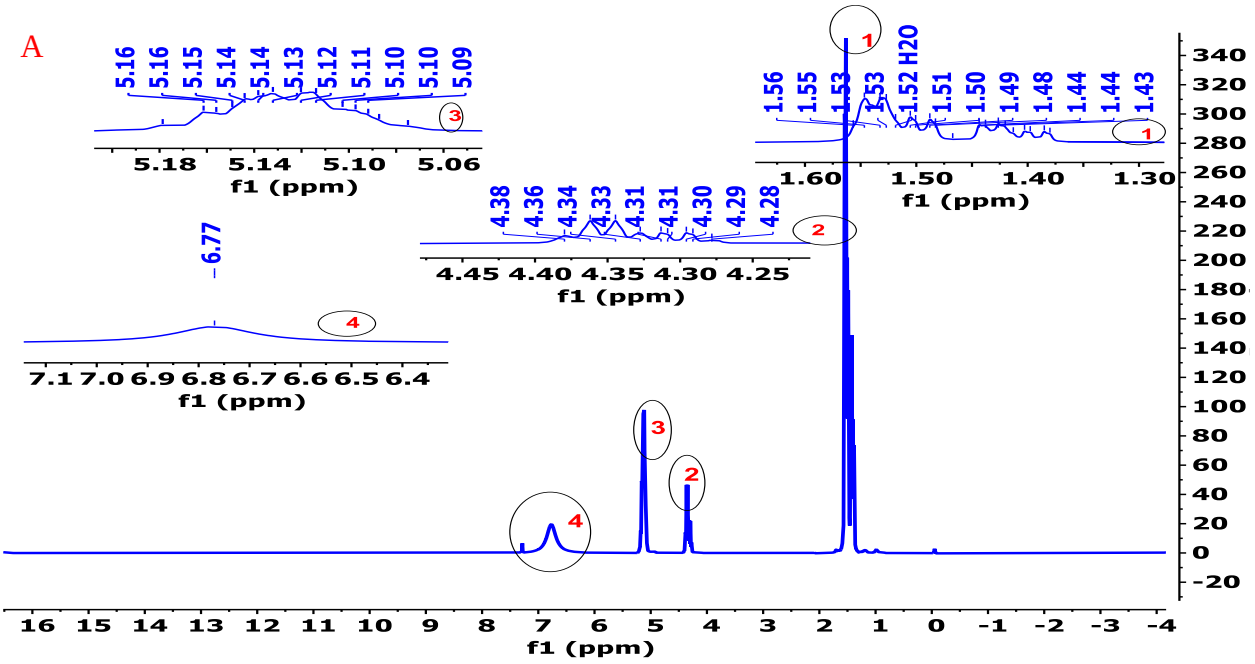

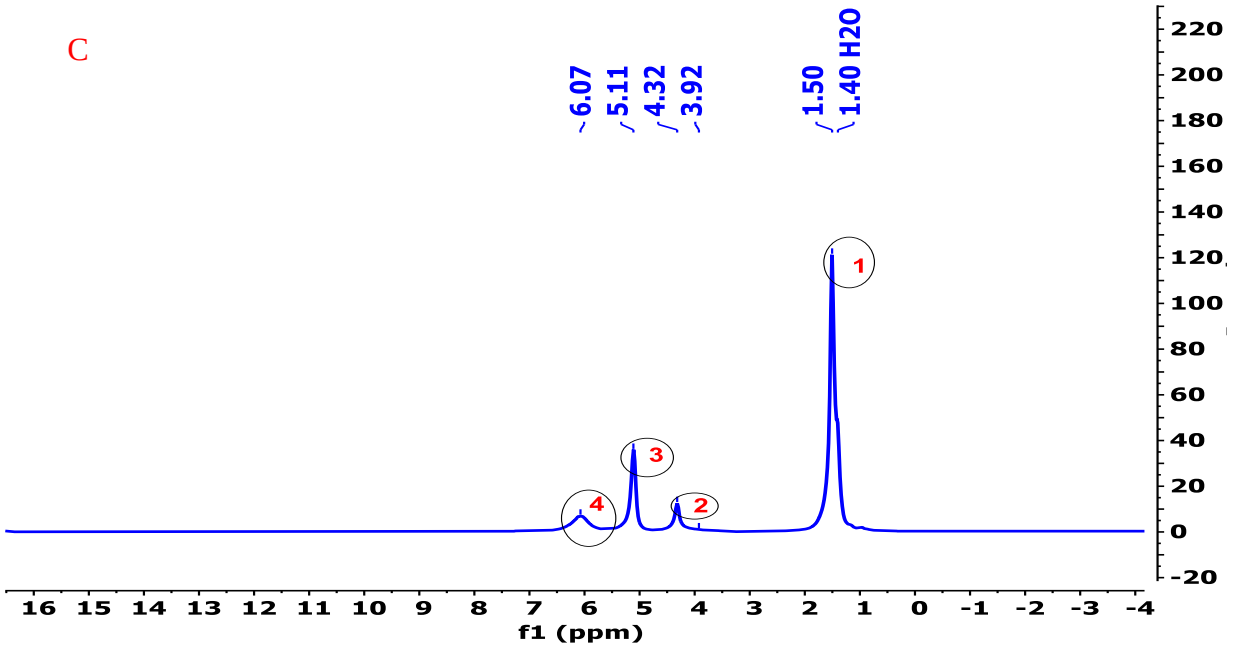

Figure 4.9. IH-NMR analysis, A) LAO, B) LAO-g-GA(h), and C) LAO-g-GA(l).

4.2. Characterization of U-e-LAO-g-GA

4.2.1. FTIR Analysis for U-e-LAO-g-GAs and Pure Urea

As shown in the Figure 4.10 below, the FTIR spectrum of U-e-LAO-g-GAs and pure urea, the peak at 3455 cm-1of O-H and N – H stretching becomes broaden for LRU-e-LAO-g-GA and HRU-e-LAO-g-GAs relative to pure urea, indicates there is an interaction between urea and LAO-g-GAs, especially due to hydrogen bonding interaction (Sempeho et al., 2015). The C=O stretching frequency for HRU-e-LAO-g-GA and LRU-e-LAO-g-GA has 1664 cm-1 similar to pure urea (Sempeho et al., 2015) , however, additional peak C=O stretching was observed at 1750 cm-1 for only HRU-e-LAO-g-GA and LRU-e-LAO-g-GA due to the presence LAO-g-GA**.**. And it is also observed that the C-O stretching frequency is shifted from 1160 cm-1 of pure urea to 1162 cm-1 and 1202 cm-1 for LRU-e-LAO-g-GA and HRU-e-LAO-g-GA, respectively, this also suggests that there is an interaction through hydrogen bonding between the amino groups of urea and the carboxylic groups of LAO-g-GA (Castro-Enríquez et al., 2012). The peak at the wavenumber around 1627 cm-1 and 1455 cm-1 for all U-e-LAO-g-GAs and pure urea shows N-H deformation and C–N stretching, respectively (Sempeho et al., 2015).

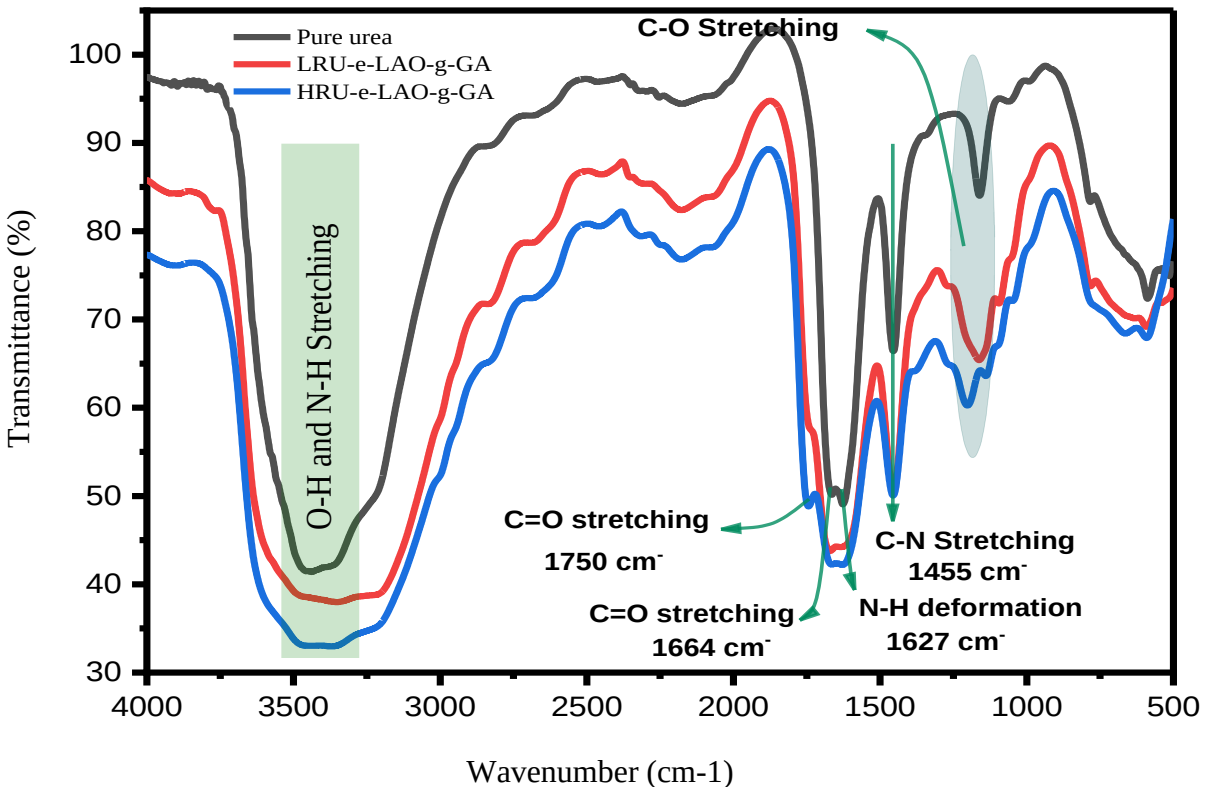

Figure 4.10. FTIR result for U-e-LAO-g-GAs and pure urea.

4.2.2. The Effect of pH on the Urea Release Rate

The urea release rate for the three selected U-e-LAO-g-GAs (i.e., HRU-e-LAO-g-GA, MRU-e-LAO-g-GA, and LRU-e-LAO-g-GA) in buffer solutions at pH 4, 7, and 10 at room temperature was evaluated as shown in Figure 4.11a, b&c, below. The figures, Figure 4a, b&c were plotted from the experimental result data's tabulated in Appendix-5a, b&c, respectively. The pH values were selected by considering extreme pH values (4 and 10) and soil pH is commonly close to 7 because soil is composed of alkaline and silica-based materials (Dórame-Miranda et al., 2018; Heuchan et al., 2019). From the experiment, it was observed that, as the pH of the medium increased, the urea release rate decreases. As shown in the figure 4.11a, at pH 4, the urea from a sample coded HRU-e-LAO-g-GA releases almost completely (99.69%) within 15 hours' of incubation in a solution, and from those samples coded MRU-e-LAO-g-GA and LRU-e-LAO-g-GA, the percent of urea released was 80.71% and 71.25%, respectively within the same time of incubation (15hrs). At pH 7 shown in Figure 4.11b, a highly released sample, which is coded by HRU-e-LAO-g-GA takes 23hrs of incubation to release 99.51% of its urea, whereas samples coded

by MRU-e-LAO-g-GA and LRU-e-LAO-g-GA releases 83.78% and 74.22% of urea, respectively. And at pH 10 shown in Figure 4.11c, a highly released sample HRU-e-LAO-g-GA takes 29hrs of incubation to release 99.82% of its urea, while samples coded by MRU-e-LAO-g-GA and LRU-e-LAO-g-GA releases only 85.02% and 74.27% of its urea, respectively, within this long time of incubation (29hrs).

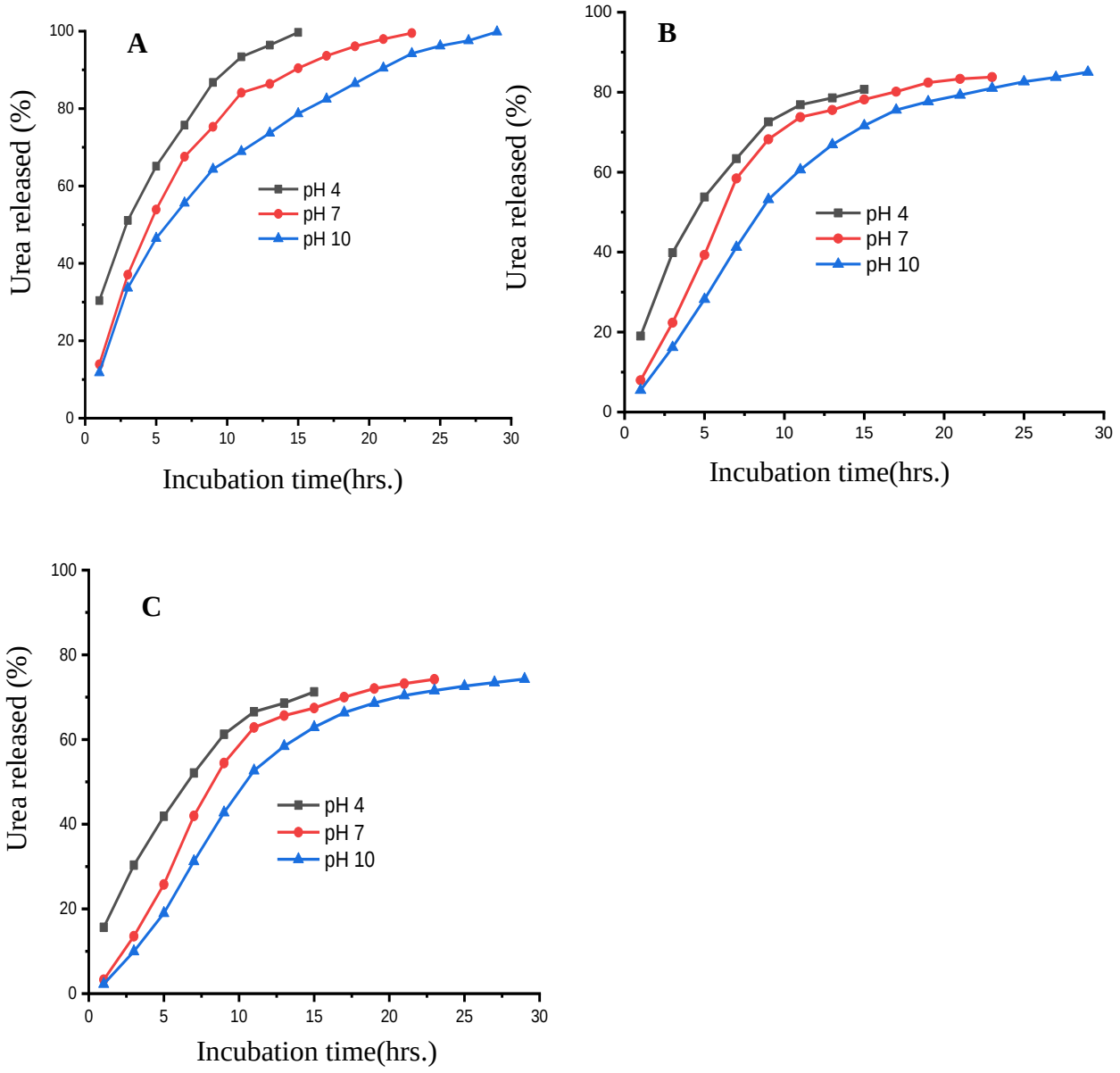

Figure 4.11. The percent of urea released as a function of time at different pH values, A) HRU-e-LAO-g-GA, B) MRU-e-LAO-g-GA and C) LRU-e-LAO-g-GA.

The effect of pH on the urea release rate of U-e-LAO-g-GAs depends on the protonation of the amino groups of urea. Based on the pH of the medium, urea can be protonated or deprotonated. More H^+ ions were conducted into the solution when the pH of the solution medium decreases, and as a result, the amino groups present in urea were protonated with those H^+ ions. Since H^+ ions from the solution occupy the bond sites of the amino groups of urea, the carboxyl groups of LAO-g-GA can't be attached easily with the urea molecules. Therefore, at pH 4, the amino groups of urea present in its ionized state (NH_3^+). Consequently, since the bond sites were occupied by H^+ ions, there is an electrical repulsion between non-ionized carboxyl groups (-COOH) of LAO-g-GA and ionized amino groups (NH_3^+) of urea, causing fast release. When the buffer solution is prepared to pH 7, the amine groups in urea continue to be in their non-ionized state (NH_2**)** (Dórame-Miranda et al., 2018), while the carbonyl groups in the LAO-g-GA, on the other hand, are expected to be in both their ionized ($-COO^-$) and non-ionized (-COOH) forms**.** As a result, there is a rise in the interaction between the anime groups of urea and the carboxyl groups of LAO-g-GA through hydrogen bonding. This causes to decrease the release rate of urea. As the pH rises, the amino groups of urea were not protonated and remain in the form of primary amine (NH_2), and the carboxyl groups of LAO-g-GA were expected to acquire its ionized ($-COO^-$) forms. As a result, the interaction between the carbonyl groups of LAO-g-GA and the amine groups of urea through hydrogen bonding increases when the pH of a medium reaches pH 10. As the number of hydrogen bonds between a LAO-g-GA and urea increases, the amount of urea released into the medium gradually decreases.

Although the urea release rate of all U-e-LAO-g-GAs were affected by the pH value of the medium, the degree of its effect differs from sample to sample. From experimental results tabulated in Appendix-5a, b&c, when we observe the urea release rate of all samples at a specific time of incubation (for example at 15hrs) in order to understand the effect of pH on the urea release rate of each individual sample separately, the sample coded by HRU-e-LAO-g-GA releases: 99.69% at pH 4, 90.44 % at pH 7, and 78.69 % at pH 10. The sample coded by MRU-e-LAO-g-GA releases: 80.71% at pH 4, 78.18% at pH 7, and 71.64% at pH 10; and the sample coded by LRU-e-LAO-g-GA release: 71.2% at pH 4, 67.42% at pH 7, and 62.89% at pH 10. This suggests that, in comparison to other samples, the sample coded by HRU-e-LAO-g-GA was greatly affected by pH. Specifically, it rises by 21% when the pH is lowered from pH 10 to pH 4. At the same time sample coded by MRU-e-LAO-g-GA increases by 9.07% and sample coded by LRU-e-LAO-g-

GA increases by 8.31%. The U-e-LAO-g-GAs, formulated by dispersing urea into a highly grafted LAO-g-GAs (i.e. LRU-e-LAO-g-GA) can resist the effect of pH on its urea release rate. This might be due to, in LRU-e-LAO-g-GA, the urea was encapsulated within a long chains of LAO-g-GA, as the gap between these long molecular chains of highly grafted LAO-g-GAs was too small and its surface become strong, the solution can't be reached the urea easily by penetrating through this very small chain gaps as well as it is unable to penetrate through the strong surface of LAO-g-GA. Therefore, the amino group of urea takes long time to be protonated with the H^+ of the solution at lower pH (i.e. pH 4), implies the carboxyl groups of LAO-g-GA, which is present in the amino acids of GA can be attached easily with non-ionized amine groups of urea through hydrogen bonding.

4.2.3. The Effect of Temperature on the Urea Release Rate

The Figure 4.12a, b&c below shows the temperature effect on urea release rate of the selected U-e-LAO-g-GAs (i.e., HRU-e-LAO-g-GA, MRU-e-LAO-g-GA, and LRU-e-LAO-g-GA) at 25 ^{0}C, 35 ^{0}C and 45 ^{0}C, respectively. The figures were plotted from the experimental result data's tabulated in Appendix-6a, b&c. The temperature values were selected according to the literatures Dórame-Miranda et al., (2018) and Husby et al., (2019), and as illustrated in Husby et al.,(2019), the high nutrient release rate were reported at the range of 35 ^{0}C - 40 ^{0}C, so in this case 25 ^{0}C and 45 ^{0}C were selected as an extreme valus to study the nutrient release rate. As shown in Figure 4.12a, b&c, the urea release rate in all U-e-LAO-g-GAs increases with the increase temperature. This is because the kinetic energy of urea molecules in the LAO-g-GA increases at a higher temperature, which rises the average molecular diffusion rate of urea, causes to increases its release rate. And the hydrogen bonds have weaker energies than regular valence bonds when the temperature rises, the bond is more likely to breakdown (Rodríguez-Félix et al., 2012). As shown in the figure 4.12a, at 25 ^{0}C, the urea in a sample coded by HRU-e-LAO-g-GA was dissolved almost completely, 99.73% of its urea was released into a deionized water within 23hrs of incubation in a deionized water. Whereas samples coded by MRU-e-LAO-g-GA and LRU-e-LAO-g-GA releases 84.44% and 73.56%, respectively, within this 23hrs of incubation. At 35 ^{0}C, shown in Figure 4.12b, the sample coded by HRU-e-LAO-g-GA takes 19hrs to release 99.87% of its urea, whereas samples MRU-e-LAO-g-GA and LRU-e-LAO-g-GA releases 83.38% and 74.76%, respectively on the same time of incubation (19hrs). And at 45 ^{0}C shown in figure 4.12c, the sample coded by HRU-e-LAO-g-GA takes 17hrs only to release 99.6% of its urea, whereas, samples coded

by MRU-e-LAO-g-GA and LRU-e-LAO-g-GA releases 83.96% and 75.87%, respectively within 17hrs of incubation.

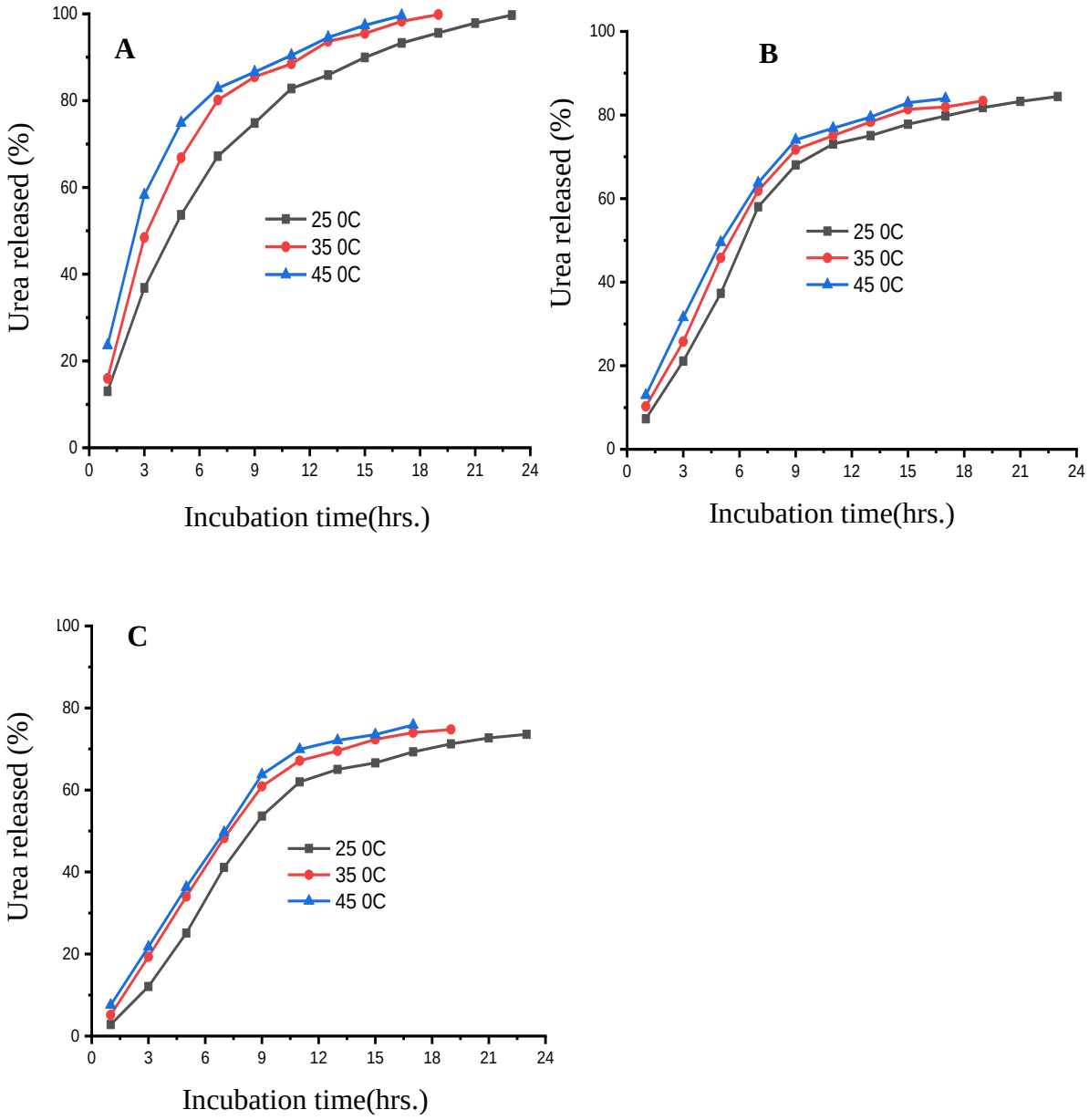

Figure 4.12. The percent of urea released as a function of time at different temperatures, A) HRU-e-LAO-g-GA, B) MRU-e-LAO-g-GA and C) LRU-e-LAO-g-GA.

As illustrated in the Figure 4.12a, b&c, the effect of temperature on urea release rate was most evident during the first hours of release periods. This phenomenon is attributed to the system receiving more energy, which facilitates the dissociation of interactions through hydrogen bonding

between the amino group of urea and the carbonyl group of LAO-g-GA, leads to increase the urea release rate. And as shown in the Figure 4.12a, b&c, the urea release rate of all samples becomes very slow after a certain hour (~9hrs) at each temperature condition. This is because, in the experiment conditions, the urea encapsulated in an insoluble component of LAO-g-GAs could only be released after being degraded into soluble, which is a very slow process.

4.2.4. The Effect of Urea Concentration on Urea Release Rate

The Figure 4.13a, b&c below, illustrates the effect of urea concentrations on urea release rate of the three selected U-e-LAO-g-GAs (i.e., HRU-e-LAO-g-GA, MRU-e-LAO-g-GA, and LRU-e-LAO-g-GA), at 70%, 75%, and 80% of urea concentrations, respectively. The values of the urea concentrations were selected based on the preliminary experiment results. The figures were plotted from the experimental result data's tabulated in Appendix-7a, b&c. From the experiment, it was observed that, as the urea concentration encapsulated into the synthesized LAO-g-GAs increases, the rate of urea released from each U-e-LAO-g-GAs also increases. As shown in the Figure 4.14a, when all U-e-LAO-g-GAs contains 70% of urea, the urea from the sample coded by HRU-e-LAO-g-GA releases almost completely (99.76%) within 25hrs' of incubation, whereas from those samples coded by MRU-e-LAO-g-GA and LRU-e-LAO-g-GA, the percent of urea released within this long time of incubation (25hrs) was 84.43% and 73.76 %, respectively. But, When the amount of urea contained in all U-e-LAO-g-GAs increases to 75%, as shown in Figure 4.11b, a highly released sample, which was coded by HRU-e-LAO-g-GA takes 23hrs of incubation to release 99.51% of its urea, and those samples coded by MRU-e-LAO-g-GA and LRU-e-LAO-g-GA releases 83.78% and 74.22%, respectively. And when the amount of urea contained in all U-e-LAO-g-GAs further increases to 80%, a highly released sample, which was coded by HRU-e-LAO-g-GA takes only 21hrs to release 99.83% of urea, whereas those samples coded by MRU-e-LAO-g-GA and LRU-e-LAO-g-GA releases 85.63% and 75.67% within the same time of incubation (21hrs) as illustrated in Figure 4.11c. This is due to the fact that as the amount of urea encapsulated within each LAO-g-GAs increases, the LAO-g-GAs molecular chains expands, accordingly, the gap between the molecular chains widens, and also its surface strength weakens. As a result, more water was able to enter into LAO-g-GAs through the gaps as well as through its surface, which causes to increases the urea release rate.

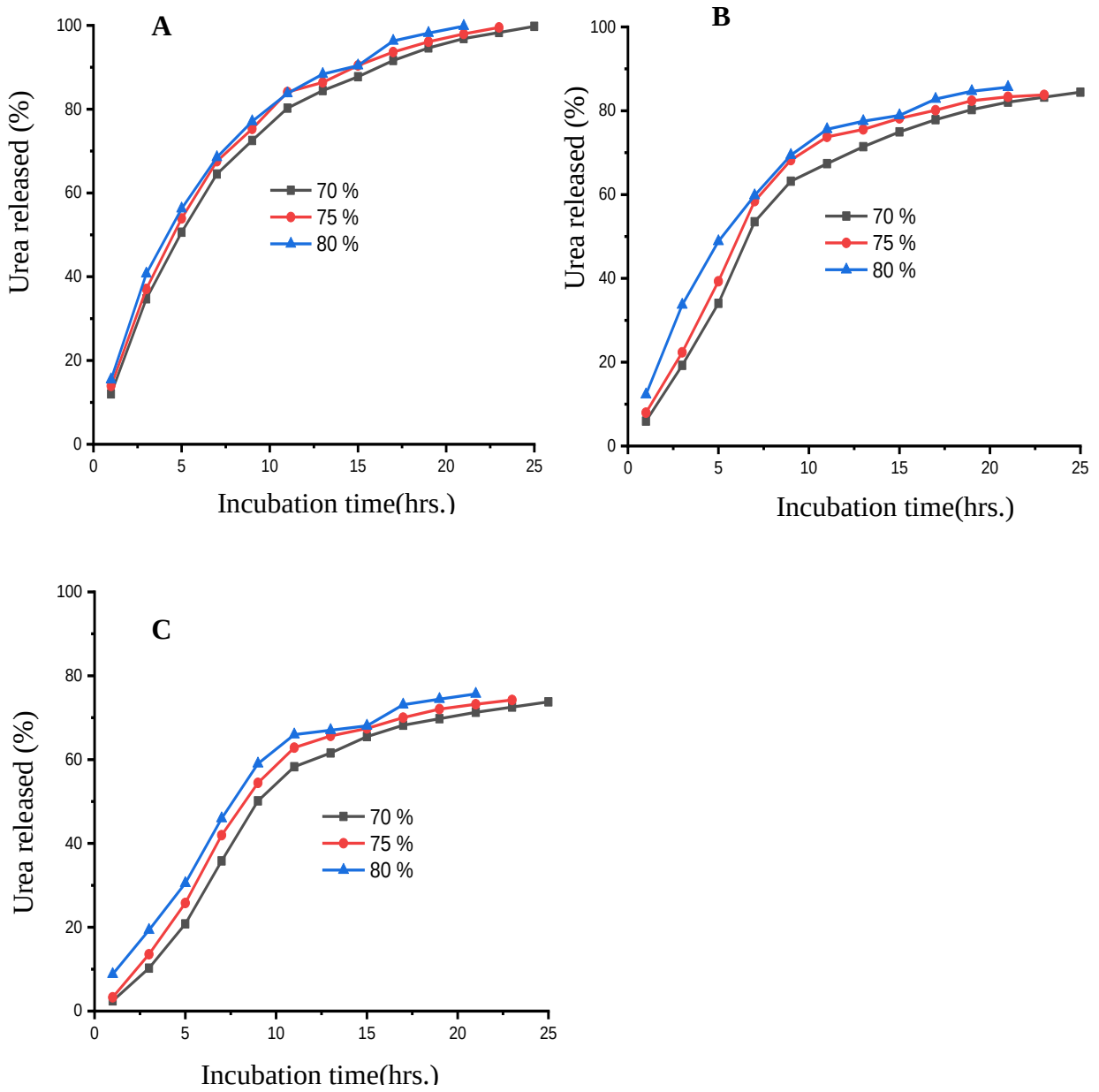

Figure 4.13. The percent of urea released as a function of time at different urea concentration, A) HRU-e-LAO-g-GA, B) MRU-e-LAO-g-GA and C) LRU-e-LAO-g-GA.

At the beginning of the urea release periods, the urea release rate from all U-e-LAO-g-GAs was fast with the increase in urea concentration. This is because of the urea content difference on the surface of each U-e-LAO-g-GAs. As sown in the Figure 4.13a, b&c, in each U-e-LAO-g-GA which contains 80% urea, the urea release rate was much faster at the beginning urea release

periods as compared with those U-e-LAO-g-GAs synthesized in the same conditions, containing 75% and 70% urea concentrations. And then, the urea release rate difference gradually decreases due to most of the urea present on the surface of each individual U-e-LAO-g-GAs was released and then the release rate of the remaining urea from each U-e-LAO-g-GAs depends on the water penetration ability through molecular chains of LAO-g-GAs as well as it depends on the rate at which in soluble LAO-g-GAs become soluble through hydrolytic degradation. Generally, after the urea present on the surfaces of the samples were released, the remaining urea release rate depends on the grafting efficiency of LAO-g-GAs in which the urea was encapsulated.

4.2.5. Urea Release Rate in Soil

The release behaviors of U-e-LAO-g-GAs and commercial urea fertilizer in soil were also evaluated as shown in Figure 4.14 below. The figure was plotted from the experimental result data's tabulated in Appendix-8. From the experimental results it was observed that the urea release rate in soil was slower as compared to its release rate in distilled water. This is due to the fact that the sample in the soil was in an environment of extreme conditions. During the release process the U-e-LAO-g-GA surface was connected with soil particles, in this way the soil condition around the U-e-LAO-g-GAs might be changed. Hence, this leads to decrease the free water exchange rate between the soil and the U-e-LAO-g-GAs, reduces the diffusion rate of water into the U-e-LAO-g-GA. Consequently, the urea release rate of U-e-LAO-g-GA in soil becomes less relative to that was in water. Besides, as the urea release rate test in the distilled water condition was static and in the soil condition was dynamic, the water might leach out with less absorbency of urea, as a result the release of urea into a leachate was reduced (Gungula et al., 2021). The Figure 4.14 shows that the release rate of pure urea in the soil rapidly reaches its equilibrium within the first 10 days of incubation. Whereas, from U-e-LAO-g-GAs, the high released sample coded HRU-e-LAO-g-GA releases 98.67% of its urea after 30 days of incubation, demonstrating that even the highly released sample (i.e., HRU-e-LAO-g-GA) from those U-e-LAO-g-GAs was able to effectively reduces the urea release rate in the soil, over a period of time (30 days) almost 3 times longer than that was observed for a pure urea fertilizer (10days). At this long time incubation (30 days), U-e-LAO-g-GAs coded by MRU-e-LAO-g-GA and LRU-e-LAO-g-GA releases only 83% and 72%, respectively. The observed release rate of pure urea was 62.22% within 24hrs of incubation. This also implies more than half of the essential nutrient N from pure urea was released within this short time (24hrs), which is very fast relative to plants nutrient requirement for their long lifetime.

Whereas the urea release rates for HRU-e-LAO-g-GA, MRU-e-LAO-g-GA and LRU-e-LAO-g-GA were 21.5%**,** 13.67% and 9.17%, respectively in the first 24hrs of incubation, which indicates that the U-e-LAO-g-GAs were favorable to reduce the N loss through leaching in soil, and the environmental and human health probloms caused by the utilization of commercial urea fertilizers can be reduced while using U-e-LAO-g-GAs.

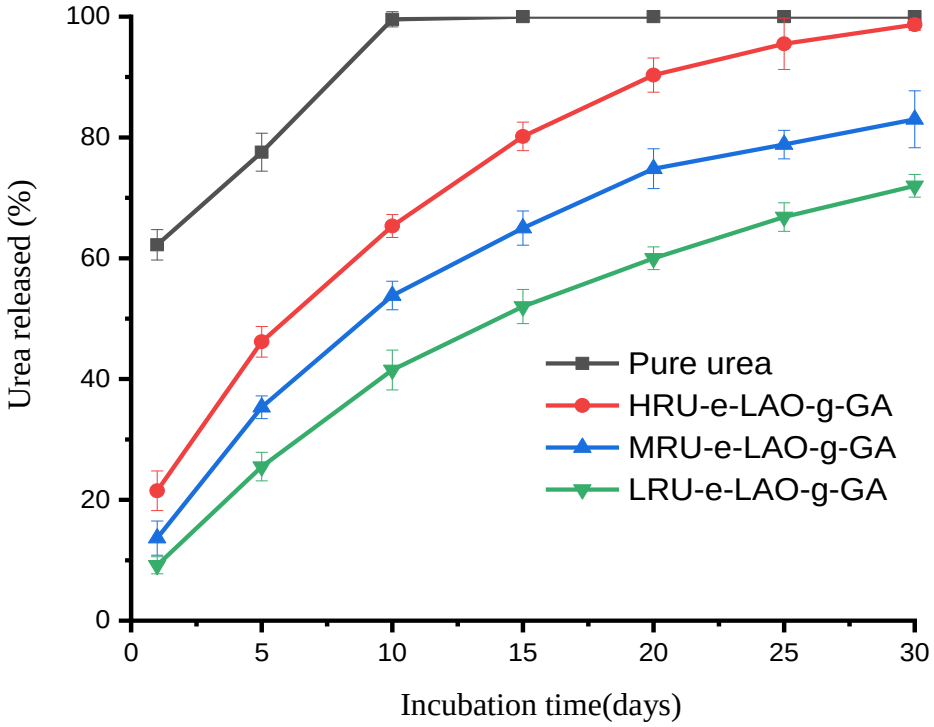

Figure 4.14. Urea release rate in soil

4.2.6. Soil Degradation Rate of U-e-LAO-g-GAs Relative to Pure Urea

The soil degradation experiments were conducted to understand the degradation rate of U-e-LAO-g-GAs relative to the commercial urea fertilizer. And the effect of grafting efficiency on the soil degradation rate of U-e-LAO-g-GAs was also investigated during the experimental result analysis. The results of soil degradation rate of U-e-LAO-g-GAs and commercial urea fertilizer are shown in Figure 4.15 below, in which the figure was plotted from the experimental result data's tabulated in Appendix-9b. As illustrated in the Figure 4.16, it was observed that the weight loss of all U-e-LAO-g-GAs and pure urea increases with the increase in incubation time. The commercial urea (pure urea) degrads completely within 3 days of incubation in the soil i.e., its weight loss reachs 100% within 3 days of incubation. Whereas, those U-e-LAO-g-GAs i.e., HRU-e-LAO-g-GA,

MRU-e-LAO-g-GAs, and LRU-e-LAO-g-GA losses only 40.8%, 25.5%, and 18.8% of their weights, respectively within the first 3 days of incubation. The LRU-e-LAO-g-GAs fertilizer showed the lowest weight loss (68.3% only) on the 25th days of incubation, while the weight loss for the high urea released U-e-LAO-g-GA (i.e., HRU-e-LAO-g-GA) reachs 99.75%, and MRU-e-LAO-g-GA releases 87.75% within this 25 days of incubation, demonstrating that all U-e-LAO-g-GAs were degraded in soil, but it takes longer time to be fully decompose relative to commercial urea fertilizer. And from those U-e-LAO-g-GAs, LRU-e-LAO-g-GAs takes long time to degrade in soil relative to other U-e-LAO-g-GAs. This is because, the grafting efficiency of LAO-g-GA in which U-e-LAO-g-GAs were formulated have an influence on its soil degradation rate. As shown in the Figure 4.15, when the grafting efficiency of LAO-g-GA in which U-e-LAO-g-GAs were formulated increases, the percent of degradation rate decreases. This is due to the fact that, in highly grafted LAO-g-GAs, its molecular chains are more densely packed together, implies GA and urea inclusions in the graft copolymer were well protected, as a result, microorganisms in the soil can't esily acess it to break down, causes to slow down its degradation rate as compared to other U-e-LAO-g-GAs which were formulated by encapsulatiing urea into a low grafted LAO-g-GAs (Nikolic et al., 2014).

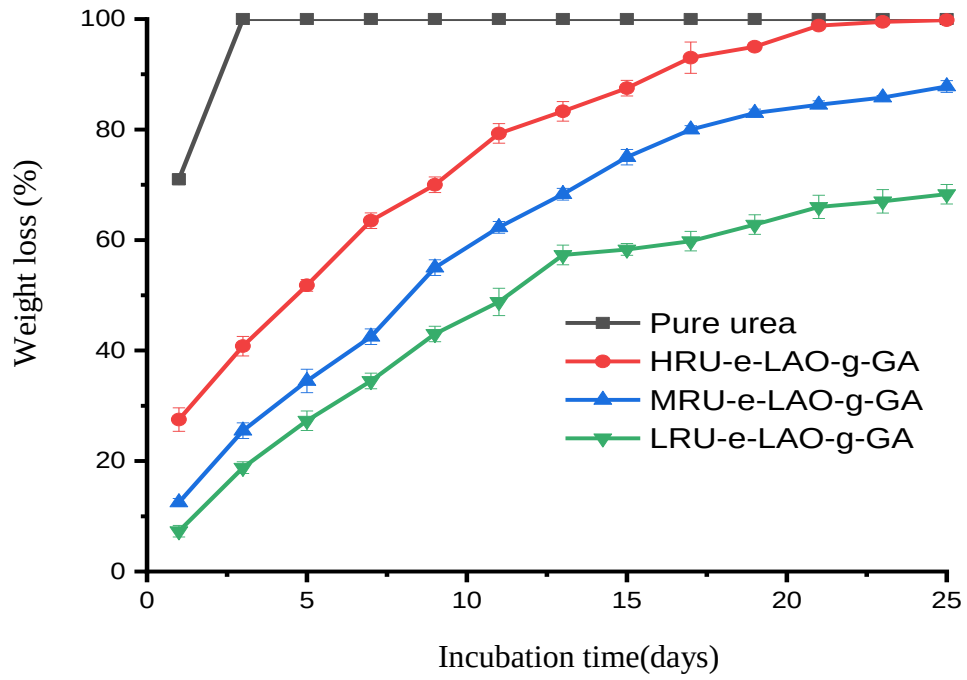

Figure 4.15. Weight loss (%) for the three selected U-e-LAO-g-GAs and pure urea exposed to soil for 25 days.

In this case, since urea was dispersed in every parts of the formulated U-e-LAO-g-GAs, and the essential nutrient nitrogen was released from each parts through degradation when it was exposed to soil as shown in Figure 4.16 below, it can address the issue of the essential nutrient N being lost due to an irregular release by the disintegration of coating layers while using coating mechanisms. It can also solve the soil structure and the nutrient balance problomes of using non-biodegradable materials for coating as well as encapsulating purposes, since it completely degrads in soil.

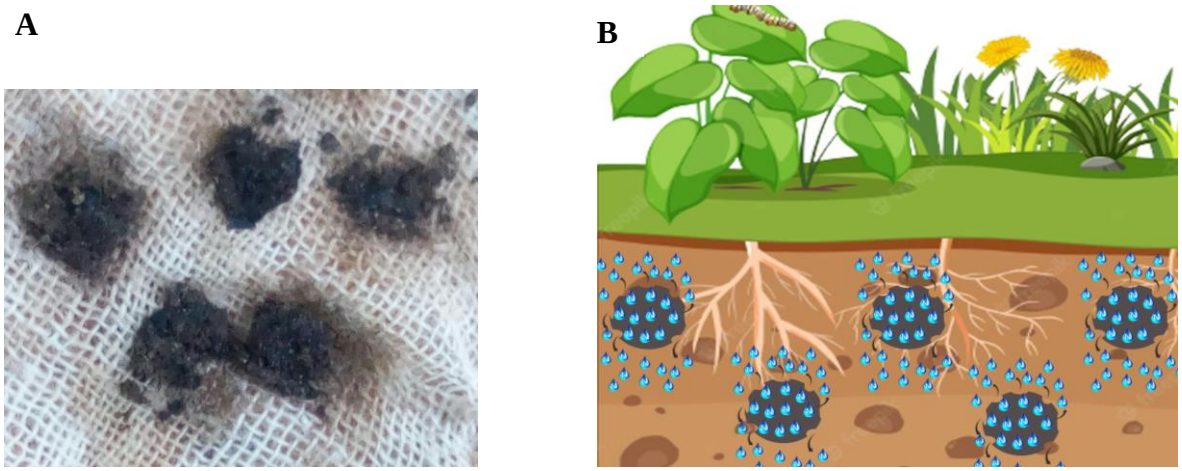

Figure 4.16**.** The release of N through degradation A) degradation of U-e-LAO-g-GAs in soil, B) the N delivery system

4.2.7. The Effect of Urea Concentration on the Soil Degradation Rate

The Figure 4.17 a, b&c below shows the effect of urea concentration (i.e., at 70%, 75%, and 80%) on the soil degradation rate of HRU-e-LAO-g-GA, MRU-e-LAO-g-GA, and LRU-e-LAO-g-GA, respectively. The figures, Figure 4.17a, b&c were plotted from the experimental result data's tabulated in Appendix-9a, b&c. The experimental results indicate that, as the urea concentration increase the soil degradation rate also increases in all U-e-LAO-g-GAs. As illustrated in the Figure 4.17a, the sample coded HRU-e-LAO-g-GAs takes 25 days to lose 98.8% of its weight when urea concentration is 70%, but when its urea concentration becomes 75%, it takes only 21 days to lose the same amount of its weight (98.8%). When urea concentration is further increased to 80%, the degradation rate increases and it only takes 19 days to lose nearly the same amount of its weight (98.6%). And the Figure 4.17b below shows that the sample coded MRU-e-LAO-g-GA loses 83.8% of its weight within 25 days of incubation when it contains 70% urea, while the weight loss increases to 87.8% when the urea concentration was increased to 75%, and to 91.8% when the urea

concentration was further increased to 80%. Similarly, as illustrated in Figure 4.17c, the sample coded LRU-e-LAO-g-GA, losses less weight (64.8%) within 25 days of incubation when its urea content was 70%, whereas, when its urea concentration raises to 75%, its weight loss reaches 68.3%, and when its urea concentration further increases to 80%, its weight loss also increases and reaches 72.5% within the same time periods of incubation (25days). This is due to the fact that, as discussed in the effect of urea concentration on the urea release rate above, the amount of urea encapsulated in the LAO-g-GA increases, the LAO-g-GAs molecular chains expands and its bond strength weakens, as a result, the microorganisms in the soil can break down it easily. Generally, in this soil degradation rate experiment, the result demonstrates, not only its urea release rate in water, but also its soil degradation rate in soil was greatly influenced by the grafting efficiency of LAO on the GA backbone.

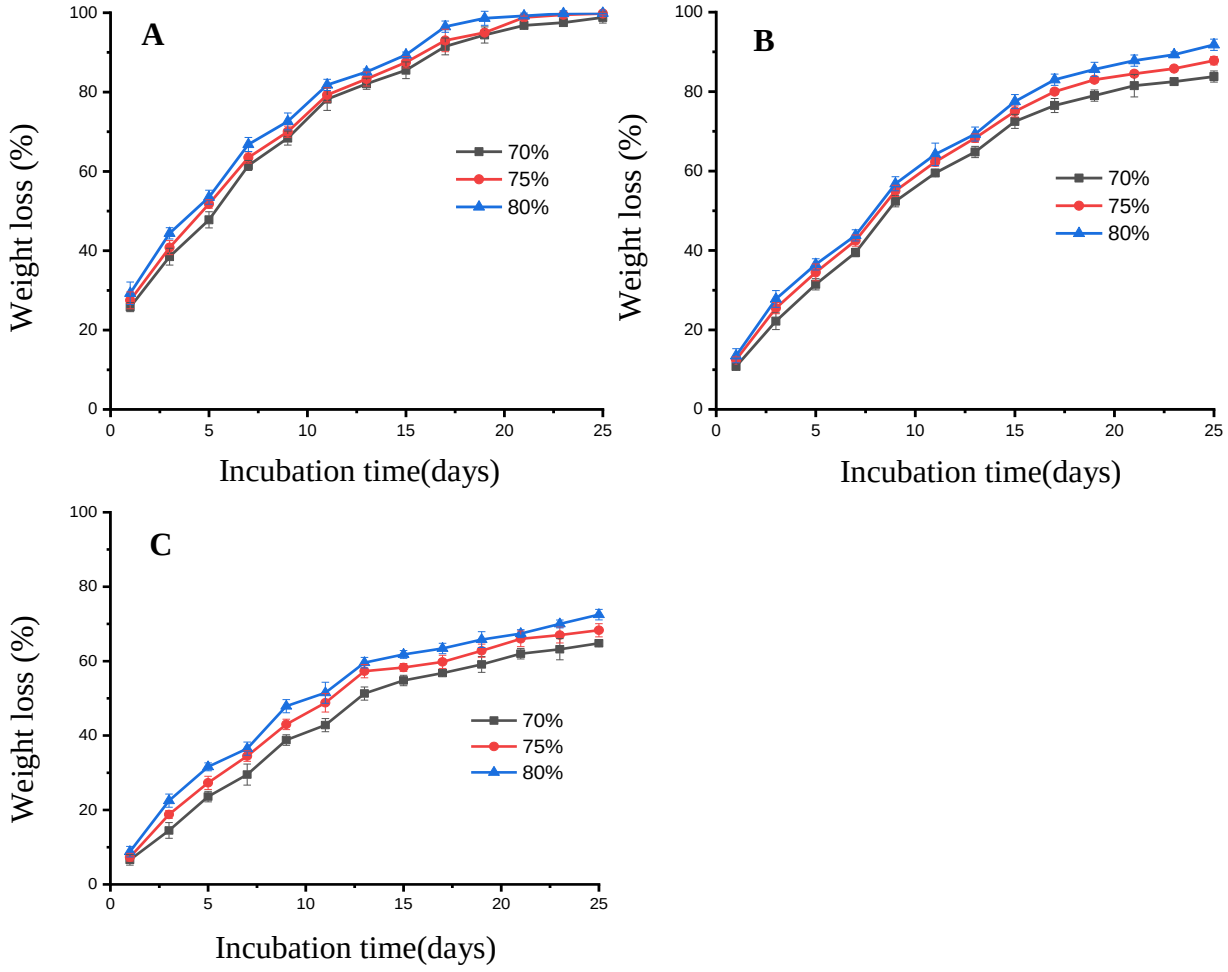

Figure 4.17. The effect of urea concentration on the soil degradation rate, A) HRU-e-LAO-g-GAs B) MRU-e-LAO-g-GAs, and C) LRU-e-LAO-g-GAs

4.2.8. Total Nitrogen Release Rate and its Release Kinetics Behaviors in Water

The nitrogen release rate of U-e-LAO-g-GAs and commercial urea in water was evaluated using kjeldhal method, as illustrated in the Figure 4.18 below. The figure was plotted from the experimental result data's tabulated in Appendix-10. As shown in the figure 4.18 below, pure urea releases 98% of its nitrogen content with in an hour, which is almost similar to the results documented in literatures Gungula et al., (2021)(97%), and Muslim et al., (2015)(100%). However, the nitrogen release rate for U-e-LAO-g-GAs coded by HRU-e-LAO-g-GA, MRU-e-LAO-g-GA, and LRU-e-LAO-g-GA were 12.15%, 6.94%, and 2.9%, respectively within an hour of incubation in a distilled water. The reason why LRU-e-LAO-g-GA release slower is due to the fact that the LAO-g-GA which was used for the formulation of LRU-e-LAO-g-GA has the highest grafting efficiency relative to the other synthesized LAO-g-GA, the highest grafting efficiency has the lowest release rate as discussed earlier. From those U-e-LAO-g-GAs, HRU-e-LAO-g-GA releases its nitrogen content almost completely (99.95%) within 25hrs of incubation, whereas fertilizer coded by MRU-e-LAO-g-GA attained 85.04%, and LRU-e-LAO-g-GA releases only 76.14% of nitrogen within this long time incubation (25hrs).

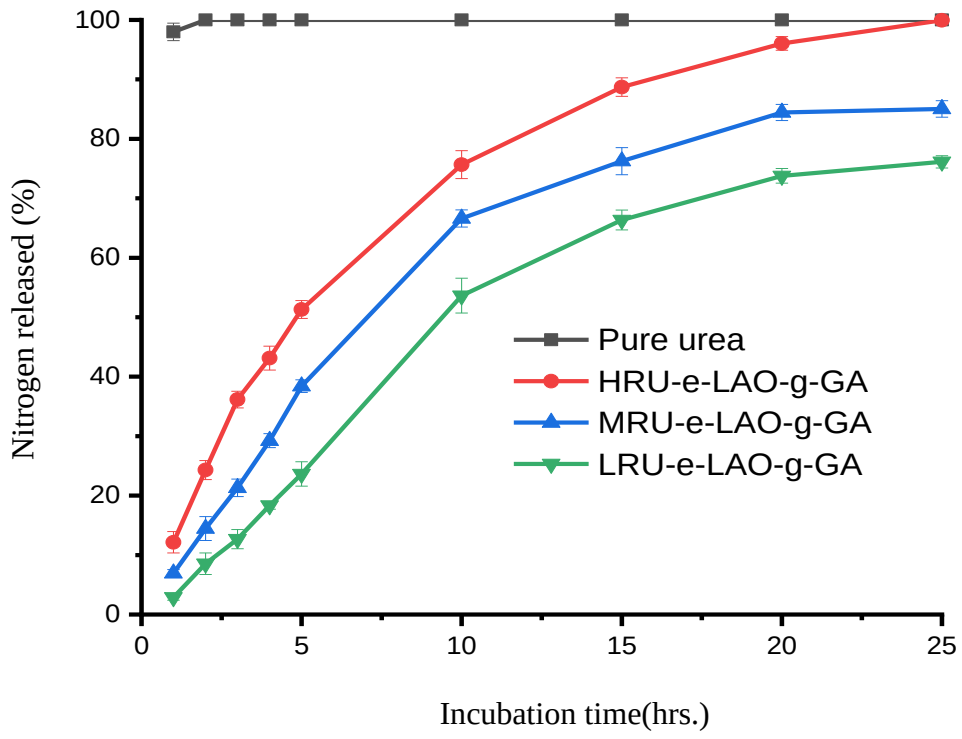

Figure 4.18. Nitrogen release rate in water

As illustrated in Appendix-5B and Appendix-10, the percent of nitrogen release rate for U-e-LAO-g-GAs, which was determined by using Kjeldhal method is almost similar to the percent of urea release rate, which was evaluated by measuring its refractive index using ABBE Digital Refractometer. Therefore, it is possible to use either of the two methods to determine the release rate of a synthesized U-e-LAO-g-GA.

The nitrogen release kinetics for all the mathematical model equations is shown in Table 4.6 below and their linear fit graphs were illustrated in Appendices-11-14. For Korsmeyer-Peppas model, the fraction of nitrogen release used was only below 60%, because of a large difference between experimental results and model calculation data above 60% nitrogen release (Kaavessina et al., 2021). The nutrient release mechanism can be classified as diffusion control, erosion control or a combination of those mechanisms. Higuchi model is applicable if the release of nutrient is largely governed by diffusion through water-filled pores in the matrix and a good fit to Korsmeyer–Peppas equation indicates a combined effect of diffusion and erosion mechanisms for nutrient release (Limmatvapirat et al., 2008). In this case, the release kinetics shows a good fit on to Higuchi equation with the correlation coefficient ($R^2 > 0.96$) for all U-e-LAO-g-GAs (i.e., $R^2 = 0.969$ for HRU-e-LAO-g-GA, $R^2 = 0.962$ for MRU-e-LAO-g-GA, and $R^2 = 0.972$ for LRU-e-LAO-g-GA), suggests that the release mechanism might be a diffusion-controlled release. However, the release kinetics has a best fit on Korsmeyer-Peppas equation relative to the other model equations with correlation coefficient ($R^2 > 0.99$) for all U-e-LAO-g-GAs (i.e., $R^2 = 0.993$ for HRU-e-LAO-g-GA, $R^2 = 0.999$ for MRU-e-LAO-g-GA, and $R^2 = 0.992$ for LRU-e-LAO-g-GA), implies the release mechanism was not a pure diffusion controlled release rather it was a combined effect of diffusion and erosion release mechanisms. Besides, since all U-e-LAO-g-GAs have a good fit on the Korsmeyer-Peppas equation the type of diffusion can be determined by calculating the release exponent (n). If the value of release exponent (n) is less than 0.45, it is Fichian diffusion release, n lies between 0.45 and 0.89 for anomalous transport (non Fickian diffusion release), n is 0.89 for case II transport through swelled matrixes and for super case II transport, the value of n is greater than 0.89 (Ahmed et al., 2019; Bhuyan et al., 2018). In this case as shown in the Table 4.6 below, the value of the release exponent (n) in in all U-e-LAO-g-GAs were greater than 0.89 (i.e., n = 0.899 for HRU-e-LAO-g-GA, n = 1.05 for MRU-e-LAO-g-GA, and n = 1.288 for LRU-e-LAO-g-GA)**,** indicating that the nitrogen released from the U-e-LAO-g-GAs followed the super case-II

transport mechanism. This is done by an erosion mechanism and macromolecular relaxation of the LAO-g-GA chains (Kopač et al., 2021; Limmatvapirat et al., 2008).

Table 4.6. Modeling of the release kinetics data for U-e-LAO-g-GAs

Kinetic models		Sample Code		
		HRU-e-LAO-g-GA	MRU-e-LAO-g-GA	LRU-e-LAO-g-GA
Korsmeyer-Peppas	$K_i(hr^{-n})$	0.12608	0.06911	0.03097
	n	0.89929	1.05004	1.28844
	R^2	0.9932	0.99905	0.99923
Higuchi	$K_H(g/hr^{1/2})$	1.68729	1.61635	1.55171
	R^2	0.9693	0.96274	0.97296
Zero order	$K_0(g/hr)$	0.26456	0.25419	0.24745
	R^2	0.88769	0.88691	0.92165
1^{st} order	K(g/hr)	0.06838	0.08599	0.11141
	R^2	0.69547	0.71056	0.7265
Best fit model		Korsmeyer-Peppas	Korsmeyer-Peppas	Korsmeyer-Peppas
Type of diffusion		Super Case II Transport	Super Case II Transport	Super Case II Transport

From the U-e-LAO-g-GA, nitrogen probably diffuses through its outer layer that erodes and droplets containing dissolved nitrogen released into the aqueous medium. This conclusion is supported by the visual observation of the U-e-LAO-g-GA (i.e., MRU-e-LAO-g-GA) before and after release in the test solutions. The photograph in the Figure 4.19a shows at the time when the samples were immersed/before they undergo erosion, whereas photograph in Figure 4.19b shows that the U-e-LAO-g-GA starts to erode after 5 hours of incubation and the droplets that contain the nitrogen diffuses in to the aqueous medium. And after a long time of incubation (24hrs), it is clearly visible that the eroded parts of the U-e-LAO-g-GA undergo floating over water as shown in the Figure 4.19c. The results from the evaluation of nitrogen release mechanism using various kinetic models and the experimental observations confirms that the release kinetics of nitrogen from the U-e-LAO-g-GAs was with a combined effect of erosion and diffusion mechanisms.

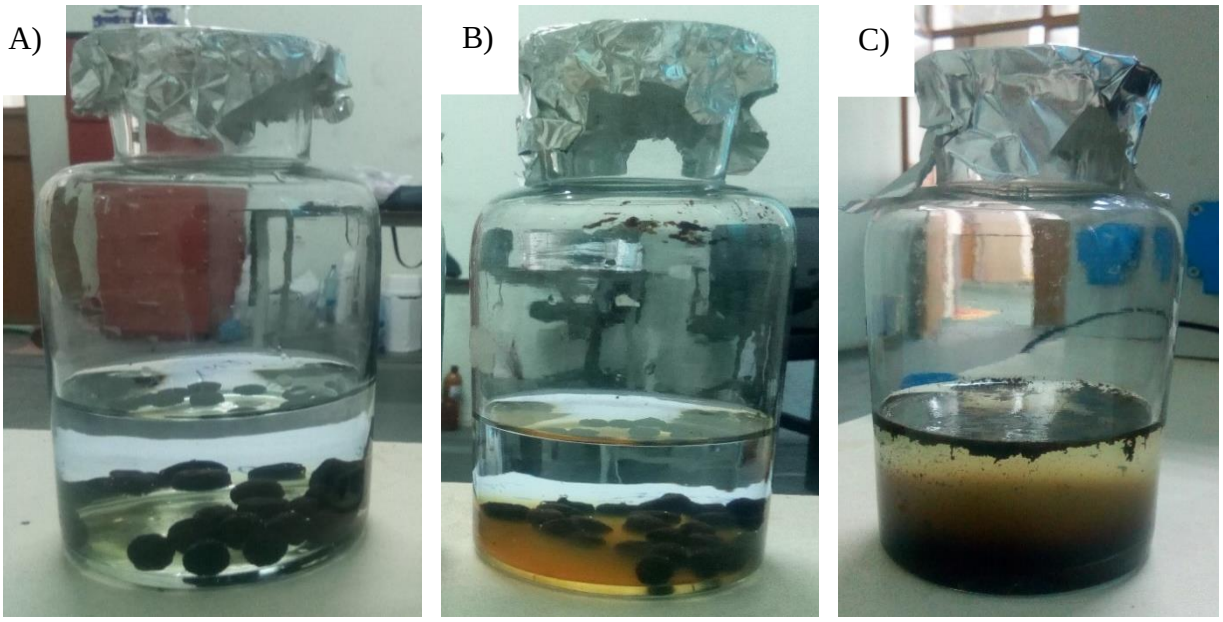

Figure 4.19. A photograph shows the combined effects of erosion and diffusion on the release of N from the U-e-LAO-g-GAs in water. A) at the time of immersion, B) after 5hrs, and C) after 24hrs of incubation.

The erosion (hydrolytic degradation) of U-e-LAO-g-GA's was also confirmed by measuring the acidity (pH) change of the solution over time. The chemical hydrolysis that might take place during the immersion of U-e-LAO-g-GA in water has the potential to break the ester bonds that are present in the LAO-g-GA. The breaking of ester bonds produces carboxylic acid and alcohol. In fact, the presence of carboxylic acid affects the solution's acidity. Instead, when urea dissolves in water, it initially has a tendency to be alkaline (Kaavessina et al., 2021). The combined properties of urea and carboxylic acid dissolved in water were therefore described by the observed pH values of solutions. The similar tendency was present in all samples of U-e-LAO-g-GAs, as shown in table 4.7 below. Over the immersion time range, the pH progressively increases and then starts to decline for all U-e-LAO-g-GAs. This is because, initially, the release of urea from the U-e-LAO-g-GAs raises the pH of the solution, but when LAO-g-GA begins to break down, the rise in carboxylic acid causes the pH of the solution to decline.

Table 4.7. Changes in acidity (pH) during the nitrogen release test

Time (hrs)	pH of the solutions		
	HRU-e-LAO-g-GA	MRU-e-LAO-g-GA	LRU-e-LAO-g-GA
0	7.00 ± 0.02	7.00 ± 0.02	7.00 ± 0.02
1	7.42 ± 0.01	7.31 ± 0.04	7.15 ± 0.01
3	7.47 ± 0.02	7.36 ± 0.01	7.21 ± 0.03
5	7.37 ± 0.04	7.42 ± 0.01	7.26 ± 0.02
7	7.32 ± 0.04	7.39 ± 0.02	7.32 ± 0.02
9	7.26 ± 0.02	7.36 ± 0.03	7.35 ± 0.04
11	7.19 ± 0.03	7.33 ± 0.03	7.39 ± 0.02
13	7.13 ± 0.02	7.28 ± 0.02	7.36 ± 0.03
15	7.08 ± 0.01	7.23 ± 0.04	7.33 ± 0.03
17	7.01 ± 0.06	7.19 ± 0.01	7.28 ± 0.02
19	6.94 ± 0.02	7.16 ± 0.06	7.24 ± 0.02
21	6.87 ± 0.02	7.12 ± 0.02	7.19 ± 0.04
23	6.82 ± 0.01	7.09 ± 0.02	7.14 ± 0.06
25	6.75 ± 0.02	7.04 ± 0.01	7.11 ± 0.02

The acidity of the solutions also exhibits that the hydrolytic degeradation of a U-e-LAO-g-GAs depends on the grafting efficiency of the LAO-g-GAs in which the U-e-LAO-g-GAs were formulated. As illustrated in the Table 4.7, the hydrolytic degradation decreases when the grafting efficiency of LAO-g-GA increases. This is becouse at high grafting efficiency of LAO-g-GA, the gap between the molecular chains becomes narrow and its surface streangth increases, accordingly, the amount water penetrated through the gap as well as through its surface, which causes to break down the ester bonds, decreases. And also the time at which the pH of all U-e-LAO-g-GAs starts to decline was different, this implies, the initial degradation time for those U-e-LAO-g-GAs was different. As illustrated in the Table 4.7, the pH valus for the samples coded HRU-e-LAO-g-GA, MRU-e-LAO-g-GA, and LRU-e-LAO-g-GA starts to decline after 3, 5 and 11hrs of incubation, respectively. This implies the hydrolytic degradation time of HRU-e-LAO-g-GA, MRU-e-LAO-g-GA, and LRU-e-LAO-g-GA was initiated around 3, 5 and 11hrs of incubation, respectively.

5. CONCLUSION AND RECOMMENDATION

5.1. Conclusion

A new type of controlled dissolution rate fertilizer with an improved soil degradation rate was formulated successfully by encapsulating urea into a biodegradable lactic acid oligomer grafted gum acacia (LAO-g-GA). The properties of a synthesized LAO-g-GA as well as the urea encapsulated lactic acid oligomer grafted gum acacia (U-e-LAO-g-GA) were characterized using different physiochemical techniques. The effect of independent variables (i.e., reaction temperature, reaction time, and GA to LA mixing ratio) on the grafting efficiency of LAO-g-GAs, and on the urea release rate of U-e-LAO-g-GAs was studied. The results exhibits that the grafting efficiency of LAO-g-GAs and the urea release rate of U-e-LAO-g-GAs were inversely proportional. When the grafting efficiency reach's it's maximum value (66.12%) (at reaction temperature 180 ^{0}C, reaction time 2hrs, and GA to LA mixing ratio 10.4 w/w%), the urea release rate reach's it's minimum value (15.3%). The grafting of lactic acid oligomer (LAO) chains at O-H and N-H functional groups of gum acacia (GA) backbone was confirmed with the help of FTIR and NMR analyses. The effect of the grafting efficiency of LAO-g-GA on its solubility and hydrophobicity was also studied. The results exhibits that as the grafting efficiency of LAO-g-GA increases, both its solubility in chloroform and its hydrophobicity increases. The LAO-g-GA(l), which have the highest grafting efficiency (66.12%) has a high percentage solubility in chloroform (77.5%), whereas LAO-g-GA (h), which have the lowest grafting efficiency (41.5%) has a low percentage solubility (57.6%). Similarly, the hydrophobicity of LAO-g-GA(l), which was evaluated using contact angle analysis, results, the maximum contact angle (79^0) (high hydrophobicity) was obtained at maximum grafting efficiency (66.12%), whereas a minimum contact angle (39^0) (low hydrophobicity) was obtained at minimum grafting efficiency (41.5%). The effect of pH, temperature, and urea concentration on the urea release rate of U-e-LAO-g-GAs was also determined. Since, the increase in temperature causes to increases the molecular diffusion rate of urea in the LAO-g-GAs, the urea release rate increases with the increase in temperature. Similarly, as the urea concentration encapsulated into the LAO-g-GA increases, the urea release rate also increases. This is due to, the large amount of urea encapsulated into the LAO-g-GAs causes to expand its molecular chains. But, when the pH of the medium increases, the amount of urea released from U-e-LAO-g-GA decreases, this is due to the increase in the interaction between

the carboxyl groups of LAO-g-GA and the amine groups of urea. The soil degradation rate and the urea release rate in soil were also studied. The commercial urea (pure urea) degrades completely within 3 days of incubation in the soil, whereas those U-e-LAO-g-GAs coded HRU-e-LAO-g-GA, MRU-e-LAO-g-GA, and LRU-e-LAO-g-GA losses only 40.8%, 25.5%, and 18.8% of their weights, respectively with in the first 3days incubation. This indicates that all U-e-LAO-g-GAs were degraded in soil, but it takes longer time to be fully decompose relative to the commercial urea fertilizer. The degradation rate of U-e-LAO-g-GAs decrease with the increase in grafting efficiency of LAO-g-GA. And as the urea concentration encapsulated into LAO-g-GA increases, the soil degradation rate also increases. The total nitrogen release rate of U-e-LAO-g-GAs as compared with pure urea in water was studied using Kjeldhal method. And the release kinetics of nitrogen from U-e-LAO-g-GAs was studied using four different kinetic models. From those model equations Korsmeyer-Peppas equation has a best fit with correlation coefficients ($R^2 > 0.99$) for all U-e-LAO-g-GAs, and the value of the release exponent (n) in all U-e-LAO-g-GAs were greater than 0.89. This indicates that the nitrogen release from the U-e-LAO-g-GA**s** followed the super case-II transport mechanism, and the release kinetics of nitrogen from U-e-LAO-g-GAs was a combined effect of diffusion and erosion controlled releases mechanisms.

Generally, this research revealed a successful controlled dissolution rate fertilizer without residue that damages the soil structure and the nutrient balance in the soil, since it degrades completely in the soil. The grafting efficiency of LAO-g-GA can be controlled by varying the values of its synthesizing factors (i.e. reaction temperature, reaction time and GA to LA mixing ratio) during the poly-condensation reaction of GA and LA. Therefore, since the grafting efficiency is inversely proportional to the nitrogen release rate, accordingly, the control of nitrogen release rate in water was achieved simply by controlling the grafting efficiency of LAO-g-GA.

5.2. Recommendation

- In this study an effective control of the release rate of urea in the water was performed by encapsulating urea into a hydrophobic and biodegradable LAO-g-GA, however further study can be done on its effectiveness study by planting crops and measuring the yield. And the assessment of the costs and feasibility of utilizing a formulated U-e-LAO-g-GA should be done.
- In the present investigation of U-e-LAO-g-GA, the effect parameters such as pH, temperature, and urea concentration on the urea release rate shows an excellent characteristic. However, the effect of parameters such as urease enzyme and other micro-organisms present in soil should be considered.
- The synthesized LAO-g-GA, which was used to formulate a U-e-LAO-g-GA also shows an excellent characteristic in its grafting efficiency, solubility, and hydrophobicity tests, however, it needs further characterization for further engineering applications other than a urea holding matrix.
- Since, the hydrolytic degradation of the synthesized LAO-g-GA can be controlled by controlling the grafting efficiency of LAO on the backbone of GA, and since it is nontoxic, it can be used especially for a controlled drug delivery system.

REFERENCES

Abalos, D., Jeffery, S., Sanz-Cobena, A., Guardia, G., & Vallejo, A. (2014). Meta-analysis of the effect of urease and nitrification inhibitors on crop productivity and nitrogen use efficiency. *Agriculture, Ecosystems and Environment*, *189*, 136–144.

Abd El-Aziz, M. E., Salama, D. M., Morsi, S. M. M., Youssef, A. M., & El-Sakhawy, M. (2021). Development of polymer composites and encapsulation technology for slow-release fertilizers. *Reviews in Chemical Engineering*.

Abdelrahman, M., Alwossabi, A., Elamin, E. S., & Ahmed, E. M. M. (2021). Natural Excipients Applications in Conventional Pharmaceutical Formulations-Part I Medicinal & Aromatic Plants Natural Excipients Applications in Conventional Pharmaceutical Formu-lations-Part I. *Medicinal & Aromatic Plants*, *10*(7), 1–10. https://www.researchgate.net/publication/353879340

Adebayo, E. F., Tame, V. T., Mavakumba, H., & Joseph, J. (2021). *2 3 4 5*. *October*.

Affendi, N. M. N., Mansor, N., & Mathialagan, R. (2020). Development and characterization of allicin using palm stearin as a binder on urea granules. *Journal of Plant Nutrition*, *43*(5), 621–628.

Ahmed, L., Atif, R., Eldeen, T. S., Yahya, I., Omara, A., & Eltayeb, M. (2019). Study the Using of Nanoparticles as Drug Delivery System Based on Mathematical Models for Controlled Release. *International Journal of Latest Technology in Engineering, Management & Applied Science*, *8*(5), 52–56.

Ali, M., Maqsood, M. A., Aziz, T., & Awan, M. I. (2020). Neem (Azadirachta indica) oil coated urea improves nitrogen use efficiency and maize growth in an alkaline calcareous soil. *Pakistan Journal of Agricultural Sciences*, *57*(3), 675–684.

Amalraj, A., Haponiuk, J. T., Thomas, S., & Gopi, S. (2020). Preparation, characterization and antimicrobial activity of polyvinyl alcohol/gum arabic/chitosan composite films incorporated with black pepper essential oil and ginger essential oil. *International Journal of Biological Macromolecules*, *151*, 366–375.

Ambrosio-Martín, J., Fabra, M. J., Lopez-Rubio, A., & Lagaron, J. M. (2015). Melt polycondensation to improve the dispersion of bacterial cellulose into polylactide via melt compounding: enhanced barrier and mechanical properties. *Cellulose*, *22*(2), 1201–1226.

Ameen, S. M. (2017). *Springer briefs in molecular science lactic acid in the food industry*.

An, X., Wu, Z., Qin, H., Liu, X., He, Y., Xu, X., Li, T., & Yu, B. (2021). Integrated co-pyrolysis and coating for the synthesis of a new coated biochar-based fertilizer with enhanced slow-release performance. *Journal of Cleaner Production*, *283*, 124642.

Antille, D. L., Hoekstra, N. J., & Lalor, S. T. J. (2015). Field-Scale Evaluation of Calcium Ammonium Nitrate, Urea, and Urea Treated with N-(N-Butyl) Thiophosphoric Triamide Applied to Grassland in Ireland. *Communications in Soil Science and Plant Analysis*, *46*(11), 1345–1361.

Azeem, B., KuShaari, K., & Man, Z. (2016). Effect of Coating Thickness on Release Characteristics of Controlled Release Urea Produced in Fluidized Bed Using Waterborne Starch Biopolymer as Coating Material. *Procedia Engineering*, *148*(December), 282–289.

Azeem, B., KuShaari, K., Naqvi, M., Keong, L. K., Almesfer, M. K., Al-Qodah, Z., Naqvi, S. R., & Elboughdiri, N. (2020). Production and characterization of controlled release urea using biopolymer and geopolymer as coating materials. *Polymers*, *12*(2), 1–30.

Banea, M. D., & Da Silva, L. F. M. (2009). Adhesively bonded joints in composite materials: An overview. *Proceedings of the Institution of Mechanical Engineers, Part L: Journal of Materials: Design and Applications*, *223*(1), 1–18.

Barak, S., Mudgil, D., & Taneja, S. (2020). Exudate gums: chemistry, properties and food applications – a review. *Journal of the Science of Food and Agriculture*, *100*(7), 2828–2835.

Bealer, E. J., Onissema-karimu, S., Rivera-galletti, A., Francis, M., Wilkowski, J., & Hu, X. (2020). Protein – Polysaccharide Composite Materials : *Polymers*, 1–28.

Beig, B., Niazi, M. B. K., Jahan, Z., Hussain, A., Zia, M. H., & Mehran, M. T. (2020). Coating materials for slow release of nitrogen from urea fertilizer: a review. *Journal of Plant Nutrition*, *43*(10), 1510–1533.

Bhuyan, M. M., Okabe, H., Hidaka, Y., Dafader, N. C., Rahman, N., & Hara, K. (2018). Synthesis of pectin-N, N-dimethyl acrylamide hydrogel by gamma radiation and application in drug delivery (in vitro). *Journal of Macromolecular Science, Part A: Pure and Applied Chemistry*, *55*(4), 369–376.

Byrne, M. P., Tobin, J. T., Forrestal, P. J., Danaher, M., Nkwonta, C. G., Richards, K., Cummins, E., Hogan, S. A., & O'Callaghan, T. F. (2020). Urease and nitrification inhibitors-As mitigation tools for greenhouse gas emissions in sustainable dairy systems: A

review. *Sustainability (Switzerland)*, *12*(15), 1–35.

Cantarella, H., Otto, R., Soares, J. R., & Silva, A. G. de B. (2018). Agronomic efficiency of NBPT as a urease inhibitor: A review. *Journal of Advanced Research*, *13*, 19–27.

Castillo Martinez, F. A., Balciunas, E. M., Salgado, J. M., Domínguez González, J. M., Converti, A., & Oliveira, R. P. de S. (2013). Lactic acid properties, applications and production: A review. *Trends in Food Science and Technology*, *30*(1), 70–83.

Castro-Enríquez, D. D., Rodríguez-Félix, F., Ramírez-Wong, B., Torres-Chávez, P. I., Castillo-Ortega, M. M., Rodríguez-Félix, D. E., Armenta-Villegas, L., & Ledesma-Osuna, A. I. (2012). Preparation, characterization and release of urea from wheat gluten electrospun membranes. *Materials*, *5*(12), 2903–2916.

Chen, S., Yang, M., Ba, C., Yu, S., Jiang, Y., Zou, H., & Zhang, Y. (2018). Preparation and characterization of slow-release fertilizer encapsulated by biochar-based waterborne copolymers. *Science of the Total Environment*, *615*, 431–437.

Chezanoglou, E., & Goula, A. M. (2021). Co-crystallization in sucrose: A promising method for encapsulation of food bioactive components. *Trends in Food Science and Technology*, *114*(February), 262–274.

Cui, C., & Liu, W. (2021). Recent advances in wet adhesives: Adhesion mechanism, design principle and applications. *Progress in Polymer Science*, *116*, 101388.

Dimkpa, C. O., Andrews, J., Fugice, J., Singh, U., Bindraban, P. S., Elmer, W. H., Gardea-Torresdey, J. L., & White, J. C. (2020). Facile Coating of Urea With Low-Dose ZnO Nanoparticles Promotes Wheat Performance and Enhances Zn Uptake Under Drought Stress. *Frontiers in Plant Science*, *11*(February), 1–12.

Dimkpa, C. O., Fugice, J., Singh, U., & Lewis, T. D. (2020). Development of fertilizers for enhanced nitrogen use efficiency – Trends and perspectives. *Science of the Total Environment*, *731*, 139113.

Ding, H., Zhang, Y. S., Li, W. H., Zheng, X. Z., Wang, M. K., Tang, L. N., & Chen, D. L. (2016). Nutrients Release from a Novel Gel-Based Slow/Controlled Release Fertilizer. *Applied and Environmental Soil Science*, *2016*.

Dórame-Miranda, R. F., Rodríguez-Félix, D. E., López-Ahumada, G. A., Castro-Enriquez, D. D., Quiroz-Castillo, J. M., Márquez-Ríos, E., & Rodríguez-Félix, F. (2018). Effect of pH and temperature on the release kinetics of urea from wheat-gluten membranes obtained by

electrospinning. *Polymer Bulletin*, *75*(11), 5305–5319.

El-Ghamry, A., El-Naggar, E. S., Elgorban, A. M., Gao, B., Ahmad, Z., & Mosa, A. (2021). Double coating as a novel technology for controlling urea dissolution in soil: A step toward improving the sustainability of nitrogen fertilization approaches. *Sustainability (Switzerland)*, *13*(19).

El Assimi, T., Blažic, R., Vidović, E., Raihane, M., El Meziane, A., Baouab, M. H. V., Khouloud, M., Beniazza, R., Kricheldorf, H., & Lahcini, M. (2021). Polylactide/cellulose acetate biocomposites as potential coating membranes for controlled and slow nutrients release from water-soluble fertilizers. *Progress in Organic Coatings*, *156*(April).

Feng, C., Lü, S., Gao, C., Wang, X., Xu, X., Bai, X., Gao, N., Liu, M., & Wu, L. (2015). "smart" Fertilizer with Temperature- and pH-Responsive Behavior via Surface-Initiated Polymerization for Controlled Release of Nutrients. *ACS Sustainable Chemistry and Engineering*, *3*(12), 3157–3166.

Fertahi, S., Bertrand, I., Ilsouk, M., Oukarroum, A., Amjoud, M. B., Zeroual, Y., & Barakat, A. (2020). New generation of controlled release phosphorus fertilizers based on biological macromolecules: Effect of formulation properties on phosphorus release. In *International Journal of Biological Macromolecules* (Vol. 143).

Fertahi, S., Ilsouk, M., Zeroual, Y., Oukarroum, A., & Barakat, A. (2021). Recent trends in organic coating based on biopolymers and biomass for controlled and slow release fertilizers. *Journal of Controlled Release*, *330*(September 2020), 341–361.

Fu, J., Wang, C., Chen, X., Huang, Z., & Chen, D. (2018). Classification research and types of slow controlled release fertilizers (SRFs) used - a review. *Communications in Soil Science and Plant Analysis*, *49*(17), 2219–2230.

Gafar, S. M., & Abdel-Kader, N. M. (2020). Dosimetric characteristics and applications of cross-linking and degradation of a natural biopolymer Gum Acacia. *Radiochimica Acta*, *108*(3), 223–229.

Galloway, J. N., Townsend, A. R., Erisman, J. W., Bekunda, M., Cai, Z., Freney, J. R., Martinelli, L. A., Seitzinger, S. P., & Sutton, M. A. (2008). Transformation of the nitrogen cycle: Recent trends, questions, and potential solutions. *Science*, *320*(5878), 889–892.

Ganetri, I., Essamlali, Y., Amadine, O., Danoun, K., Aboulhrouz, S., & Zahouily, M. (2021). Controlling factors of slow or controlled-release fertilizers. In *Controlled Release*

Fertilizers for Sustainable Agriculture. Elsevier Inc.

Gopinath, V., Saravanan, S., Al-Maleki, A. R., Ramesh, M., & Vadivelu, J. (2018). A review of natural polysaccharides for drug delivery applications: Special focus on cellulose, starch and glycogen. *Biomedicine and Pharmacotherapy*, *107*(April), 96–108.

Gungula, D. T., Andrew, F. P., Joseph, J., Kareem, S. A., Barminas, J. T., Adebayo, E. F., Saddiq, A. M., Tame, V. T., Dere, I., Ahinda, W. J., & Ator, R. (2021). Formulation and characterization of water retention and slow-release urea fertilizer based on Borassus aethiopum starch and Maesopsis eminii hydrogels. *Results in Materials*, *12*, 100223.

Gupta, A., & Hussain, N. (2014). A critical study on the use, application and effectiveness of organic and inorganic fertilizers. *Journal of Industrial Pollution Control*, *30*(2), 191–193.

Hammad, H. M., Khaliq, A., Abbas, F., Farhad, W., Fahad, S., Aslam, M., Shah, G. M., Nasim, W., Mubeen, M., & Bakhat, H. F. (2020). Comparative Effects of Organic and Inorganic Fertilizers on Soil Organic Carbon and Wheat Productivity under Arid Region. *Communications in Soil Science and Plant Analysis*, *51*(10), 1406–1422.

Hasanuzzaman, M., Fujita, M., Oku, H., Nahar, K., & Hawrylak-Nowak, B. (2018). Plant nutrients and abiotic stress tolerance. In *Plant Nutrients and Abiotic Stress Tolerance*.

Heinrich, L. A. (2019). Future opportunities for bio-based adhesives-advantages beyond renewability. *Green Chemistry*, *21*(8), 1866–1888.

Hermida, L.; Agustian, J. Slow release urea fertilizer synthesized through recrystallization of urea incorporating natural bentonite using various binders. Environ. Technol. Innov. 2019, 13, 113–121

Herrera, J. M., Rubio, G., Häner, L. L., Delgado, J. A., Lucho-Constantino, C. A., Islas-Valdez, S., & Pellet, D. (2016). Emerging and established technologies to increase nitrogen use efficiency of cereals. *Agronomy*, *6*(2), 11–18.

Heuchan, S. M., Fan, B., Kowalski, J. J., Gillies, E. R., & Henry, H. A. L. (2019). Development of Fertilizer Coatings from Polyglyoxylate-Polyester Blends Responsive to Root-Driven pH Change. *Journal of Agricultural and Food Chemistry*, *67*(46), 12720–12729.

Husby, C. E., Niemiera, A. X., Wright, R. D., & Harris, J. R. (2019). 369 Influence of Temperature and Product on Nutrient Release Patterns of Three Polymer-coated Fertilizers. *HortScience*, *35*(3), 456A – 456.

Hussain, M. J., Karim, A. J. M. S., Solaiman, A. R. M., Islam, M. S., & Rahman, M. (2017). Effect of Urea Super Granule and Prilled Urea on Yield and Yield Attributes of Broccoli

(*Brassica oleracea* var. *italica* L.). *The Agriculturists*, *14*(2), 95–112.

Iftime, M. M., Ailiesei, G. L., Ungureanu, E., & Marin, L. (2019). Designing chitosan based eco-friendly multifunctional soil conditioner systems with urea controlled release and water retention. *Carbohydrate Polymers*, *223*(June), 115040.

Janke, C. K., Moody, P., & Bell, M. J. (2020). Three-dimensional dynamics of nitrogen from banded enhanced efficiency fertilizers. *Nutrient Cycling in Agroecosystems*, *118*(3), 227–247.

Jia, C., Zhang, M., & Lu, P. (2020). Preparation and characterization of polyurethane-/MMT nanocomposite-coated urea as controlled-release fertilizers. *Polymer-Plastics Technology and Materials*, *59*(9), 975–984.

Jintakanon, N., Opaprakasit, P., Petchsuk, A., & Opaprakasit, M. (2008). Controlled-release materials for fertilizer based on lactic acid polymers. *Advanced Materials Research*, *55–57*, 905–908.

Kaavessina, M., Distantina, S., & Shohih, E. N. (2021). A slow-release fertilizer of urea prepared via melt blending with degradable poly(Lactic acid): Formulation and release mechanisms. *Polymers*, *13*(11).

Kalita, N. K., Sarmah, A., Bhasney, S. M., Kalamdhad, A., & Katiyar, V. (2021). Demonstrating an ideal compostable plastic using biodegradability kinetics of poly(lactic acid) (PLA) based green biocomposite films under aerobic composting conditions. *Environmental Challenges*, *3*(January), 100030.

Katiyar, V., & Tripathi, N. (2019). *Functionalizing gum arabic for adhesive and food packaging applications*. *8*(April), 8–11.

Khan, M. J., Malik, A., Zaman, M., Khan, Q., ur Rehman, H., & Kalimullah. (2014). Nitrogen use efficiency and yield of maize crop as affected by Agrotain coated urea in arid calcareous soils. *Soil and Environment*, *33*(1), 1–6.

Komesu, A., Martins Martinez, P. F., Lunelli, B. H., Oliveira, J., Wolf MacIel, M. R., & MacIel Filho, R. (2017). Study of lactic acid thermal behavior using thermoanalytical techniques. *Journal of Chemistry*, *2017*.

Kopač, T., Lisac, A., Mravljak, R., Ručigaj, A., Krajnc, M., & Podgornik, A. (2021). Bacteriophage delivery systems based on composite polyhipe/nanocellulose hydrogel particles. *Polymers*, *13*(16).

Kora, A. J. (2021). Exudate Tree Gums: Properties and Applications. *Polysaccharides*, 205–220.

Kumar, D., Devakumar, C., Kumar, R., Panneerselvam, P., Das, A., & Shivay, Y. S. (2011). Relative efficiency of prilled urea coated with major neem (Azadirachta indica A. Juss) oil components in lowland irrigated rice of the Indo-Gangetic plains. *Archives of Agronomy and Soil Science*, *57*(1), 61–74.

Lamsen, M. R. (2019). *TRACE : Tennessee Research and Creative Exchange Encapsulation of Vitamin D3 in Gum Arabic to Improve Application in Beverages and Enhance Bioavailability*.

Lasisi, A. A., Akinremi, O. O., & Kumaragamage, D. (n.d.). *Efficacy of a new NBPT formulation in reducing ammonia volatilization from urea-based fertilizers*. *i*, 1–34.

Lawrencia, D., Wong, S. K., Low, D. Y. S., Goh, B. H., Goh, J. K., Ruktanonchai, U. R., Soottitantawat, A., Lee, L. H., & Tang, S. Y. (2021). Controlled release fertilizers: A review on coating materials and mechanism of release. *Plants*, *10*(2), 1–26.

Le, P. T., & Nguyen, K. T. (2020). Hydrophobizing cellulose surfaces via catalyzed transesterification reaction using soybean oil and starch. *Heliyon*, *6*(11), e05559.

Li, L.; Sun, Y.; Cao, B.; Song, H.; Xiao, Q.; Yi, W. Preparation and performance of polyurethane/mesoporous silica composites for coated urea. Mater. Des. 2016**,** 99**, 21–25.**

Li, L., Wang, M., Wu, X., Yi, W., & Xiao, Q. (2021). Bio-based polyurethane nanocomposite thin coatings from two comparable POSS with eight same vertex groups for controlled release urea. *Scientific Reports*, *11*(1), 1–12.

Limmatvapirat, S., Limmatvapirat, C., Puttipipatkhachorn, S., Nunthanid, J., Luangtana-anan, M., & Sriamornsak, P. (2008). Modulation of drug release kinetics of shellac-based matrix tablets by in-situ polymerization through annealing process. *European Journal of Pharmaceutics and Biopharmaceutics*, *69*(3), 1004–1013.

Liu, G., Zotarelli, L., Li, Y., Dinkins, D., Wang, Q., & Ozores-Hampton, M. (2014). Controlled-Release and Slow-Release Fertilizers as Nutrient Management Tools 1. *Tampabay.Wateratlas.Usf.Edu*, 1–7.

Liu, L., Shen, T., Yang, Y., Gao, B., Li, Y. C., Xie, J., Tang, Y., Zhang, S., Wang, Z., & Chen, J. (2018). Bio-based Large Tablet Controlled-Release Urea: Synthesis, Characterization, and Controlled-Released Mechanisms. *Journal of Agricultural and Food Chemistry*.

Liu, X., Chen, L., Hua, Z., Mei, S., Wang, P., & Wang, S. (2020). Comparing ammonia

volatilization between conventional and slow-release nitrogen fertilizers in paddy fields in the Taihu Lake region. *Environmental Science and Pollution Research*, *27*(8), 8386–8394.

Llive, L. M., Perullini, M., Santagapita, P. R., Schneider-Teixeira, A., & Deladino, L. (2020). Controlled release of fertilizers from Ca(II)-alginate matrix modified by yerba mate (Ilex paraguariensis) waste. *European Polymer Journal*, *138*(June), 109955.

Lyu, Y., Yang, X., Pan, H., Zhang, X., Cao, H., Ulgiati, S., Wu, J., Zhang, Y., Wang, G., & Xiao, Y. (2021). Impact of fertilization schemes with different ratios of urea to controlled release nitrogen fertilizer on environmental sustainability, nitrogen use efficiency and economic benefit of rice production: A study case from Southwest China. *Journal of Cleaner Production*, *293*, 126198.

Ma, Z., Yue, Y., Feng, M., Li, Y., Ma, X., Zhao, X., & Wang, S. (2019). Mitigation of ammonia volatilization and nitrate leaching via loss control urea triggered H-bond forces. *Scientific Reports*, *9*(1), 1–9.

Madzokere, T. C., Murombo, L. T., & Chiririwa, H. (2020). Nano-based slow releasing fertilizers for enhanced agricultural productivity. *Materials Today: Proceedings*, *45*, 3709–3715.

Maharana, T., Pattanaik, S., Routaray, A., Nath, N., & Sutar, A. K. (2015). Synthesis and characterization of poly(lactic acid) based graft copolymers. In *Reactive and Functional Polymers* (Vol. 93). Elsevier B.V.

McClements, D. J., & Öztürk, B. (2021). Utilization of nanotechnology to improve the handling, storage and biocompatibility of bioactive lipids in food applications. *Foods*, *10*(2), 1–17.

Mishra, M. M., Mishra, D. K., Mishra, P., & Behari, K. (2015). Synthesis and characterization of a novel graft copolymer of partially carboxymethylated guar gum and N-vinylformamide. *Carbohydrate Polymers*, *115*, 776–784.

Mohammadbagheri, Z., Rahmati, A., & Hoshyarmanesh, P. (2021). Synthesis of a novel superabsorbent with slow-release urea fertilizer using modified cellulose as a grafting agent and flexible copolymer. *International Journal of Biological Macromolecules*, *182*, 1893–1905.

Mohammed, A. M. E. (2017). Estimation of the Active Components in Gum Arabic Collected from Western Sudan. *International Journal of Science and Research*, *6*(3), 1262–1282.

Mohanty, S., Nayak, A. K., Bhaduri, D., Swain, C. K., Kumar, A., Tripathi, R., Shahid, M.,

Behera, K. K., & Pathak, H. (2021). Real-time application of neem-coated urea for enhancing N-use efficiency and minimizing the yield gap between aerobic direct-seeded and puddled transplanted rice. *Field Crops Research*, *264*(January), 108072.

Musa, H. H., Ahmed, A. A., & Musa, T. H. (2019). Chemistry, Biological, and Pharmacological Properties of Gum Arabic. *Reference Series in Phytochemistry*, 797–814.

Musa, T. H., Musa, I. H., Osman, W., Campbell, M. C., & Musa, H. H. (2021). A bibliometric analysis of global scientific research output on Gum Arabic. *Bioactive Carbohydrates and Dietary Fibre*, *25*(May 2020), 100254.

Naz, M. Y., & Sulaiman, S. A. (2016). Slow release coating remedy for nitrogen loss from conventional urea: A review. *Journal of Controlled Release*, *225*, 109–120.

Nikolic, V., Velickovic, S., & Popovic, A. (2014). Biodegradation of polystyrene-graft-starch copolymers in three different types of soil. *Environmental Science and Pollution Research*, *21*(16), 9877–9886.

Niu, Y., & Li, H. (2012). Controlled release of urea encapsulated by starch-g-poly(vinyl acetate). *Industrial and Engineering Chemistry Research*, *51*(38), 12173–12177.

Nutrient Release Patterns of Controlled Release Fertilizers Used in. (2010). 1–80.

Olson, R. A., & Kurtz, L. T. (2015). Crop nitrogen requirements, utilization, and fertilization. *Nitrogen in Agricultural Soils*, *22*, 567–604.

Pan, M., Qian, W., Wang, Y., Wu, C., & Huang, H. (2021). Effect of dimethoxymethane (DMM) additive on combustion and emission characteristics under different working conditions in CI engines. *Fuel*, *284*(July 2020), 119304.

Pereira, E.I.; da Cruz, C.C.T.; Solomon, A.; Le, A.; Cavigelli, M.A.; Ribeiro, C. Novel slow-release nanocomposite nitrogen fertilizers: The impact of polymers on nanocomposite properties and function. Ind. Eng. Chem. Res. 2015**,** 54**,** 3717–3725

Qi, Q., Deng, Y., Gu, S., Gao, M., Hasegawa, J. Y., Zhou, G., Lv, X., Lv, W., & Yang, Q. H. (2019). L-Cysteine-Modified Acacia Gum as a Multifunctional Binder for Lithium-Sulfur Batteries. *ACS Applied Materials and Interfaces*, *11*(51), 47956–47962.

Rajan, M., Shahena, S., Chandran, V., & Mathew, L. (2021). Controlled release of fertilizers—concept, reality, and mechanism. In *Controlled Release Fertilizers for Sustainable Agriculture*. Elsevier Inc.

Ransom, C. J., Jolley, V. D., Blair, T. A., Sutton, L. E., & Hopkins, B. G. (2020). Nitrogen

release rates from slow- And controlled-release fertilizers influenced by placement and temperature. *PLoS ONE*, *15*(6 June), 1–21.

Razavi, S., Janfaza, S., Tasnim, N., Gibson, D. L., & Hoorfar, M. (2021). Microencapsulating polymers for probiotics delivery systems: Preparation, characterization, and applications. *Food Hydrocolloids*, *120*(May), 106882.

Rehman, A., Nawaz, M., Chattha, M. U., Khan, I., Chattha, M. B., Hussain, F., Ayub, M. A., Iqbal, M. M., Ahmed, F., Aslam, M. T., Khan, F. A., Kharal, M., & Hassan, M. U. (2021). Neem Coated Urea Improves the Productivity, Nitrogen Use Efficiency and Economic Return of Wheat Crop. *International Journal of Agriculture and Biology*, *26*(3), 450–460.

Reque, P. M., & Brandelli, A. (2021). Encapsulation of probiotics and nutraceuticals: Applications in functional food industry. *Trends in Food Science and Technology*, *114*(May), 1–10.

Riveiro, A., Maçon, A. L. B., del Val, J., Comesaña, R., & Pou, J. (2018). Laser surface texturing of polymers for biomedical applications. *Frontiers in Physics*, *5*(FEB).

Rodríguez-Félix, D. E., Pérez-Martínez, C. J., Castillo-Ortega, M. M., Pérez-Tello, M., Romero-García, J., Ledezma-Pérez, A. S., Del Castillo-Castro, T., & Rodríguez-Félix, F. (2012). PH- and temperature-sensitive semi-interpenetrating network hydrogels composed of poly(acrylamide) and poly(c-glutamic acid) as amoxicillin controlled-release system. *Polymer Bulletin*, *68*(1), 197–207.

Ruser, R., & Schulz, R. (2015). The effect of nitrification inhibitors on the nitrous oxide (N2O) release from agricultural soils-a review. *Journal of Plant Nutrition and Soil Science*, *178*(2), 171–188.

Saha, S. K., Rahman, S. M. A., Rahman, F. H., & Pramanik, S. (2021). *Nanofertlizers-A Potential Alternative to Chemical Fertilizers*. *2*(6), 32–37.

Salarbashi, D., Jahanbin, K., Tafaghodi, M., & Fahmideh-Rad, E. (2021). Prunus armeniaca gum exudates: An overview on purification, structure, physicochemical properties, and applications. *Food Science and Nutrition*, *9*(2), 1240–1255.

Salimi, M., Motamedi, E., Motesharezedeh, B., Hosseini, H. M., & Alikhani, H. A. (2020). Starch-g-poly(acrylic acid-co-acrylamide) composites reinforced with natural char nanoparticles toward environmentally benign slow-release urea fertilizers. *Journal of Environmental Chemical Engineering*, *8*(3), 103765.

Sarkar, A., Biswas, D. R., Datta, S. C., Dwivedi, B. S., Bhattacharyya, R., Kumar, R., Bandyopadhyay, K. K., Saha, M., Chawla, G., Saha, J. K., & Patra, A. K. (2021). Preparation of novel biodegradable starch/poly(vinyl alcohol)/bentonite grafted polymeric films for fertilizer encapsulation. *Carbohydrate Polymers*, *259*(September 2020), 117679.

Schneider, R. V., Waibel, K. A., Arndt, A. P., Lang, M., Seim, R., Busko, D., Bräse, S., Lemmer, U., & Meier, M. A. R. (2018). Sequence-definition in stiff conjugated oligomers. *Scientific Reports*, *8*(1), 6–13.

Seleiman, M. F., Almutairi, K. F., Alotaibi, M., Shami, A., Alhammad, B. A., & Battaglia, M. L. (2021). Nano-fertilization as an emerging fertilization technique: Why can modern agriculture benefit from its use? *Plants*, *10*(1), 1–27.

Sempeho, S. I., Kim, H. T., Mubofu, E., Pogrebnoi, A., Shao, G., & Hilonga, A. (2015). Encapsulated urea-Kaolinite Nanocomposite for controlled release fertilizer formulations. *Journal of Chemistry*, *2015*.

Sha, Z., Lv, T., Staal, M., Ma, X., Wen, Z., Li, Q., Pasda, G., Misselbrook, T., & Liu, X. (2020). Effect of combining urea fertilizer with P and K fertilizers on the efficacy of urease inhibitors under different storage conditions. *Journal of Soils and Sediments*, *20*(4), 2130–2140.

Shan, P., Liu, H., Li, D., Zhou, R., Huang, S., Cai, P., Wang, Z., Lu, Y., Li, Z., & Li, Z. (2021). Thiol-ene Click Chemistry Using Triethylamine Gas as a Promoter to Make Coated Slow-release Fertilizer. *Chemical Engineering Journal Advances*, *8*, 100189.

Silva, I. A. A., de Macedo, O. F. L., Cunha, G. C., Oliveira, R. V. M., & Romão, L. P. C. (2021). Using water hyacinth (Eichhornia crassipes) biomass and humic substances to produce urea-based multi-coated slow release fertilizer. *Cellulose*, *28*(6), 3691–3701.

Singh, B. (2019). Neem coated urea as a source of nitrogen for plants. *Journal of Eco-Friendly Agriculture*, *14*(1), 43–54.

Singh, R. P. (2012). Organic fertilizers: Types, production and environmental impact. In *Organic Fertilizers: Types, Production and Environmental Impact* (Issue May).

Skorupka, M., & Nosalewicz, A. (2021). Ammonia volatilization from fertilizer urea—A new challenge for agriculture and industry in view of growing global demand for food and energy crops. *Agriculture (Switzerland)*, *11*(9).

Sulieman, A. M. E. H. (2018). Gum Arabic as Thickener and Stabilizing Agents in Dairy

Products. In *Gum Arabic: Structure, Properties, Application and Economics*. Elsevier Inc.

Taha, G., Farahat, S., Elnggar, E., & AL Molakab, M. (2016). Creation & Characterization of Different Coated Urea Materials & Their Impact as Controlled Release Fertilizers. *Journal of Soil Sciences and Agricultural Engineering*, *7*(10), 793–800.

Technology, M. O. F., Technology, P., & Sachan, R. (2018). *STUDIES ON HIGH HEAT RESISTANT ACRYLIC ADHESIVE*. 1–54.

Tripathi, N. (2016). *Dedicated to my beloved Parents & little Sister Shalini*.

Tripathi, N., & Katiyar, V. (2018). Lactic acid oligomer (OLLA) grafted gum arabic based green adhesive for structural applications. *International Journal of Biological Macromolecules*, *120*, 711–720.

Umar, W., Czinkota, I., Gulyás, M., Aziz, T., & Hameed, M. K. (2022). Development and characterization of slow release N and Zn fertilizer by coating urea with Zn fortified nano-bentonite and ZnO NPs using various binders. *Environmental Technology and Innovation*, *26*, 102250.

Watson, C. J., Akhonzada, N. A., Hamilton, J. T. G., & Matthews, D. I. (2008). Rate and mode of application of the urease inhibitor N-(n-butyl) thiophosphoric triamide on ammonia volatilization from surface-applied urea. *Soil Use and Management*, *24*(3), 246–253.

Xia, H., Riaz, M., Zhang, M., Liu, B., Li, Y., El-Desouki, Z., & Jiang, C. (2022). Biochar-N fertilizer interaction increases N utilization efficiency by modifying soil C/N component under N fertilizer deep placement modes. *Chemosphere*, *286*(P1), 131594.

Xiaoyu, N., Yuejin, W., Zhengyan, W., Lin, W., Guannan, Q., & Lixiang, Y. (2013). A novel slow-release urea fertiliser: Physical and chemical analysis of its structure and study of its release mechanism. *Biosystems Engineering*, *115*(3), 274–282.

Zafar, N., Niazi, M. B. K., Sher, F., Khalid, U., Jahan, Z., Shah, G. A., & Zia, M. (2021). Starch and polyvinyl alcohol encapsulated biodegradable nanocomposites for environment friendly slow release of urea fertilizer. *Chemical Engineering Journal Advances*, *7*, 100123.

Zhang, L., Tian, H., Zhang, M., Wu, L., Guo, W., Fang, F., Sun, X., Zhong, Z., Du, L., & Liu, Z. (2022). Preparation and Properties of Bio-Based Polyurethane Controlled Release Urea Coating with Photosensitivity. *ACS Omega*, *7*(10), 8558–8569.

Zhang, X., Davidson, E. A., Mauzerall, D. L., Searchinger, T. D., Dumas, P., & Shen, Y. (2015). Managing nitrogen for sustainable development. *Nature*, *528*(7580), 51–59.

Zhao, C., Tian, H., Zhang, Q., Liu, Z., Zhang, M., & Wang, J. (2021). Preparation of urea-containing starch-castor oil superabsorbent polyurethane coated urea and investigation of controlled nitrogen release. *Carbohydrate Polymers*, *253*(July 2020), 117240.

Zonatto, F., Muniz, E. C., Tambourgi, E. B., & Paulino, A. T. (2017). Adsorption and controlled release of potassium, phosphate and ammonia from modified Arabic gum-based hydrogel. *International Journal of Biological Macromolecules*, *105*, 363–369.

Zuki, M. M. M., Jaafar, N. M., Sakimin, S. Z., & Yusop, M. K. (2020). N-(n-Butyl) thiophosphoric triamide (NBPT)-coated urea (NCU) improved maize growth and nitrogen use efficiency (NUE) in highly weathered tropical soil. *Sustainability (Switzerland)*, *12*(21), 1–11.

Zulfiqar, F., Navarro, M., Ashraf, M., Akram, N. A., & Munné-Bosch, S. (2019). Nanofertilizer use for sustainable agriculture: Advantages and limitations. *Plant Science*, *289*(September).

APPENDICES

Appendix-1. The Effect of Three Factors on the Dissolution of U-e-LAO-g-GAs as Preliminary Investigation to Select the Levels of Factors

Samples No.	Reaction Temperature (^{0}C)	GA to LA Mixing ratio	Reaction time (hrs.)	Dissolution time
1	150	1:6	1	7.5 min
2	150	1:6	2	8 min
3	150	1:6	3	9 min
4	150	1:10	1	5.5 min
5	150	1:10	2	6 min
6	150	1:10	3	7 min
7	150	1:14	1	4.5 min
8	150	1:14	2	5.5 min
9	150	1:14	3	6 min
10	180	1:6	1	>2 month
11	180	1:6	2	>2 month
12	180	1:6	3	Unable to disperse urea powder
13	180	1:10	1	>2 months
14	180	1:10	2	>2 months
15	180	1:10	3	>2 months
16	180	1:14	1	>2 months
17	180	1:14	2	>2 months
18	180	1:14	3	>2 months
19	210	1:6	1	Unable to disperse urea powder
20	210	1:6	2	Unable to disperse urea powder
21	210	1:6	3	Unable to disperse urea powder
22	210	1:10	1	>2 months
23	210	1:10	2	Unable to disperse urea powder

24	210	1:10	3	Unable to disperse urea powder
25	210	1:14	1	>2 months
26	210	1:14	2	>2 months
27	210	1:14	3	Unable to disperse urea powder

N.B: This was done after encapsulating the same amount of urea in each synthesized LAO-g-GAs

A) Samples Completely Dissolved Within 4.5 – 9.0 Minutes.

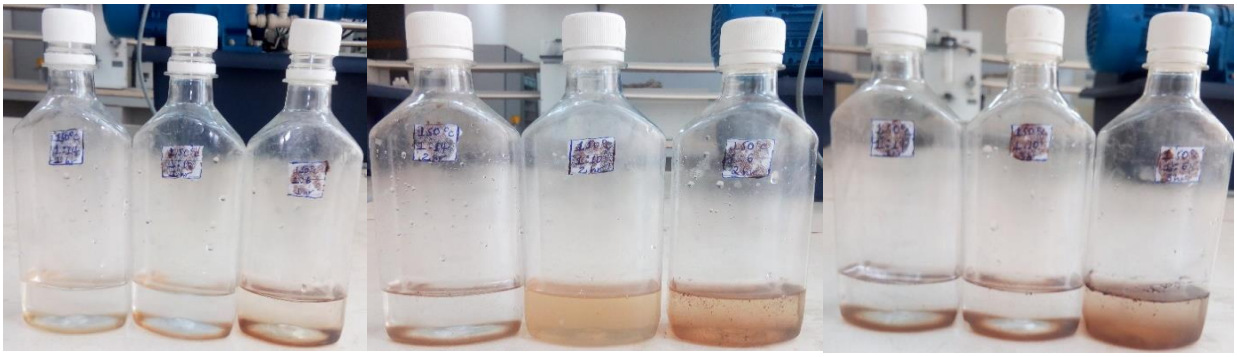

B) Samples Which Are Unable to Disperse Urea Powder (Degraded Samples).

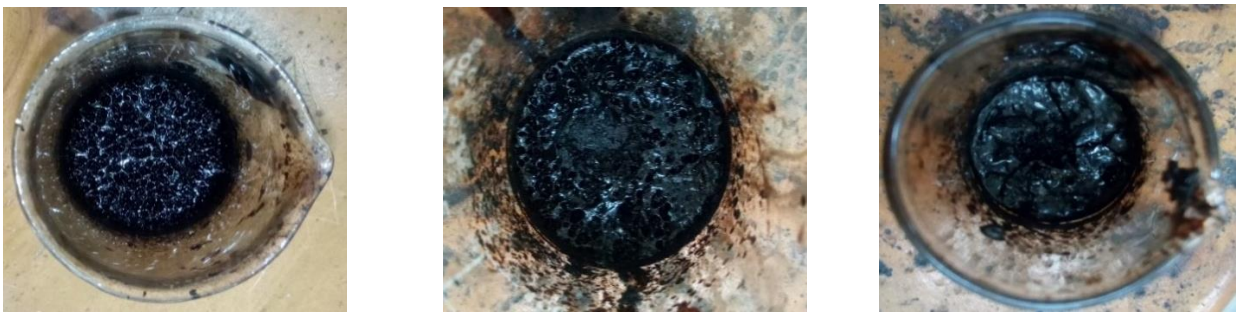

C) Samples that Don't Dissolve Completely Within 2 Months.

Appendix-2. Measured Refractive Index (nD) Values of Pure Urea

Concentration (g/100 mL)	nD-1	nD-2	nD-3	Average nD
0.2	1.33307	1.33306	1.33307	1.333067
0.4	1.33343	1.33339	1.33342	1.3334
0.6	1.33363	1.33360	1.33359	1.333647
0.8	1.33399	1.33399	1.33399	1.33399
1.0	1.33431	1.33430	1.33429	1.3343
1.2	1.33456	1.33453	1.33452	1.334553

Appendix-3. Standard Calibration Curve of Pure Urea

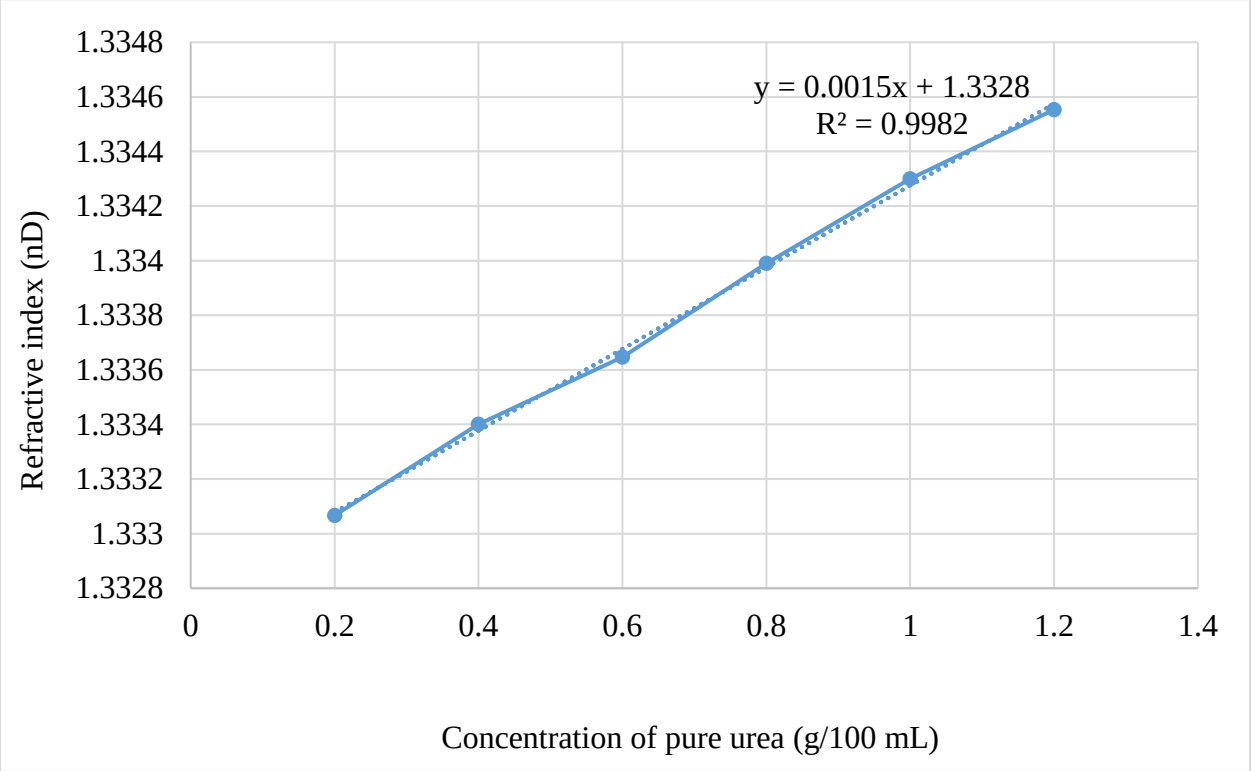

Appendix-4. Contact Angle Image of LAO-g-GAs

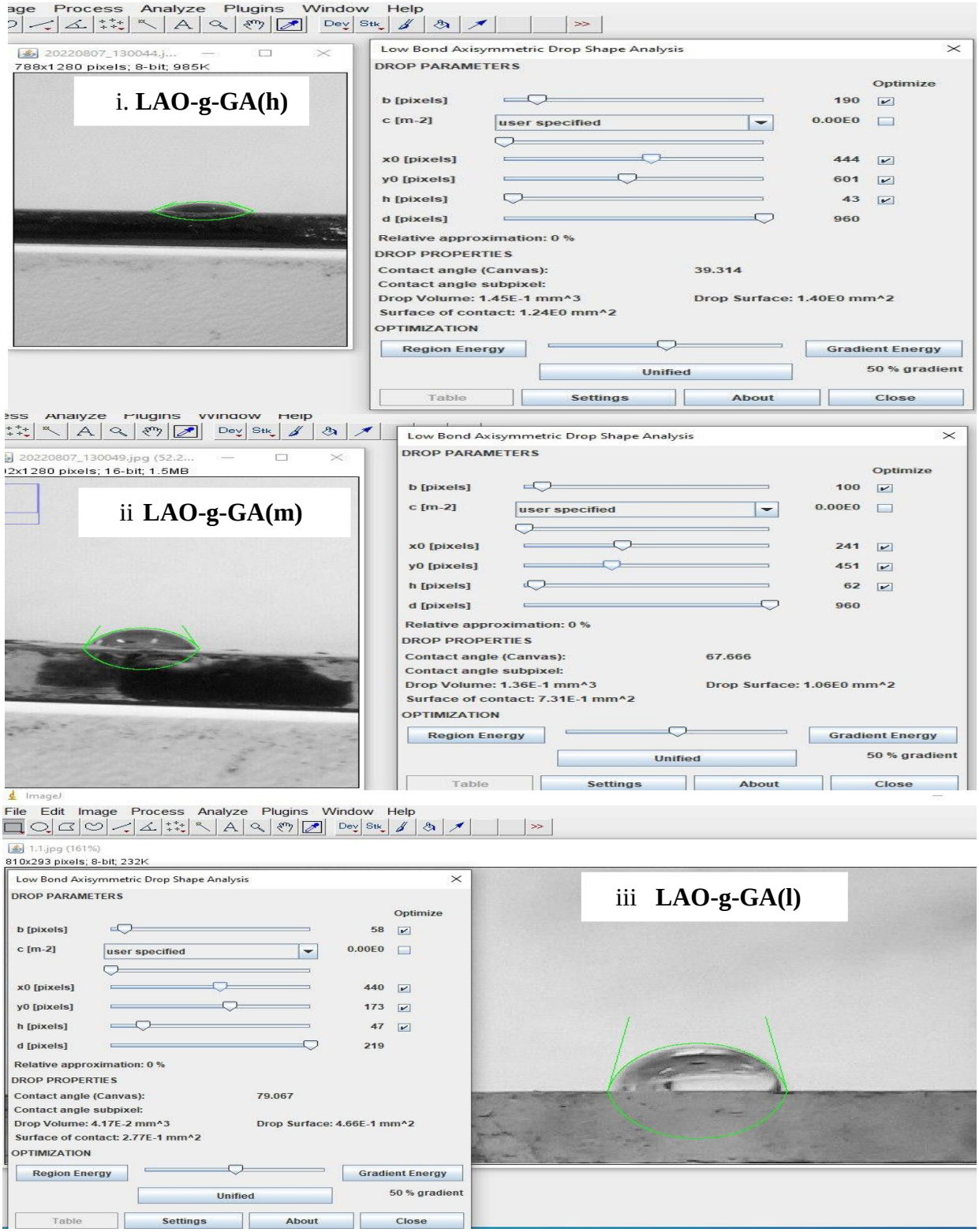

Appendix-5A. The Urea Release Rate (%) for U-e-LAO-g-GAs at pH 4

Time(hrs.)	HRU-e-LAO-g-GA		MRU-e-LAO-g-GA		LRU-e-LAO-g-GA	
	nD-avg	UR-avg (%)	nD-avg	UR-avg (%)	nD-avg	UR-avg (%)
1	1.33622	30.4 ± 0.06	1.33494	19.02 ± 0.06	1.33456	15.65 ± 0.06
3	1.33854	51.06 ± 0.03	1.33729	39.87 ± 0.03	1.33621	30.34 ± 0.03
5	1.34012	65.11 ± 0.09	1.33885	53.78 ± 0.06	1.33751	41.87 ± 0.00
7	1.34132	75.73 ± 0.06	1.33993	63.38 ± 0.06	1.33866	52.09 ± 0.06
9	1.34256	86.76 ± 0.06	1.34096	72.58 ± 0.03	1.33969	61.24 ± 0.00
11	1.34331	93.38 ± 0.03	1.34144	76.84 ± 0.03	1.34028	66.54 ± 0.03
13	1.34365	96.4 ± 0.03	1.34164	78.58 ± 0.06	1.34052	68.6 ± 0.00
15	1.34401	99.69 ± 0.15	1.34188	80.71 ± 0.06	1.34082	71.25 ± 0.03

Appendix-5B. The Urea Release Rate (%) for U-e-LAO-g-GAs at pH 7

Time(hrs.)	HRU-e-LAO-g-GA		MRU-e-LAO-g-GA		LRU-e-LAO-g-GA	
	nD-avg	UR-avg (%)	nD-avg	UR-avg (%)	nD-avg	UR-avg (%)
1	1.33406	13.91 ± 0.03	1.33369	7.96 ± 0.09	1.33317	3.29 ± 0.06
3	1.33697	37.07 ± 0.06	1.33532	22.36 ± 0.03	1.33432	13.56 ± 0.03
5	1.33886	53.91 ± 0.03	1.33722	39.29 ± 0.06	1.33309	25.78 ± 0.06
7	1.34040	67.56 ± 0.06	1.33937	58.44 ± 0.09	1.33752	41.96 ± 0.06
9	1.34127	75.29 ± 0.06	1.34047	68.22 ± 0.03	1.33892	54.44 ± 0.03
11	1.34226	84.09 ± 0.06	1.34110	73.78 ± 0.06	1.33987	62.84 ± 0.06
13	1.34252	86.4 ± 0.06	1.34130	75.56 ± 0.06	1.34018	65.64 ± 0.03
15	1.34297	90.44 ± 0.03	1.34159	78.18 ± 0.03	1.34038	67.42 ± 0.03
17	1.34333	93.64 ± 0.03	1.34181	80.13 ± 0.03	1.34067	70.00 ± 0.03
19	1.34361	96.09 ± 0.00	1.34207	82.4 ± 0.06	1.33280	72.04 ± 0.09
21	1.34382	97.96 ± 0.06	1.34217	83.33 ± 0.09	1.34103	73.2 ± 0.09
23	1.34399	99.51 ± 0.09	1.34222	83.78 ± 0.03	1.34115	74.22 ± 0.06

Appendix-5C. The Urea Release Rate (%) for U-e-LAO-g-GAs at pH 10

Time(hrs.)	HRU-e-LAO-g-GA		MRU-e-LAO-g-GA		LRU-e-LAO-g-GA	
	nD-avg	UR-avg (%)	nD-avg	UR-avg (%)	nD-avg	UR-avg (%)
1	1.33412	11.78 ± 0.06	1.33341	5.47 ± 0.06	1.333055	2.27 ± 0.06
3	1.33658	33.64 ± 0.06	1.33462	16.18 ± 0.00	1.33392	9.96 ± 0.12
5	1.33803	46.49 ± 0.12	1.33597	28.22 ± 0.06	1.33494	18.98 ± 0.18
7	1.33905	55.6 ± 0.06	1.33744	41.24 ± 0.12	1.33632	31.24 ± 0.06
9	1.34004	64.36 ± 0.12	1.33878	53.16 ± 0.00	1.33761	42.76 ± 0.12
11	1.34055	68.93 ± 0.06	1.33962	60.62 ± 0.12	1.33873	52.67 ± 0.06
13	1.34109	73.69 ± 0.12	1.34032	66.89 ± 0.06	1.33938	58.44 ± 0.06
15	1.34165	78.69 ± 0.12	1.34086	71.64 ± 0.12	1.33988	62.89 ± 0.06
17	1.34208	82.49 ± 0.12	1.34130	75.56 ± 0.12	1.34027	66.36 ± 0.06
19	1.34253	86.49 ± 0.12	1.34153	77.64 ± 0.18	1.34052	68.62 ± 0.12
21	1.34298	90.49 ± 0.12	1.34172	79.29 ± 0.12	1.34072	70.4 ± 0.12
23	1.34340	94.22 ± 0.18	1.34192	81.02 ± 0.06	1.34085	71.56 ± 0.5
25	1.34362	96.22 ± 0.09	1.34210	82.63 ± 0.06	1.34097	72.62 ± 0.06
27	1.34377	97.56 ± 0.09	1.34222	83.73 ± 0.06	1.34107	73.47 ± 0.09
29	1.34403	99.82 ± 0.12	1.34237	85.02 ± 0.06	1.34116	74.27 ± 0.06

Appendix-6A. The Urea Release Rate (%) for U-e-LAO-g-GAs at 25 ^{0}C

Time(hrs.)	HRU-e-LAO-g-GA		MRU-e-LAO-g-GA		LRU-e-LAO-g-GA	
	nD-avg	UR-avg (%)	nD-avg	UR-avg (%)	nD-avg	UR-avg (%)
1	1.334265	13.02 ± 0.06	1.33362	7.29 ± 0.12	1.33312	2.8 ± 0.06
3	1.33695	36.84 ± 0.06	1.33518	21.11 ± 0.06	1.33416	12.09 ± 0.12
5	1.33884	53.69 ± 0.12	1.33700	37.33 ± 0.12	1.33563	25.11 ± 0.18
7	1.34036	67.2 ± 0.00	1.33933	58.04 ± 0.12	1.33743	41.11 ± 0.18
9	1.34122	74.84 ± 0.12	1.34046	68.04 ± 0.06	1.33884	53.64 ± 0.06
11	1.34212	82.8 ± 0.06	1.34102	73.07 ± 0.12	1.33977	61.96 ± 0.12

13	1.34247	85.91 ± 0.06	1.34125	75.07 ± 0.06	1.34012	65.02 ± 0.06
15	1.34292	89.96 ± 0.00	1.34155	77.78 ± 0.00	1.34030	66.62 ± 0.18
17	1.34330	93.29 ± 0.18	1.34178	79.78 ± 0.12	1.34060	69.29 ± 0.18
19	1.34356	95.6 ± 0.06	1.34200	81.78 ± 0.12	1.34082	71.24 ± 0.06
21	1.34381	97.87 ± 0.00	1.34217	83.24 ± 0.06	1.34098	72.68 ± 0.06
23	1.34402	99.73 ± 0.12	1.34230	84.44 ± 0.12	1.34108	73.56 ± 0.06

Appendix-6B. The Urea Release Rate (%) for U-e-LAO-g-GAs at 35 ^{0}C

Time(hrs.)	HRU-e-LAO-g-GA		MRU-e-LAO-g-GA		LRU-e-LAO-g-GA	
	nD-avg	UR-avg (%)	nD-avg	UR-avg (%)	nD-avg	UR-avg (%)
1	1.33460	16 ± 0.12	1.33396	10.27 ± 0.06	1.33338	5.16 ± 0.12
3	1.33825	48.44 ± 0.12	1.33570	25.78 ± 0.12	1.33498	19.33 ± 0.06
5	1.34032	66.84 ± 0.12	1.33796	45.82 ± 0.06	1.33663	34 ± 0.06
7	1.34182	80.13 ± 0.06	1.33976	61.87 ± 0.06	1.33823	48.27 ± 0.12
9	1.34242	85.47 ± 0.06	1.34087	71.73 ± 0.12	1.33965	60.89 ± 0.12
11	1.34276	88.49 ± 0.06	1.34125	75.07 ± 0.06	1.34036	67.16 ± 0.06
13	1.34334	93.69 ± 0.12	1.34162	78.36 ± 0.06	1.34063	69.56 ± 0.06
15	1.34355	95.51 ± 0.06	1.34196	81.38 ± 0.06	1.34094	72.36 ± 0.12
17	1.34386	98.27 ± 0.06	1.34202	81.91 ± 0.06	1.34113	74 ± 0.06
19	1.34404	99.87 ± 0.06	1.34218	83.38 ± 0.12	1.34121	74.76 ± 0.00

Appendix-6C. The Urea Release Rate (%) for U-e-LAO-g-GAs at 45 ^{0}C

Time(hrs.)	HRU-e-LAO-g-GA		MRU-e-LAO-g-GA		LRU-e-LAO-g-GA	
	nD-avg	UR-avg (%)	nD-avg	UR-avg (%)	nD-avg	UR-avg (%)
1	1.33546	23.64 ± 0.12	1.33426	12.93 ± 0.06	1.33365	7.56 ± 0.12
3	1.33936	58.27 ± 0.06	1.33635	31.56 ± 0.12	1.33525	21.73 ± 0.06
5	1.34123	74.89 ± 0.18	1.33838	49.56 ± 0.18	1.33689	36.31 ± 0.06
7	1.34212	82.84 ± 0.12	1.33998	63.78 ± 0.06	1.33839	49.69 ± 0.26
9	1.34254	86.58 ± 0.12	1.34113	74.04 ± 0.12	1.33998	63.78 ± 0.06
11	1.34298	90.44 ± 0.06	1.34145	76.84 ± 0.06	1.34067	69.91 ± 0.06
13	1.34344	94.58 ± 0.12	1.34175	79.51 ± 0.06	1.34091	72.09 ± 0.00
15	1.34376	97.38 ± 0.06	1.34213	82.93 ± 0.12	1.34107	73.51 ± 0.12
17	1.34401	99.6 ± 0.32	1.34225	83.96 ± 0.18	1.34134	75.87 ± 0.18

Appendix-7A. The Urea Release Rate (%) for U-e-LAO-g-GAs (70% Urea Concentration)

Time(hrs.)	HRU-e-LAO-g-GA		MRU-e-LAO-g-GA		LRU-e-LAO-g-GA	
	nD-avg	UR-avg (%)	nD-avg	UR-avg (%)	nD-avg	UR-avg (%)
1	1.33407	12.04 ± 0.06	1.33343	5.95 ± 0.20	1.33306	2.43 ± 0.06
3	1.33645	34.71 ± 0.06	1.33482	19.23 ± 0.14	1.33388	10.24 ± 0.06
5	1.33812	50.62 ± 0.06	1.33638	34.05 ± 0.06	1.33499	20.81 ± 0.06
7	1.33958	64.52 ± 0.06	1.33842	53.52 ± 0.14	1.33656	35.81 ± 0.14
9	1.34042	72.52 ± 0.06	1.33944	63.19 ± 0.06	1.33807	50.14 ± 0.06
11	1.34123	80.24 ± 0.06	1.33988	67.38 ± 0.06	1.33892	58.29 ± 0.14
13	1.34167	84.43 ± 0.06	1.34030	71.43 ± 0.14	1.33927	61.57 ± 0.2
15	1.34202	87.76 ± 0.06	1.34067	74.95 ± 0.14	1.33968	65.48 ± 0.06
17	1.34242	91.62 ± 0.00	1.34098	77.86 ± 0.06	1.33996	68.19 ± 0.14
19	1.34274	94.62 ± 0.06	1.34123	80.29 ± 0.14	1.34013	69.76 ± 0.2
21	1.34296	96.86 ± 0.12	1.34142	82.05 ± 0.06	1.34029	71.29 ± 0.06
23	1.34312	98.29 ± 0.14	1.34154	83.24 ± 0.14	1.34042	72.52 ± 0.06
25	1.34328	99.76 ± 0.06	1.34167	84.43 ± 0.06	1.34055	73.76 ± 0.06

Appendix-7B. The Urea Release Rate (%) for U-e-LAO-g-GAs (75% Urea Concentration)

Time(hrs.)	HRU-e-LAO-g-GA		MRU-e-LAO-g-GA		LRU-e-LAO-g-GA	
	nD-avg	UR-avg (%)	nD-avg	UR-avg (%)	nD-avg	UR-avg (%)
1	1.33437	13.91 ± 0.06	1.33370	7.96 ± 0.18	1.33317	3.29 ± 0.12
3	1.33697	37.07 ± 0.12	1.33532	22.36 ± 0.06	1.33433	13.56 ± 0.06
5	1.33887	53.91 ± 0.06	1.33722	39.29 ± 0.12	1.33570	25.78 ± 0.12
7	1.34040	67.56 ± 0.12	1.33938	58.44 ± 0.18	1.33752	41.96 ± 0.12
9	1.34127	75.29 ± 0.12	1.34048	68.22 ± 0.06	1.33893	54.44 ± 0.06
11	1.34226	84.09 ± 0.12	1.34110	73.78 ± 0.12	1.33987	62.84 ± 0.12
13	1.34252	86.4 ± 0.12	1.34130	75.56 ± 0.12	1.34019	65.64 ± 0.06
15	1.34298	90.44 ± 0.06	1.34160	78.18 ± 0.06	1.34039	67.42 ± 0.06
17	1.34334	93.64 ± 0.06	1.34182	80.13 ± 0.06	1.34068	70 ± 0.06
19	1.34361	96.09 ± 0.00	1.34207	82.4 ± 0.12	1.34091	72.04 ± 0.18
21	1.34382	97.96 ± 0.12	1.34218	83.33 ± 0.18	1.34104	73.2 ± 0.18
23	1.34399	99.51 ± 0.18	1.34223	83.78 ± 0.06	1.34115	74.22 ± 0.12

Appendix-7C. The Urea Release Rate (%) for U-e-LAO-g-GAs (80% Urea Concentration)

Time(hrs.)	HRU-e-LAO-g-GA		HRU-e-LAO-g-GA		HRU-e-LAO-g-GA	
	nD-avg	UR-avg (%)	nD-avg	UR-avg (%)	nD-avg	UR-avg (%)
1	1.33466	15.46 ± 0.06	1.33428	12.29 ± 0.06	1.33386	8.79 ± 0.06
3	1.33769	40.71 ± 0.06	1.33684	33.67 ± 0.12	1.33512	19.33 ± 0.12
5	1.33955	56.25 ± 0.12	1.33866	48.83 ± 0.12	1.33646	30.5 ± 0.00
7	1.34102	68.5 ± 0.00	1.33998	59.79 ± 0.06	1.33832	45.96 ± 0.06
9	1.34205	77.08 ± 0.12	1.34113	69.42 ± 0.12	1.33989	59.04 ± 0.06
11	1.34285	83.75 ± 0.00	1.34187	75.58 ± 0.12	1.34072	65.96 ± 0.06
13	1.34341	88.38 ± 0.18	1.34210	77.5 ± 0.12	1.34084	67 ± 0.12
15	1.34365	90.42 ± 0.12	1.34227	78.88 ± 0.06	1.34097	68.04 ± 0.18
17	1.34436	96.29 ± 0.06	1.34274	82.79 ± 0.06	1.34157	73.08 ± 0.12
19	1.34458	98.17 ± 0.06	1.34296	84.67 ± 0.12	1.34173	74.42 ± 0.12
21	1.34478	99.83 ± 0.06	1.34308	85.63 ± 0.06	1.34188	75.67 ± 0.12

Appendix-8. The Urea Release Rate (%) of U-e-LAO-g-GAs in Soil.

Time (days.)	Pure urea		HRU-e-LAO-g-GA		MRU-e-LAO-g-GA		LRU-e-LAO-g-GA	
	nD-avg	UR-avg (%)	nD-avg	UR-avg (%)	nD-avg	UR-avg (%)	nD-avg	UR-avg (%)
1	1.3398	62.22 ± 2.51	1.33522	21.5 ± 3.29	1.33434	13.67± 2.83	1.33383	9.17 ± 1.41
5	1.34153	77.56 ± 3.14	1.33799	46.17 ± 2.53	1.33678	35.33± 1.89	1.33567	25.5 ± 2.36
10	1.34400	99.56 ± 1.26	1.34015	65.33 ± 1.89	1.33886	53.83 ± 2.36	1.33747	41.5 ± 3.29
15	1.34405	100 ± 0.0	1.34182	80.17 ± 2.36	1.34011	65 ± 2.83	1.33865	52 ± 2.83
20	1.34405	100 ± 0.0	1.34296	90.33 ± 2.83	1.34122	74.83 ± 3.29	1.33955	60 ± 1.89
25	1.34405	100 ± 0.0	1.34354	95.5 ± 4.24	1.34167	78.83 ± 2.36	1.34032	66.83 ± 2.36
30	1.34405	100 ± 0.0	1.34390	98.67 ± 0.94	1.34214	83 ± 4.71	1.34090	72 ± 1.89

Appendix-9A. Weight Loss (%) for U-e-LAO-g-GAs (70% Urea Concentration)

Time(days.)	Weight loss (%)		
	HRU-e-LAO-g-GA	MRU-e-LAO-g-GA	LRU-e-LAO-g-GA
0	0	0	0
1	25.8 ± 1.14	10.8 ± 0.71	6.6 ±1.41
3	38.5 ± 2.12	22.2 ± 2.12	14.5 ± 2.12
5	47.8 ± 2.04	31.5 ± 1.41	23.6 ± 1.41
7	61.5 ± 1.27	39.5 ± 1.06	29.5 ± 2.83
9	68.4 ± 1.77	52.4 ± 1.41	38.8 ± 1.41
11	78.2 ± 2.83	59.5 ± 0.71	42.8 ± 1.77
13	82.1 ± 1.41	64.8 ± 1.41	51.3 ± 1.77
15	85.5 ± 2.12	72.5 ± 1.77	54.8 ± 1.41
17	91.5 ± 2.12	76.5 ± 1.77	56.8 ± 0.71
19	94.4 ± 2.04	79.0 ± 1.41	59.1 ± 2.12
21	96.8 ± 0.71	81.5 ± 2.83	62.0 ± 1.41
23	97.5 ± 1..77	82.5 ± 0.71	63.2 ± 2.83
25	98.8 ± 1.41	83.8 ± 1.41	64.8 ± 0.71

Appendix-9B. Weight loss (%) for U-e-LAO-g-GAs (75% Urea Concentration)

Time(days.)	Weight loss (%)			
	Pure urea	HRU-e-LAO-g-GA	MRU-e-LAO-g-GA	LRU-e-LAO-g-GA
0	0	0	0	0
1	71 ± 1	27.5 ± 2.12	12.5 ± 0.71	7.3 ±1.06
3	100 ± 0	40.8 ± 1.77	25.5 ± 1.41	18.8 ± 1.06
5	100 ±0	51.8 ± 1.06	34.5 ± 2.12	27.3 ± 1.77
7	100 ± 0	63.5 ± 1.41	42.5 ± 1.41	34.5 ± 1.41
9	100 ± 0	70.0 ± 1.41	55.0 ± 1.41	43.0 ± 1.41
11	100 ± 0	79.3 ± 1.77	62.3 ± 1.06	48.8 ± 2.47
13	100 ± 0	83.3 ± 1.77	68.3 ± 1.06	57.3 ± 1.77

15	100 ± 0	87.5 ± 1.41	75.0 ± 1.41	58.3 ± 1.06
17	100 ± 0	93.0 ± 2.83	80.0 ± 0.71	59.8 ± 1.77
19	100 ± 0	95.0 ± 0.71	83.0 ± 0.71	62.8 ± 1.77
21	100 ± 0	98.8 ± 0.35	84.5 ± 0.71	66.0 ± 2.12
23	100 ± 0	99.5 ± 0.00	85.8 ± 0.35	67.0 ± 2.12
25	100 ± 0	99.8 ± 0.35	87.8 ± 1.06	68.3 ± 1.77

Appendix-9C. Weight loss (%) for U-e-LAO-g-GAs (80% Urea Concentration)

Time(days.)	Weight loss (%)		
	HRU-e-LAO-g-GA	MRU-e-LAO-g-GA	LRU-e-LAO-g-GA
0	0	0	0
1	29.3 ± 2.83	13.5 ± 1.77	8.8 ±1.41
3	44.4 ± 1.41	27.8 ± 2.12	22.5 ± 1.77
5	53.5 ± 1.77	36.5 ± 1.41	31.6 ± 1.06
7	66.8 ± 1.77	43.8 ± 1.41	36.5 ± 1.77
9	72.6 ± 2.12	56.8 ± 1.77	47.9 ± 1.77
11	81.8 ± 1.41	64.2 ± 2.83	51.5 ± 2.83
13	85.1 ± 0.71	69.3 ± 1.77	59.6 ± 1.41
15	89.4 ± 0.71	77.5 ± 1.77	61.8 ± 1.06
17	96.5 ± 1.41	83.0 ± 1.41	63.4 ± 1.41
19	98.6 ± 1.77	85.6 ± 1.77	65.8 ± 2.12
21	99.2 ± 0.71	87.8 ± 1.41	67.4 ± 1.06
23	99.8 ± 0.00	89.3 ± 0.71	70.0 ± 1.06
25	99.9 ± 0.00	91.8 ± 1.41	72.5 ± 1.41

Appendix-10. The Nitrogen Release Rate (%) for Pure Urea and U-e-LAO-g-GAs at pH 7

Incubation Time(hrs.)	Pure urea	HRU-e-LAO-g-GA	MRU-e-LAO-g-GA	LRU-e-LAO-g-GA
1	98.06 ± 1.47	12.15 ± 1.8	6.94 ± 0.62	2.9 ± 0.49
2	100 ± 0.0	24.3 ± 1.8	14.47 ± 2.01	8.54 ± 1.81
3	100 ± 0.0	36.15 ± 1.7	21.32 ± 1.47	12.68 ± 1.61
4	100 ± 0.0	43.12 ± 1.48	29.24 ± 1.18	18.34 ± 0.64
5	100 ± 0.0	51.67 ± 1.51	38.41 ± 1.05	23.64 ± 2.05
10	100 ± 0.0	75.66 ± 2.35	66.6 ± 1.44	53.63 ± 2.93
15	100 ± 0.0	88.72 ± 1.56	76.25 ± 2.28	66.35 ± 1.67
20	100 ± 0.0	96.05 ± 1.15	84.43 ± 1.36	73.78 ± 1.22
25	100 ± 0.0	99.95 ± 0.07	85.04 ± 1.39	76.14 ± 1.03

Appendix-11. Ln of Nitrogen Release Fraction Vs Ln of Incubation Time Plot Showing Korsmeyer-Peppas Model Linear Fit.

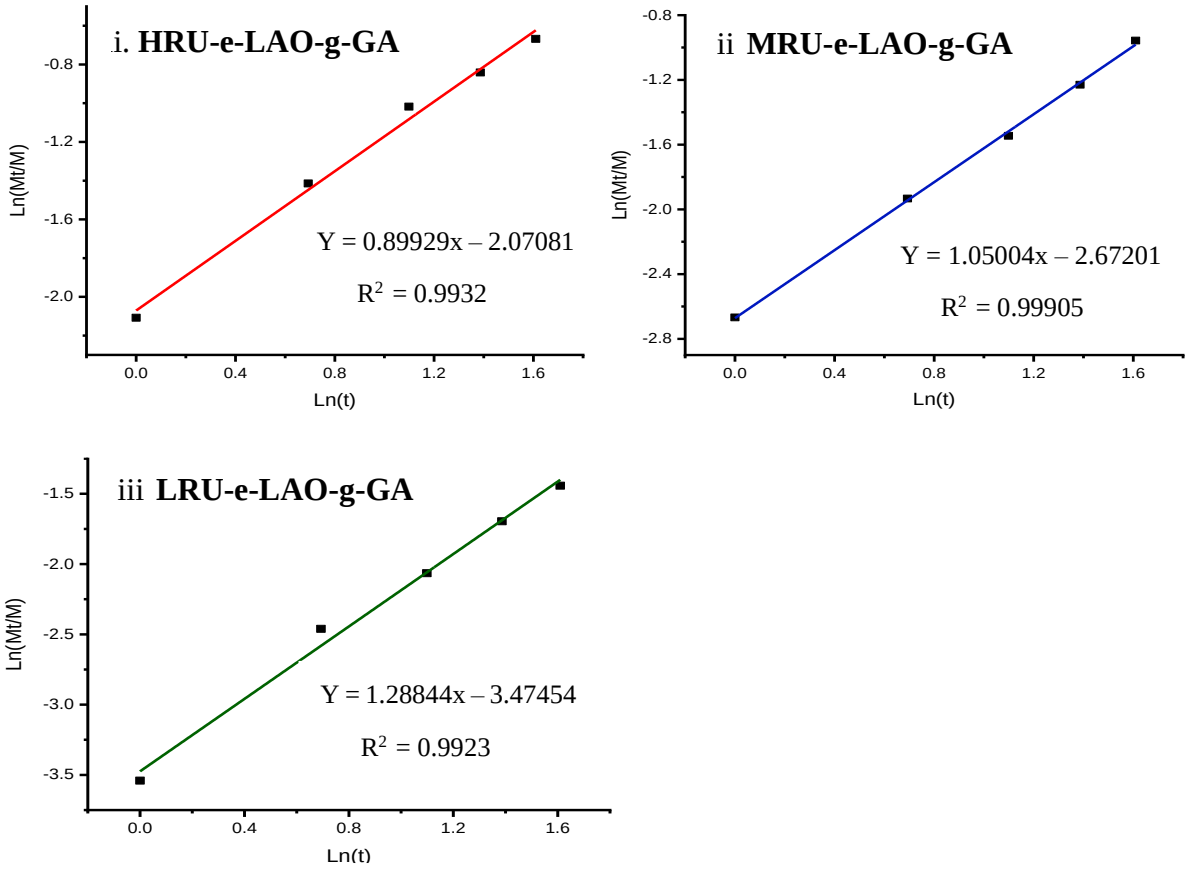

Appendix-12. Amount of Nitrogen Released Vs Square Root of Incubation Time Plot Showing Higuchi Model Linear Fit.

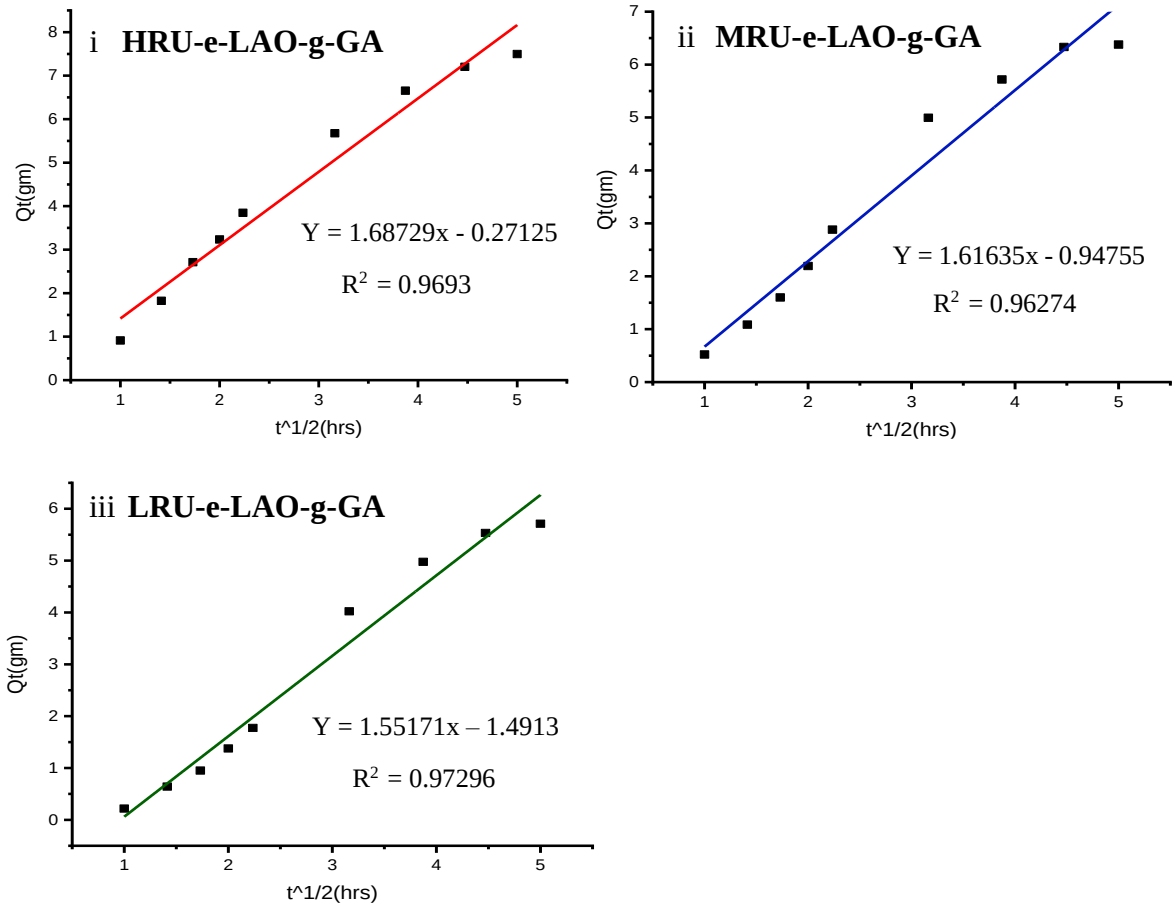

Appendix-13. Amount of Nitrogen Released Vs Incubation Time Plot Showing Zero Order Model Linear Fit.

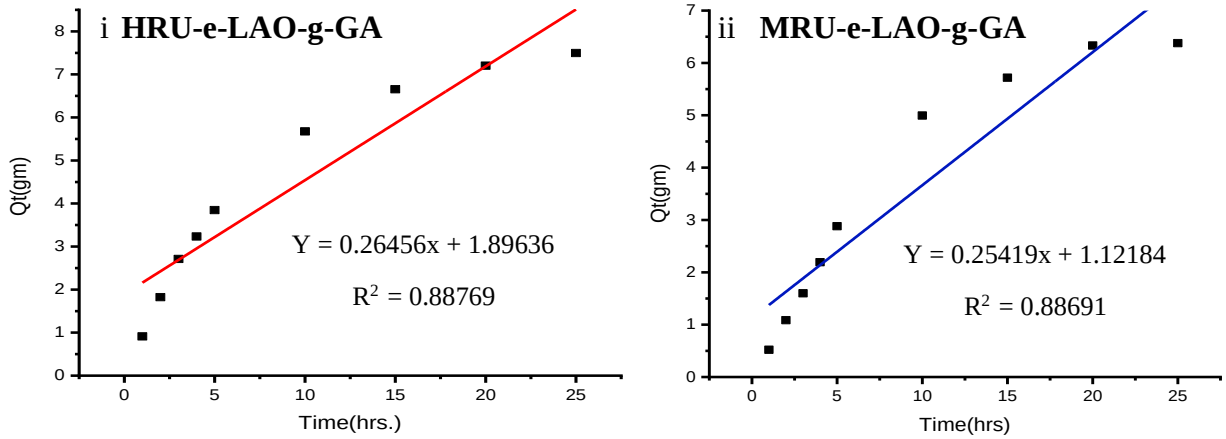

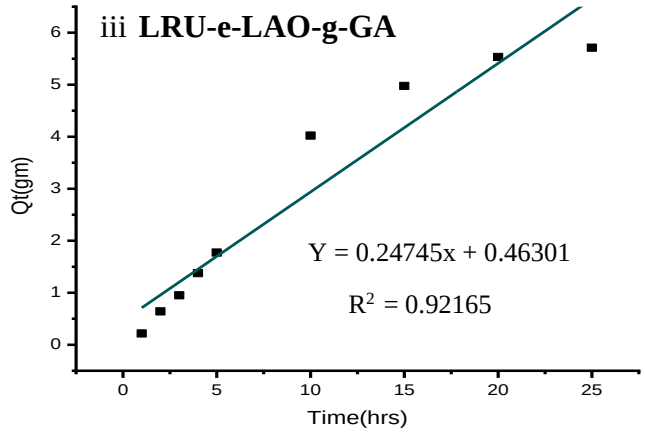

Appendix-14. Ln of Amount of Nitrogen Released Vs Incubation Time Plot Showing 1st Order Model Linear Fit.

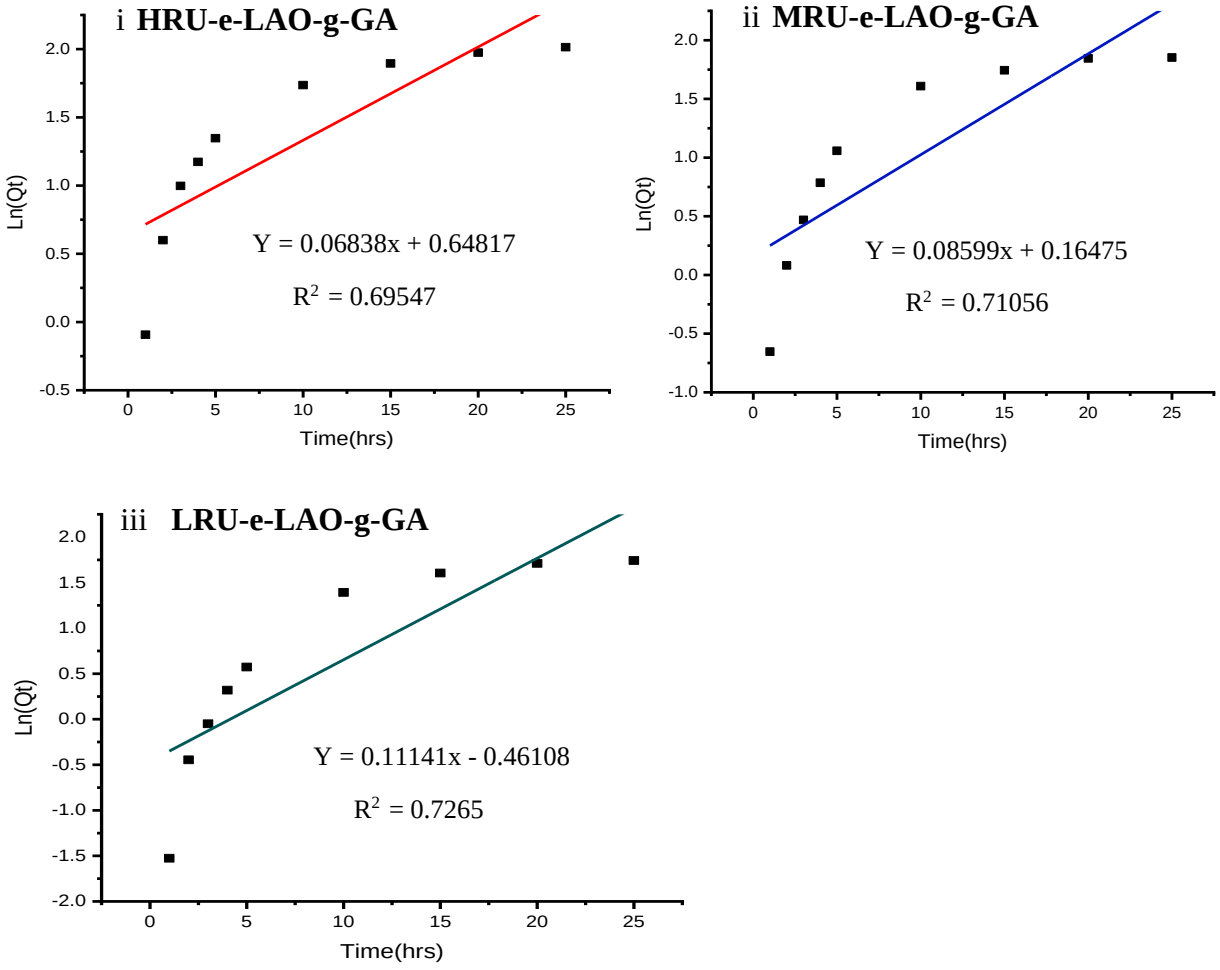

Appendix- 15. Refractive Index Measurement

Appendix-16. Conversion of Refractive Index into Urea Concentration

Using A calibration curve equation, **y = 0.0015x + 1.3328,** where, y is refractive index (nD) & x is urea concentration (Mn).

Then, Urea released (%) $= \frac{Mn}{M} * 100\%$, Where Mn is the concentration of urea released within a given time interval (i.e., calculated using the above calibration curve equation) of the experiment and M is the final concentration released in the experiment(i.e., 7.5g/100 mL).

As an example, the urea release rate at pH-4 for HRU-e-LAO-g-GA was calculated as

Time (hrs.)	nD-1	M1 (g/100 mL)	UR1 (%)	nD-2	M2 (g/100 mL)	UR2 (%)	nD-avg.	Mav (g/100 mL)	UR-avg (%)	SD
1	1.33621	2.273	30.311	1.33623	2.286	30.489	1.33622	2.28	30.4	0.06
3	1.33855	3.833	51.111	1.33854	3.826	51.022	1.338545	3.83	51.06	0.03
5	1.34014	4.893	65.244	1.34011	4.873	64.977	1.340125	4.883	65.11	0.09
7	1.34131	5.673	75.644	1.34133	5.686	75.822	1.34132	5.68	75.73	0.06
9	1.34255	6.5	86.666	1.34257	6.513	86.844	1.34256	6.506	86.75	0.06
11	1.34331	7.006	93.422	1.3433	7	93.333	1.343305	7.003	93.38	0.03
13	1.34365	7.233	96.444	1.34364	7.226	96.355	1.343645	7.23	96.4	0.03
15	1.34399	7.46	99.466	1.34404	7.493	99.911	1.344015	7.477	99.69	0.15

Where, UR (%) is the urea release rate in present, nD is refractive index & SD is standard deviation.

Appendix-17. Nitrogen Release Rate Calculation

$\text{Nitrogen release rate } (\%) = \frac{C*V}{M} * 100\%$, Where C is concentration of nitrogen in leachate (g/mL) obtained from Kjeldahl method, V is the leachate volume in each sampling (mL), and M is total nitrogen present in a fertilizer (g).

The total N in a sample which contains 7.5g of urea is 3.45g. i.e., M = 46%* 7.5g = 3.45g; and V is 100 mL.

As an example the total nitrogen release rate for HRU-e-LAO-g-GA was calculated as:

Time(hrs.)	C1*V	N1 (%)	C2*V	N2 (%)	N-avg. (%)	SD
1	0.375	10.87	0.463	13.42	12.15	1.80
2	0.797	23.1	0.879	25.5	24.3	1.70
3	1.283	37.2	1.211	35.1	36.15	1.48
4	1.507	43.68	1.468	42.56	43.12	0.79
5	1.819	52.74	1.746	50.6	51.67	1.51
10	2.553	74	2.667	77.32	75.66	2.35
15	3.099	89.82	3.023	87.62	88.72	1.56
20	3.286	95.24	3.342	96.86	96.05	1.15
25	3.446	99.9	3.450	100	99.95	0.07

Where, N1 (%) and N2 (%) are the nitrogen release rates of experiment 1 and 2, respectively.